Study Of The Dynamics And Control Of Vapor Recompression Columns.

Order Number 8909395

Study of the dynamics and control of vapor recompression columns

Muhrer, Cristian Augusto, Ph.D.

Lehigh University, 1989

U·M·I
300 N. Zeeb Rd.
Ann Arbor, MI 48106

STUDY OF THE DYNAMICS AND CONTROL OF VAPOR RECOMPRESSION COLUMNS

by

CRISTIAN A. MUHRER

A Dissertation

Presented to the Graduate Committee

of Lehigh University

in Candidacy for the Degree of

Doctor of Philosophy

in

Chemical Engineering

Lehigh University

1988

Approved and recommended for acceptance as a dissertation in partial fulfillment of the requirements for the degree of Doctor of Philosophy.

Dec. 15, 1988

(date)

William F Luyben

Professor in Charge

Special committee directing the doctoral work of Cristian A. Muhrer

William F Luyben

Dr. William Luyben, Chairman

John C. Chen

Dr. John Chen

C W Clump

Dr. Curtis Clump

Michael A Collura

Dr. Michael Collura

C Georgakis

Dr. Christos Georgakis

Kenneth F Emigholz

Dr. Kenneth Emigholz

Dec. 15, 1988

Accepted

To Carla and Francesca

Acknowledgements

I would like to thank the members of my committee for their guidance and encouragement during the course of my studies. Special thanks to Professor William Luyben for sharing his expertise and providing constant support. Thanks to Dr. Michael Collura for his collaboration and direction in this project.

I would like to express my gratitude to the Department of Chemical Engineering at the University of Concepcion, Chile, for giving me a leave of absence to pursue my education toward a Doctoral degree. In addition I appreciate the financial support of the Process Modeling and Control Center at Lehigh University.

Finally, I would like to acknowledge the friendship of my fellow graduate students in the Process Modeling and Control Center and express special appreciation for the assistance of Randel Price in editing this dissertation.

Table of Contents

List of Figures

List of Tables

Abstract

Distillation with vapor recompression represents an attractive alternative to conventional columns in some systems because it reduces considerably the energy consumption of the process. Most of the literature in the vapor recompression field has been devoted to the steady-state economic aspects.

The objective of this dissertation is to improve the understanding of the operation and control of distillation with vapor recompression. This study uses the ethanol-water and propylene-propane systems as specific typical examples.

The results show that despite the complexity added by the vapor recompression design, the process does not require a complex control structure. Control strategies designed for conventional columns can be applied to the corresponding vapor recompression columns by simply replacing heat input control with compressor control. The pressure loop will be faster than the composition loops and hence can be treated independently. For this conclusion to be valid, two conditions are necessary: (1) the composition time constants of the column should be at least 5 times larger than the pressure time constant; (2) the time constants of the reboilers of the two systems should be approximately the same. A large ratio of composition time constant to pressure time constant is typical for vapor recompression columns because the systems considered for vapor recompression represent difficult separations (low relative volatility), which result in a column with a large number of trays.

Alternative compressor control structures were examined and all were about equally effective from a control point of view. Compressor control using variable speed and variable heat transfer area were the alternatives that require the least energy consumption.

Chapter 1
Introduction

The conventional distillation column ranks among the biggest energy consumers in the chemical process industries. Consequently there is a significant incentive to reduce capital investment and to improve the energy efficiency of this expensive separation process.

In many cases, energy consumption of existing distillation plants can be reduced by improvements, such as (Mix *et al.*, 1978):

1. Better operating conditions, *e.g.* preheating the feed with product streams.
2. Smaller temperature differences across the heat exchangers.
3. Reduced reflux by increasing the number of trays.
4. Better control systems.
5. Use of adequate insulation.
6. Installation of high-efficiency packings.

However, these straightforward and simple routes for saving energy are limited and often have already been exploited. Further energy reduction can be achieved by recovering the heat released at the top of the column. To accomplish this, Danzinger (1979) and Ferre *et al.* (1985) suggest the following: for separation at high temperatures, generate low-pressure steam in the condenser that can be reused elsewhere in the plant; for dual-pressure or coupled columns, use the heat available at the top of one to heat the other; for temperature-sensitive or corrosive products, use heat pumps with an auxiliary circuit using refrigerant to transfer the energy at the top of the column to the bottom; if the top product is unsuitable for compression, use a heat pump

where the reboiler liquid is flashed and recompressed; or for systems that require direct refrigeration or have a small boiling point difference, use a heat pump with direct vapor recompression (VRC).

The choice of a heat recovery method is based on the operating and economic conditions of the process. This work will be restricted to direct VRC, in which the overhead vapor is compressed to a higher temperature so that its energy can be released in the reboiler by condensation (see Figure 2-1).

1.1 Background

Vapor recompression design has been discussed in the literature for many years. Robinson and Gilliland (1950) describe a number of ways, including vapor recompression, to reduce energy consumption in distillation processes. However, heat pump systems in distillation have been commonly accepted by industry only in recent years (Meili, 1987). Most of the literature on vapor recompression focuses on the steady-state economic aspects (capital costs, operating costs and optimal operating conditions).

Null (1976) , Mostafa (1981) and Meili and Stuecheli (1987) indicated that the use of direct VRC is convenient when the reboiler duty is high, the temperature rise across the compressor is low. direct refrigeration or chilled water is required. or the boiling point difference is small. VRC is not convenient when the column operates with inexpensive energy or when the top pressure is less than about 80 mmHg.

Ferre *et al.* (1985) analyzed two different systems: ethylbenzene-styrene and ethylbenzene-xylene. They reported a net saving of 1.3 to 1.6 millions of dollars per year, with a pay out time of 1.7 to 2.3 years. when vapor recompression was used instead of conventional distillation.

The distillation design and operating conditions to produce a fuel-grade ethanol product from typical grain fermentation broth were studied by Collura (1986). For production of 83 mole% product from 2.9 mole% feed, a design featuring vapor recompression was found to have the lowest operating cost. This work reported an optimum reflux ratio of 1.1 times the minimum reflux ratio and a pressure of 1.0 atm.

Quadri (1981) studied vapor recompression for the propylene-propane system. He found the optimum operating conditions to be a reflux ratio close to 1.2 times the minimum reflux ratio, a temperature difference in the reboiler-condenser around 8 °C and a top pressure of 10 atm.

Little has been published on the dynamics and control of vapor recompression. A dynamic modeling study by Hernandez (1981) is somewhat helpful in model development, but is limited in complexity and scope and lacks experimental verification.

The dynamics and control of the ethanol-water system were studied by Collura (1986). Interaction of the pressure control and other loops that manipulate energy input/removal appeared to be a potential source of operating difficulty. A simplified model was used for the compressor and reflux drum.

Brousse et al. (1985) are studying the steady-state operation of a packed pilot plant vapor recompression column using microcomputer controls. The system is cyclohexane-n-heptane. No experimental data has yet been reported.

1.2 Scope of Work

This dissertation examines the dynamics and control of direct vapor recompression columns. Two specific, industrially important separations are looked at in detail. These are the ethanol-water system and a hydrocarbon system of commercial interest, such as might be found in a petroleum refinery (*e.g.* a propylene-propane splitter). For both systems there are substantial economic incentives for using vapor recompression.

The first and most important objective of this dissertation was to improve the understanding of the operation and control of distillation columns with vapor recompression. Operability and control problems were explored and different control schemes were examined and evaluated. To provide a well understood frame of reference for comparison to the vapor recompression column, conventional column designs for the same chemical systems were developed and simulated.

A second objective was to study the control problems of vapor recompression columns under different process constraints, such as maximum production, column flooding, compressor surge, constant compressor speed, etc. The control schemes were tested under these conditions and appropriate changes in the control structures identified.

The study is based on computer simulation: however, experimental data from other researchers for the steady-state operation of the conventional columns was used to verify the steady-state models.

In the following chapters, the steady-state and dynamic models for both systems are presented. The control tools are described and the control aspects of each system are discussed. Finally, some generic conclusions are drawn.

Chapter 2
Steady-State Models

A number of design configurations are possible when using vapor recompression in distillation. Figure 2-1 shows a low pressure reflux drum scheme in which the reflux drum is operated essentially at the same pressure as the top of the column. An advantage of this scheme is that it minimizes the amount of work done by the compressor. The trim condenser can be manipulated in several ways in this design. It can be operated as a flooded condenser or the cooling water rate can be manipulated without directly

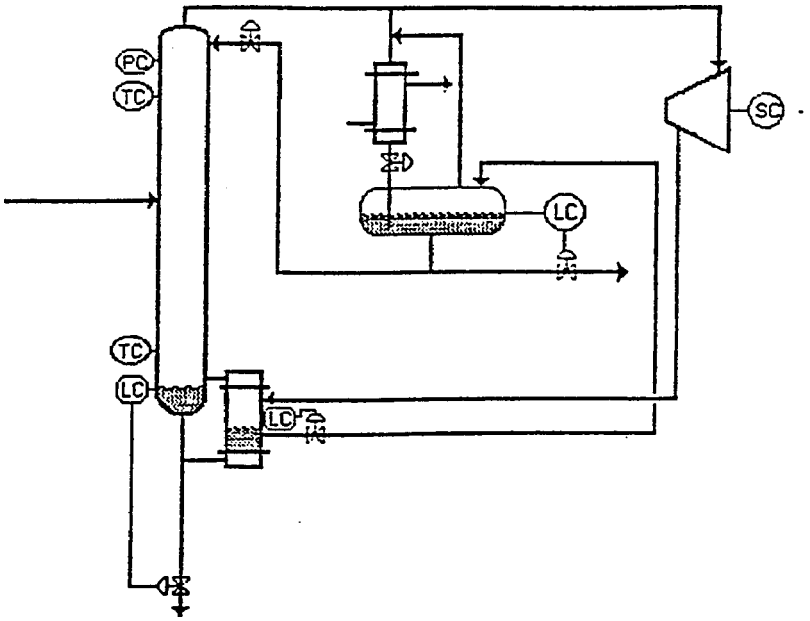

Figure 2-1: VRC design with low pressure reflux drum

restricting the flow on the process side. Figure 2-2 shows an alternative, a high pressure reflux drum scheme, in which the reflux accumulator is operated at the compressor discharge pressure. One advantage of this system is the elimination

of a refrigerated trim condenser when separating light components which condense below cooling water temperatures. Since there is no pressure let-down in the reflux accumulator, this design may also prove easier to operate than the other. Detailed models of these and other alternatives must be used to

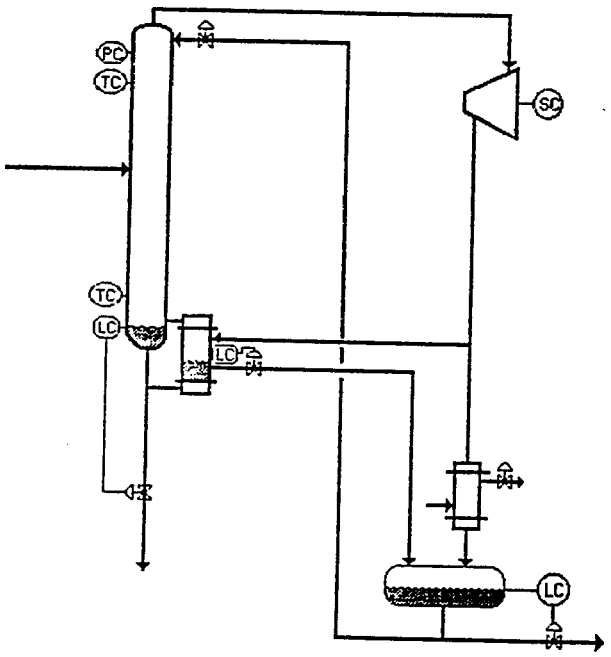

Figure 2-2: VRC design with high pressure reflux drum

determine the advantages and disadvantages of each. The design of choice varies depending on the components being separated, that is, one design may prove best for the ethanol-water system while another may be more desirable for the propylene-propane system.

Steady-state models were developed to perform design and rating calculations for the different columns to be studied. These models have been validated by comparison with real systems. Data on the ethanol-water system were obtained from pilot plant studies conducted at the University of

Concepcion (Chile). Model results match the Concepcion results when a tray efficiency of 45% is used. Propylene-propane results were used to fit data obtained by Finco (1987) for an industrial column operated by Sun Refining and Marketing. A tray efficiency of 100% was calculated from the plant data.

The purpose of the design program is to estimate the number of trays, reflux ratio and feed tray location of a distillation column for a given separation. For the vapor recompression columns this program requires the characteristic curves of the compressor to determine compressor speed for a given head and throughput.

Rating programs (Buckley et al., 1985) (Muhrer *et al.*, 1988) are useful to analyze the performance of an existing column. The goals in preparing these programs are:

- Plot the changes required in all manipulated variables to hold the controlled variables constant under typical disturbances (Luyben, 1975). This plot shows the values of manipulated variables, such as reflux ratio, reflux flow and vapor boilup, plotted against feed composition for fixed terminal compositions. Such plots (Luyben curves) can indicate whether dual composition control is necessary.

- Obtain the steady-state gains of the process. Here, for example, we need to know the change in terminal compositions due to a change in reflux flow with other manipulated variables held constant. In this procedure it is important that the changes in manipulated variables be small enough to insure that they are in the linear region (*i.e.*, constant steady-state gains). As an example, to determine the steady-state gains in the processes under study, changes on the order of 10^{-4} percent were made in the manipulated variables. Figure 2-3 shows how the gains between distillate composition and heat input vary when the size of the heat input step is decreased.

Rigorous plate-to-plate calculations were made taking into account the effects of non-equal molar overflow and variations in relative volatility. The following assumptions were made in the development of the steady-state models:

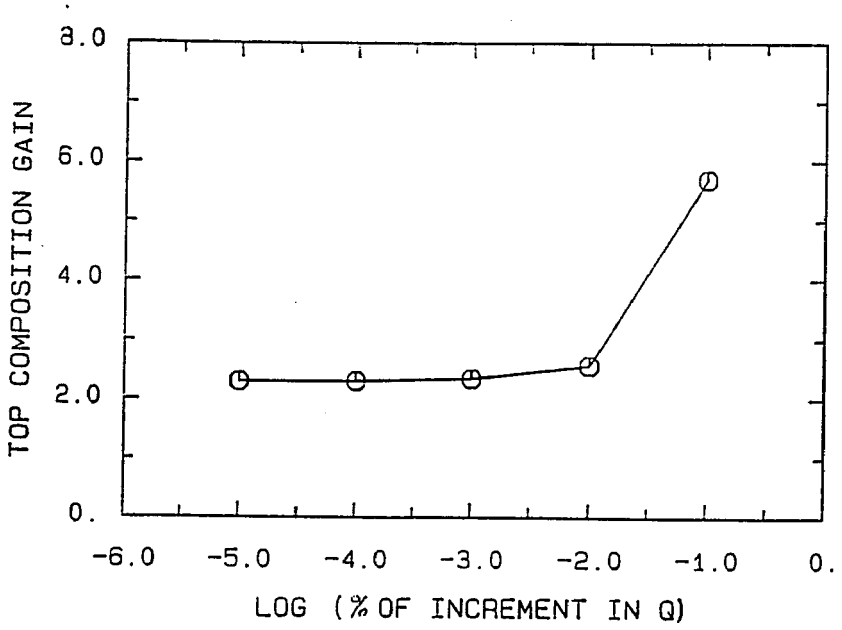

Figure 2-3: Step size influence on steady-state gain: ethanol-water

1. Complete mixing per stage
2. Adiabatic stages
3. No heat of mixing
4. Total condenser for the conventional column
5. Partial reboiler for the conventional column
6. One feed and two products (distillate and bottoms)
7. Constant pressure drop in column trays
8. Adiabatic compression with polytropic efficiency of 70%
9. Centrifugal compressor
10. Adiabatic flash of reflux
11. Condenser side of the reboiler condenser is a total condenser and the reboiler side is a partial reboiler

12. 15 °F temperature approach for reboiler-condenser design

13. 20 °F temperature approach for preheater design

In the following sections, design aspects of the different columns and systems are discussed and the base cases presented. The results of the rating programs (steady-state gains and Luyben curves) will be discussed. The thermodynamic and physical property relations are described in Appendix A. A summary of the physical design of the columns used is given in Appendix B.

2.1 Ethanol-Water System

The final design and optimum operating parameters for a standard distillation column at the base case conditions are shown in Figure 2-4. The energy consumption for this design is 117.4 million Btu/hr (120,000 lb/hr of 50 psia steam). It was found that the energy consumption is minimized when the feed is preheated as much as possible without using steam for that purpose. A 13.5 foot diameter column with 78 trays and a reflux ratio of 1.75 will produce an overhead product close to the azeotrope, 83 mol%, and a bottom product with 0.01 mol% of ethanol.

The effects of pressure and reflux ratio were studied by Collura and confirmed in this simulation. In Table 2-1 the effect of feed composition is presented. In all cases, 1.1 times the minimum reflux, a top pressure of 1.0 atm., a Murphree tray efficiency of 0.4 in the stripping section and 0.5 in the rectifying section and a pressure drop of 5.3 mmHg/tray were used to produce the desired products.

The vapor recompression design for the base case is presented in Figure 2-5. The column itself is identical to the conventional one because the operating pressure and reflux ratio are the same. The energy consumption is 8003 hp or

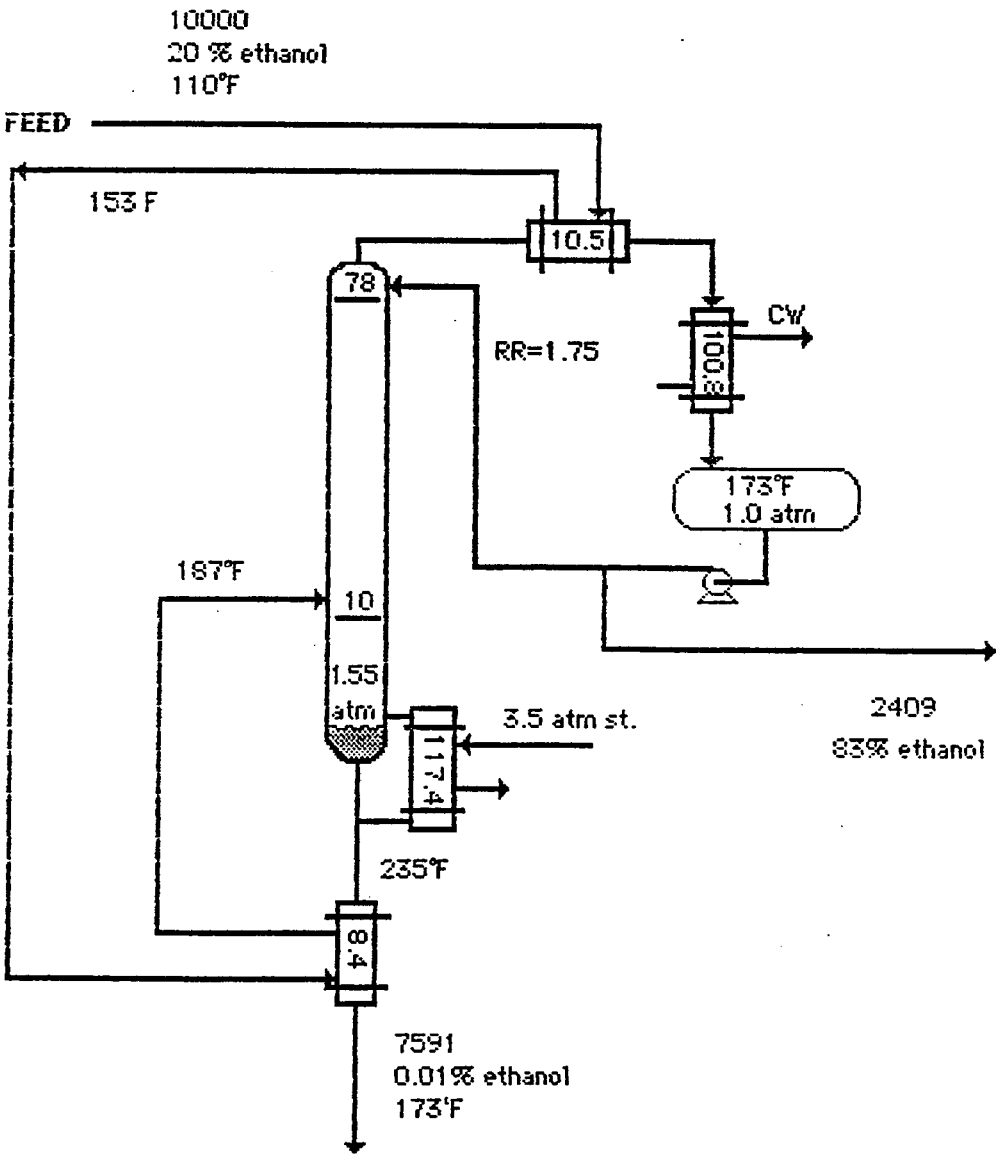

Figure 2-4: Base case conventional column: ethanol-water

The numbers without units inside the boxes are heat transfer rates in 10^6 Btu/hr, outside the boxes are flows in lbmol/hr.

Table 2-1: Feed composition effect. Conventional and vapor recompression

Conventional and Vapor Recompression					Vapor Recompression		
z	N	NF	RR	Q_R	W	hp	Q_{aux}
0.03	57	28	3.05	29.9	4.7	1855	0.6
0.05	69	25	2.04	36.4	6.2	2412	-
0.1	82	14	1.75	61.8	10.9	4264	-
0.2	78	10	1.75	117.4	20.4	8003	-
0.3	75	10	1.75	173.1	29.8	11696	-
0.4	74	11	1.75	228.6	39.2	15377	-
0.5	73	13	1.75	284.4	48.6	19078	-

N : number of trays
NF : feed tray
Q_{aux} : auxiliary reboiler duty (10^6Btu/hr)
Q_R : reboiler duty (10^6Btu/hr)
RR : reflux ratio
W : compressor work (10^6Btu/hr)
hp : compressor work (hp)
z : feed molar composition (mole fraction of ethanol)

20.4 million Btu/hr. Since the top temperature is high enough to use water to condense the excess vapor (the vapor not required to match reboiler duty) it is not necessary to compress all the overhead vapor. Therefore it is possible to use a low pressure reflux drum scheme.

The results shown in Table 2-1 indicate that the effect of feed composition

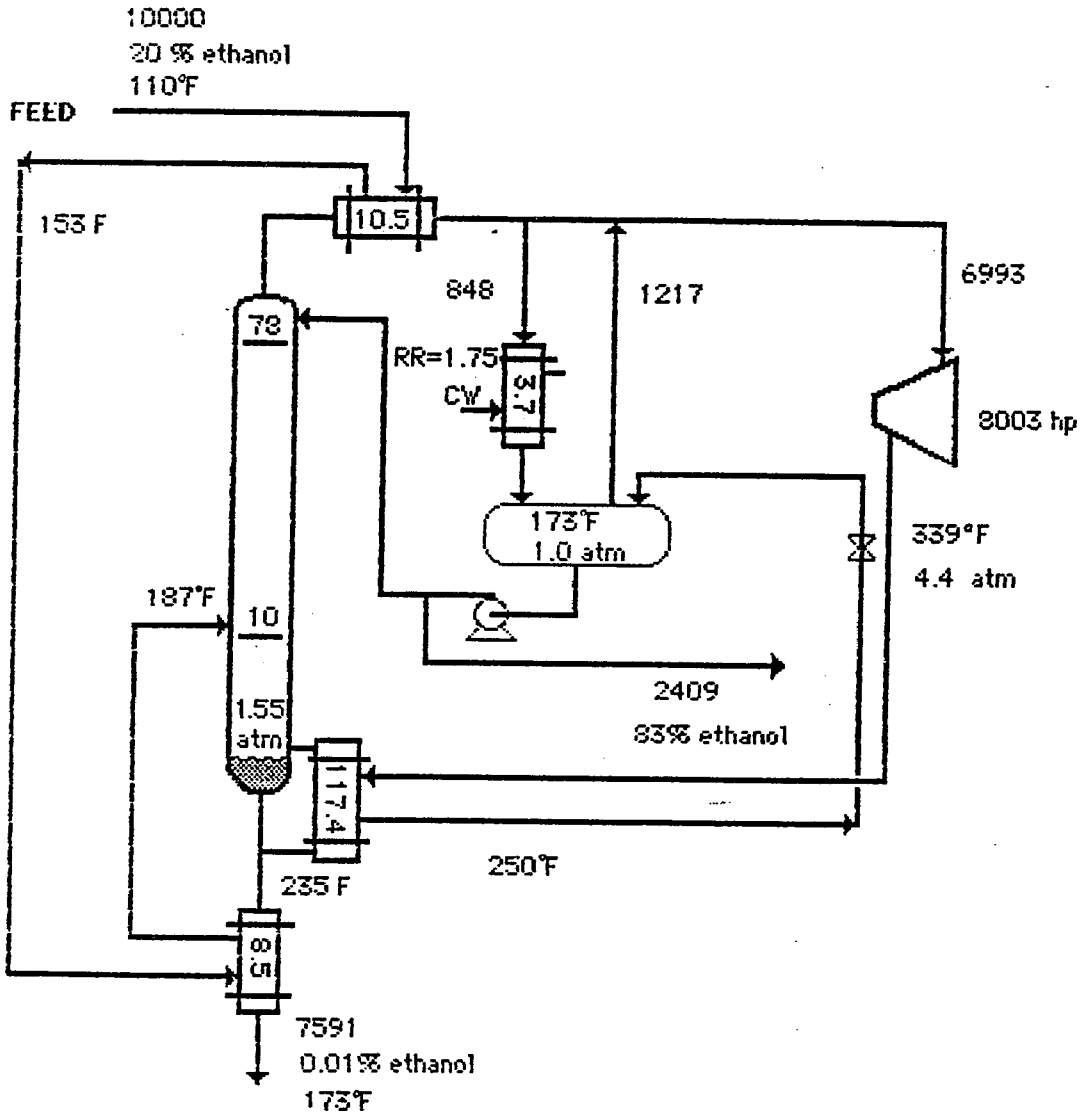

Figure 2-5: Base case vapor recompression column: ethanol-water

The numbers without units inside the boxes are heat transfer rates in 10^6 Btu/hr. outside the boxes are flows in lbmol/hr.

is similar in both the conventional and vapor recompression cases. It is interesting to note that there is not enough overhead vapor to match the reboiler duty when the feed composition is less than 5 mol% in ethanol. Therefore it is necessary to have an auxiliary reboiler . An auxiliary reboiler is also needed when the feed is subcooled to low temperatures.

The required initial investment for the base cases (20% feed composition) was calculated using published correlations (Mulet *et al.*, 1981) (Miller and Kapella, 1977) (Hall *et al.*, 1982). Costs were 1.3 and 5.5 million dollars for the conventional and vapor recompression designs respectively. Considering utility costs of $5.0/1000 lb. of steam and $0.07/KWH of electricity, the operating costs are 5.6 and 3.8 million dollars per year. These numbers indicate a 2.3 year incremental pay out time beyond the conventional column. The very large capital cost of the vapor recompression system is mostly due to the cost of the compressor. Compressor cost is a function of the compression work required. For this chemical system, the large temperature difference between the top and bottom of the column indicates the need for a large compression ratio. For systems with less temperature difference, less energy is required and capital cost and pay out time decrease (as in the propylene-propane system).

2.2 Propylene-Propane System

The base case for the conventional propylene-propane distillation is shown in Figure 2-6. It is necessary to operate at 17.6 atm. (244 psig) in order to use water in the condenser. This pressure is based on a design overhead vapor temperature of 110 °F. It is not possible to preheat the feed using a column product because the boiling points of these streams are close together. If colder cooling water were available, allowing condensation at 90 °F, the pressure can

be reduced to 15.6 atm., resulting in a 4.4 % reduction in energy consumption.

The feed composition effect is presented in Table 2-2. A reflux ratio 1.2 times the minimum, a tray efficiency of 100 %, a pressure drop of 5.3 mmHg/tray and a top temperature of 110 °F were used to produce the required products.

The same separation using vapor recompression is presented in Figure 2-7. In this case it is possible to decrease the operating pressure and hence increase the relative volatility. A high pressure reflux drum scheme is used because of the low top temperature. The temperature in the reflux drum is fixed to provide a 15 °F temperature difference in the reboiler-condenser. This design has a column with 54 fewer trays and an operating pressure 7 atmospheres lower than the conventional column. The energy consumption drops from 27.3 million Btu/hr (steam) to 3.0 million Btu/hr (electricity).

Lowering the pressure reduces energy consumption due to the increase in relative volatility. At some point, however, the reflux drum temperature will become too low to allow condensation with water. Rather than using refrigeration, it may be economical to use a two-stage compressor to raise the saturation temperature of the excess vapor so that it can be condensed with cooling water (see Figure 2-8). Thus the choice of operating pressure on the design of the vapor recompression column is quite significant, as seen in Table 2-3.

Energy consumption can be reduced somewhat by subcooling the reflux to the column. This reduces the amount of flashing of the reflux as it drops from the compressor discharge pressure to the compressor suction pressure. The last five columns of Table 2-3 show how the flow through the compressor, the flow

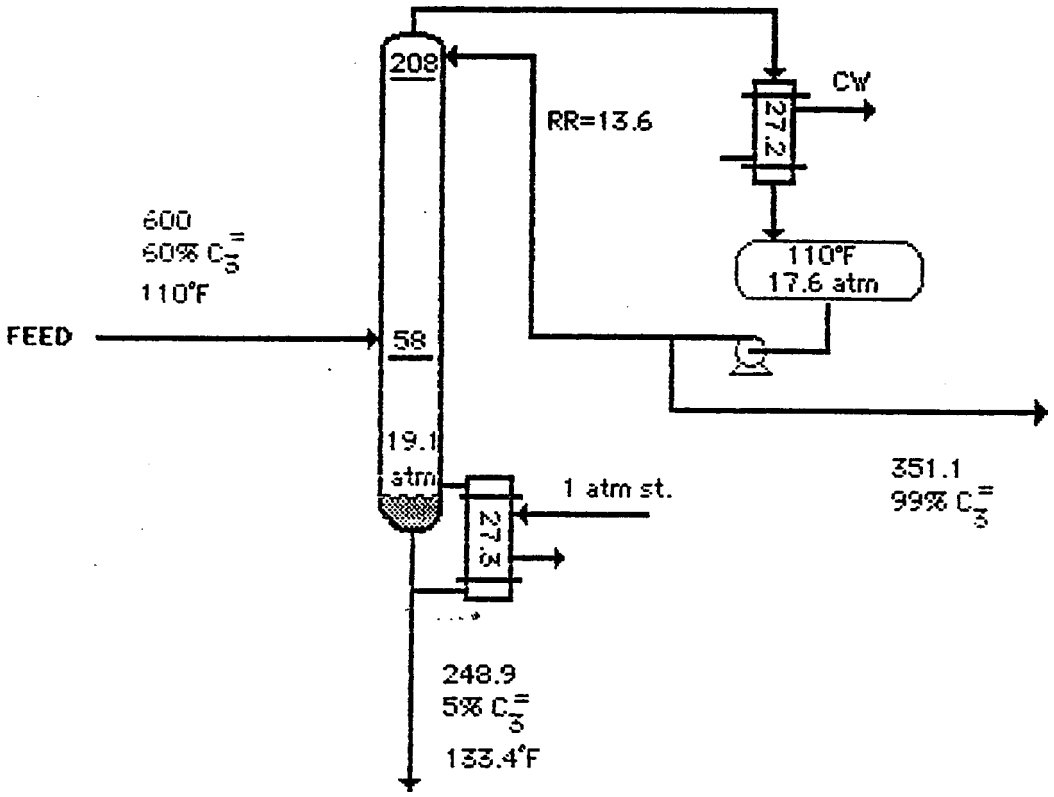

Figure 2-6: Base case conventional column: propylene-propane

The numbers without units inside the boxes are heat transfer rates in 10^6 Btu/hr, outside the boxes are flows in lbmol/hr.

Table 2-2: Feed composition effect. Conventional distillation P-P.

z	q	N	NF	RR	Q_R
0.1	1.11	106	18	66.3	11.7
0.2	1.09	131	36	34.5	18.3
0.3	1.08	149	45	23.9	21.3
0.4	1.07	166	50	18.7	23.5
0.5	1.07	185	54	15.7	25.6
0.6	1.06	208	58	13.6	27.3
0.7	1.06	243	65	12.1	28.9
0.8	1.04	259	82	10.7	29.9
0.9	1.02	220	77	9.1	29.2

through the condenser, and the compressor work change when the reflux is subcooled.

One method of subcooling the reflux is to install an auxiliary trim cooler in the reflux line (see Figure 2-9). This can be used when the reflux drum temperature is higher than 110 °F. An alternative is to subcool using the cold overhead vapor from the column. For this system, subcooling reflux shifts the minimum operating cost pressure from 12 atm. to 16 atm.; however the small decrease in energy consumption as pressure is increased is offset by an increase in the number of trays (capital cost). A review of the cost data indicates that

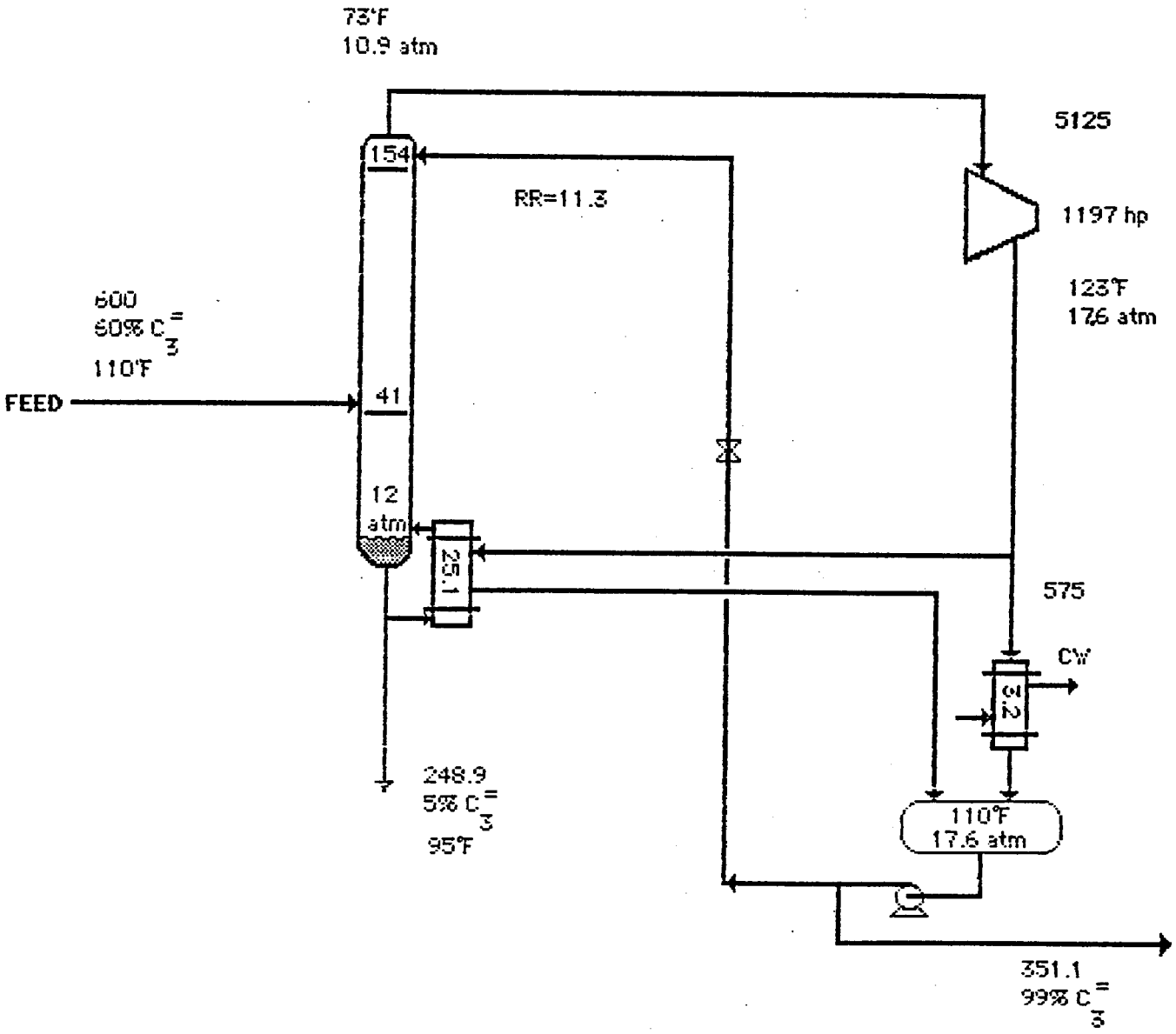

Figure 2-7: Base case vapor recompression column: propylene-propane

The numbers without units inside the boxes are heat transfer rates in 10^6 Btu/hr. outside the boxes are flows in lbmol/hr.

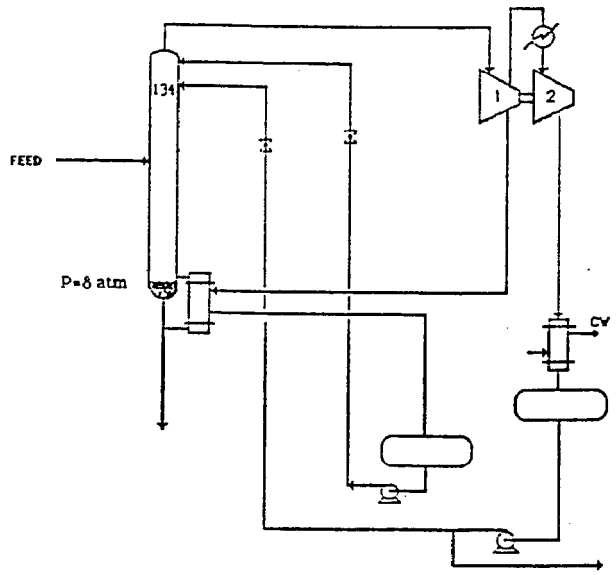

Figure 2-8: P-P vapor recompression with two-stage compressor

the optimum operating pressure seems to be about 12 atm. This is the minimum pressure that allows the use of cooling water in the condenser and does not require a two-stage compressor.

The effect of feed composition on compressor power is presented in Figure 2-10 for different operating pressures. A linear relation was found between compressor work and feed composition for a specified column pressure.

The base case design of the conventional column has a capital cost of 1.5 millions of dollars and an operating cost of 1.2 millions of dollars per year. The vapor recompression design has a capital cost of 1.85 millions of dollars and an operating cost of 0.56 millions of dollars per year. The incremental pay out time is 0.25 year for this system.

Table 2-3: Pressure effect. Vapor recompression P-P.

					no subcooled reflux				subcooled reflux				
p_b	N	RR	Q_R	t_r	F_c	F_w	hp(1)	hp(2)	F_c	F_w	hp(1)	hp(2)	RC
16	180	12.5	26.2	133	5782	567	1230	-	5087	-	1082	-	CW
15	173	12.1	25.9	128	5601	566	1217	-	5083	48.1	1104	-	CW
14	166	11.8	25.6	122	5431	567	1206	-	5087	223	1130	-	CW
12	154	11.3	25.3	110	5125	575	1197	-	4851	533	1168	-	OV
10	143	10.7	24.8	96	4846	582	1201	48.1	4609	545	1178	46.3	OV
8	134	10.3	24.6	81	4599	592	1228	112	4388	559	1210	109	OV
5	123	9.6	24.4	50	4270	640	1347	274	4094	611	1339	270	OV

p_b : bottom pressure (atm)
t_r : reflux drum temperature (°F)
F_c : flow through the compressor (lbmol/hr)
F_w : flow through the condenser (lbmol/hr)
RC : reflux coolant
CW : cooling water
OV : overhead vapor

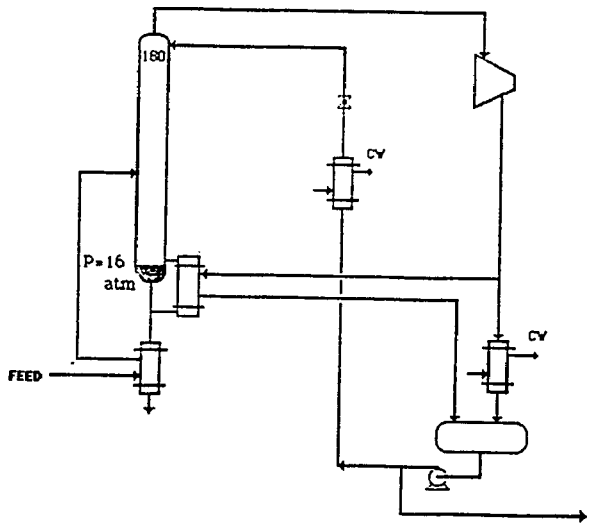

Figure 2-9: Design which subcools reflux with cooling water

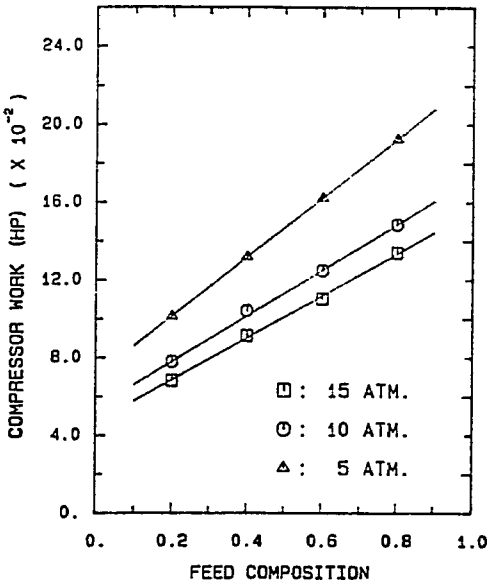

Figure 2-10: Feed composition effect on the compressor work

Chapter 3
Dynamic Models

In this chapter general dynamic models for distillation columns and compressors are described and the specific assumptions for the ethanol-water and propylene-propane systems are presented.

3.1 Distillation Column Models

Most models of a single distillation tray use one dynamic component balance for each component and one energy equation:

$$\frac{d\left[M_n^L x_{nj} + M_n^V y_{nj}\right]}{dt} = L_{n+1}\, x_{n+1,j} + V_{n-1}\, y_{n-1,j} - L_n\, x_{nj} - V_n\, y_{nj} \qquad (3.1)$$

$$j = 1, NC$$

$$\frac{d\left[M_n^L h_n + M_n^V H_n\right]}{dt} = L_{n+1}\, h_{n+1} + V_{n-1}\, H_{n-1} - L_n\, h_n - V_n H_n \qquad (3.2)$$

where:

M_n^L : liquid holdup on the nth tray
M_n^V : vapor holdup on the nth tray
x_{nj} : liquid composition of component j on the nth tray
y_{nj} : vapor composition of component j on the nth tray
L : liquid flow rate
V : vapor flow rate
h : liquid enthalpy
H : vapor enthalpy
NC : number of components

Fuentes and Luyben (1982) observed that the energy equation is usually applied in one of three alternative algebraic forms (models 1, 2 or 3) that differ in how the left hand side of equation (3.2) is approximated. Whatever algebraic form is used, the energy balance is rearranged to solve for the vapor flow rate

on each tray at each point in time.

For model 1, the energy derivative is set equal to zero, and:

$$V_n = [L_{n+1} h_{n+1} + V_{n-1} H_{n-1} - L_n h_n] / H_n \tag{3.3}$$

For model 2, the energy derivative is approximated by,

$$\frac{d[M_n^L h_n + M_n^V H_n]}{dt} \approx h_n \frac{dM_n^L}{dt} + H_n \frac{dM_n^V}{dt} \tag{3.4}$$

For model 3, the complete derivative is used:

$$\frac{d[M_n^L h_n + M_n^V H_n]}{dt} = h_n \frac{dM_n^L}{dt} + M_n^L \frac{dh_n}{dt} + H_n \frac{dM_n^V}{dt} + M_n^V \frac{dH_n}{dt} \tag{3.5}$$

and the enthalpy derivatives are calculated by the expression

$$\frac{dh_n}{dt} = \frac{h_n(t + \Delta t) - h_n(t)}{\Delta t} \tag{3.6}$$

Other basic equations for the model represent the vapor-liquid equilibrium. physical properties (see Appendix A) and liquid flow rate from each tray (usually given by the Francis weir formula). Distillate flow. bottoms flow, reflux flow and heat input are used to control levels and/or compositions.

A comparison of these models and more complex ones is given by Choe (1985) . She suggests that vapor holdup should be included when the vapor density becomes significant in comparison to the liquid density. For most common materials. this corresponds to an operating pressure greater than 5-10 atm. In cases where changes in pressure and pressure drop are significant (*e.g.*., vacuum columns) a rigorous dynamic vapor hydraulic model should be used. Solution of the modeling equations is much simpler when vapor holdup can be neglected.

Choe and Luyben (1987) give a complete description of how to solve these equations numerically. They conclude that for most constant pressure columns, the simple explicit Euler method provides the best algorithm; for variable pressure drop columns, where the rigorous vapor hydraulic model should be used, the LSODES method (Hindmarsh and Sherman, 1983) is the best algorithm.

3.2 Compressor Models

The performance of a centrifugal compressor cannot be exactly predicted from theoretical analysis. Instead it must be experimentally determined and reported in the form of performance curves. A typical set of performances curves is shown Figure 3-1. The stability limit or "surge line" denotes the minimum flow at which the compressor can operate at a given speed. Operation below the surge point could cause violent vibration to the point of permanent damage.

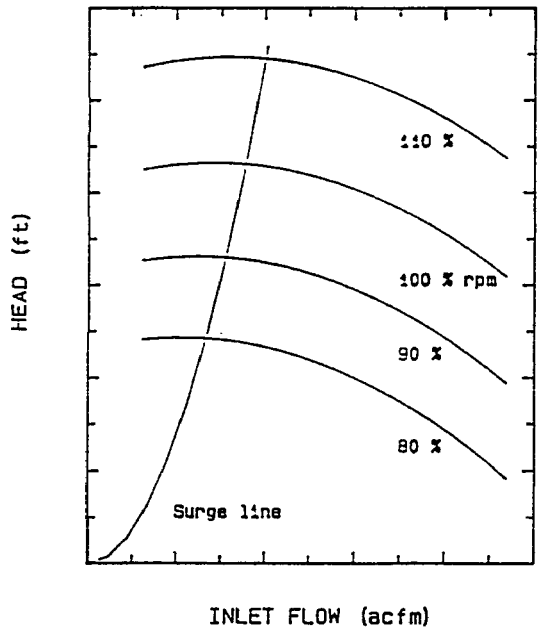

Figure 3-1: Compressor performance curves

The "head", energy per unit mass of gas in ft-lb_f/lb, is given by (Lapina, 1982)

$$H = \mu\, u^2 / g \tag{3.7}$$

μ : head coefficient
u : impeller tip speed (ft/s)
g : gravitational constant, 32.2 ft/s^2

$$u = N \pi D / 720 \tag{3.8}$$

N : impeller speed (rpm)
D : impeller diameter (in)

$$\mu = 0.54 + 5.0\,\phi - 200\,\phi^2 \tag{3.9}$$

$$\phi = \frac{700\,Q}{N\,D^3}$$

ϕ : flow coefficient
Q : inlet capacity (ft^3/min)

The relationship between head and flow coefficient (Equation (3.9)) is a correlation determined by numerically fitting a typical centrifugal compressor performance curve reported by Neerken (1975).

A typical arrangement for a centrifugal compressor with speed control is shown in Figure 3-2. The antisurge control loop (Shinskey, 1979) is designed to adjust the by-pass flow in order to keep the flow rate through the compressor above the surge value. The square of the surge flow is approximately linear with the pressure drop across the compressor. This relation supplies the set point of the antisurge controller which measures compressor inlet flow.

White (1972) has described the surge line as a parabola relating adiabatic head to the square of volumetric suction flow. The surge line is calculated as

$$H = C\,Q^2. \tag{3.10}$$

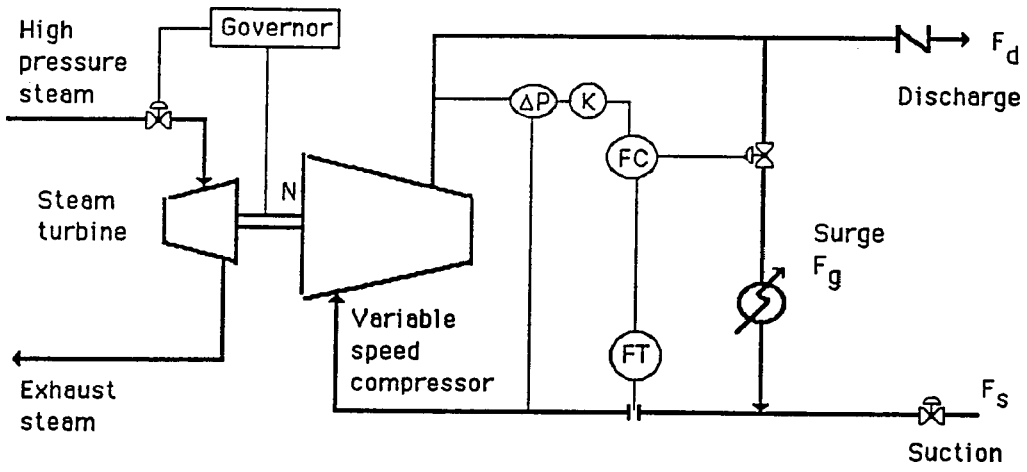

Figure 3-2: Centrifugal compressor with variable speed

To model the compressor, the system is divided into three parts: suction piping, discharge piping, and the compressor proper. Mass balance equations are written for the suction and discharge volumes. These balances can be solved for the suction and discharge pressure of the compressor (Davis and Corripio, 1974).

$$\frac{dP_s}{dt} = (F_s - F_g - F_c)\frac{z_s R T_s}{V_s} \tag{3.11}$$

$$\frac{dP_d}{dt} = (F_c - F_g - F_d)\frac{z_d R T_d}{V_d} \tag{3.12}$$

F : flow
P : pressure
R : ideal gas law constant
T : temperature
V : volume
z : compressibility factor

subscripts
c : compressor
d : discharge
g : surge
s : suction

The flows used in this calculation result from algebraic equations: F_c from the compressor curves, F_s is the flow coming out of the column plus or minus any flashed or condensed flow in the suction piping, F_d is the flow being condensed in the discharge piping and F_g is the bypass flow to avoid surge in the compressor.

3.3 Ethanol-Water System

The column operating pressure is about 1 atm. for the ethanol-water system in both the conventional and vapor recompression cases; therefore, vapor holdup is a small fraction of the total holdup ($\approx$ 2%) and is neglected. Other specific assumptions are :

- constant pressure drop (5.3 mmHg/tray)
- Murphree tray efficiency of 0.4 in the stripping section
- Murphree tray efficiency of 0.5 in the rectifying section
- temperature measurement lag of 15 seconds
- composition measurement dead time of 1 minute
- compressor speed lag of 30 seconds
- heat input lag of 30 seconds
- compressor polytropic efficiency of 70%

3.4 Propylene-Propane System

The dynamic model developed for the analysis of the conventional propylene-propane column is similar to the one used for the ethanol-water system. Due to the relatively high operating pressure, vapor holdup represents about 30% of the total holdup and is therefore considered.

The computation load was reduced by an approximation. Direct vapor dynamics were neglected, but additional liquid holdup was added to simulate the impact of the vapor holdup on the column dynamics. This model gave dynamic responses to all disturbances, which were essentially the same as the rigorous vapor holdup model proposed by Choe (1985).

Prior knowledge (Finco, 1987) suggests the use of an equimolar flow model for the propylene-propane system. This simplification gives constant vapor flow in each section of the column and removes the need for energy equations. The equimolar flow model gave realistic dynamic responses to all examined disturbances except pressure changes. Pressure effects are not seen because vapor flows are not calculated from the energy balance of each tray, but are instead assumed constant throughout the column. The equimolal overflow model requires much less computation time. Table 3-1 shows how computational time is effected by these modifications.

The following assumptions were made for this system:

- constant pressure drop (5.3 mmHg tray)
- Murphree tray efficiency of 1.0 in all the trays
- composition measurement dead time of 5 minutes
- compressor speed lag of 30 seconds
- heat input lag of 30 seconds

- compressor polytropic efficiency of 70 %

Table 3-1: Simulation times

Model	computational time / real time
vapor holdup	1/10
vapor holdup as liquid	1/15
equimolal flow	1/100

Chapter 4
Controller Design Procedure

An effective control system is essential for the efficient operation of any process. In this dissertation, multiple single-input-single-output (SISO) controllers were used to regulate the processes under consideration. This diagonal controller structure performed well, so multivariable controllers were not investigated.

This chapter outlines the controller design procedure employed. It is similar to that presented by Yu and Luyben (1986) . First, incentives for dual composition control or higher order control systems (vapor recompression) were determined. Steady-state gains were evaluated and used as an aid to select manipulated variables and eliminate unworkable pairings. Via dynamic tests, transfer functions of the process were identified and the multiple SISO controllers were tuned. Finally, the stability and robustness of the closed-loop system are checked.

4.1 Control System Order

Only the two composition control loops need to be considered for the conventional column. For the ethanol-water system, these loops control the distillate and bottoms compositions (or tray temperatures related to those compositions) by manipulating reflux rate and energy input to the reboiler. Dynamics of the loops controlling liquid levels in the column base and the reflux accumulator are slow and the column pressure control loop is very fast relative to the composition control loops. Thus the dynamics of the pressure and level loops can be neglected. Heat addition (reboiler) and removal (condenser) occur rapidly relative to column dynamics and are independent of each other.

For the vapor recompression column, the pressure loop must be considered. The reboiler and condenser are linked since the condensing overhead vapors provide the energy for reboiling the column. Changes in compressor speed do not occur instantaneously. This time lag in changes introduces some sluggishness into the dynamic response. The result is that the matrix of controlled versus manipulated variables which must be considered is 3 by 3 rather than 2 by 2.

Although dual composition control results in minimum energy consumption, interaction between the two composition loops may generate closed-loop stability problems (Rijnsdorp, 1965). To quantitatively determine the need for dual composition control or a higher order control system, Luyben curves (Chapter 2) should be generated. If one of the manipulated variables is not required to change significantly in order to hold the controlled variables constant under a typical disturbance, the control system can be reduced in order.

4.2 Steady-State Indices

Once the order of the control system has been determined it is necessary to decide on a control structure and variable pairings. Indices, evaluated from steady-state information alone, are helpful in making these decisions. Performing such a steady-state analysis reduces the number of workable combinations of control structures requiring dynamic study.

Once the controlled variables are selected, the control structures depend only on the choice of manipulated variables. For a given process, selecting different manipulated variables will produce different alternative control structures. To assess the inherent resilience of alternative control structures the most widely use indices are the Morari Resilience Index (MRI) (Morari, 1983) and the condition number (Moore, 1986).

The MRI is the minimum singular value ($\underline{\sigma}$) of the plant transfer function matrix $G(i\omega)$. The set of manipulated variables that gives the largest minimum singular value over the frequency range of interest is the best. This index can also be calculated at zero frequency using the steady-state gain matrix when transfer functions are not available.

The condition number is the ratio of the largest to the smallest singular value. The larger the condition number, the more difficult it is to compute a matrix inverse which is free of errors. In terms of the control problem, a large condition number indicates that it will be difficult to satisfy the entire set of control objectives.

In this work these indices were calculated, but since the number of choices was usually limited (2x2 systems) or/and the value of the indices were often similar, engineering judgment was often used to make the selection. In other cases, many control structures were explored before a choice was made.

At present, there is no index that quantifies the best pairing; however, a negative Relative Gain Array (RGA) (Bristol, 1966) or a negative Niederlinski Index (NI) (Niederlinski, 1971) indicates an undesirable pairing. These quantities indicate either an unstable system or a system that lacks integrity.

4.3 Transfer Function Identification

Transfer functions are used to tune the multiple SISO controllers and to study the stability and robustness of the closed-loop system. Different techniques are available in the literature to identify process transfer functions.

Classical methods include step and pulse testing (Luyben, 1973). These methods require long tests for processes with large time constants and become ineffective when the process is highly nonlinear.

Statistical methods (Ljung, 1987), which usually use a pseudo-random-binary signal (PRBS) (Davies, 1972) as input and least squares to identify the parameters of the transfer function, are becoming quite popular. In general, these methods are convenient for discrete systems but require prior knowledge of the process to define the sampling period and the characteristics of the input signal.

Recently, Luyben (1987) developed a simple and easy to use procedure to obtain transfer functions. The method, a variation of Astrom's "autotune" (relay feedback) method (Astrom and Hagglund, 1984), has been named the ATV design procedure. The ATV procedure uses Astrom's method to get critical gains and frequencies for each diagonal element of the plant transfer function matrix. It requires steady-state gains (obtained via rating programs) and the dead time. Only N tests are needed for an NxN multivariable process. The transfer functions are obtained by fitting the zero frequency and ultimate frequency data. The method has worked quite well on highly nonlinear distillation columns. Some advantages of the method are: it does not need prior knowledge of the process, it is a closed-loop test, and the test duration is less than required by classical methods.

All the transfer functions reported in this dissertation have been obtained using the ATV procedure. Pulse and PRBS tests were also performed in some cases, but similar results were obtained. The ATV method was preferred because of its simplicity and accuracy.

The technique permits the identification of two parameters. The original paper (Luyben, 1987) suggests a few simple models. Due to the underdamped characteristics of the vapor recompression systems, two additional models have

been developed. These models are:

a) Second-order underdamped system

$$G(s) = \frac{K\, e^{-Ds}}{\tau^2 s^2 + 2\,\xi\,\tau\, s + 1} \tag{4.1}$$

$$\tau = \frac{1}{\omega}\sqrt{1 - \frac{K/M}{\sqrt{1 + tan(arg\, G + \omega\, D)^2}}} \tag{4.2}$$

$$\xi = \frac{-(1 - \omega^2\,\tau^2)\, tan(arg\, G + \omega\, D)}{2\,\tau\,\omega} \tag{4.3}$$

b) First order lag and second-order underdamped system

$$G(s) = \frac{K\, e^{-D\, s}}{(\tau_1\, s + 1)\,(\tau^2\, s^2 + 2\,\xi\,\tau\, s + 1)} \tag{4.4}$$

$$M = \frac{K}{\sqrt{(1 - \tau^2\,\omega^2)^2 + 4\,\xi^2\,\tau^2\,\omega^2}\,\sqrt{1 + \tau_1^2\,\omega^2}} \tag{4.5}$$

$$-\pi = -\omega\, D + arctan\left(\frac{-2\,\xi\,\tau\,\omega}{1 - \tau^2\,\omega^2}\right) + arctan(-\omega\,\tau_1) \tag{4.6}$$

where:

D	: dead time
K	: steady-state gain
G	: system transfer function
M	: magnitude ratio
$arg\, G$	: phase angle
τ	: time constant
ω	: frequency
ξ	: damping coefficient

To evaluate model b) the damping coefficient is assumed to be one and the equations (4.5) and (4.6) are solved for τ_1 and τ. If no solution is obtained, the damping coefficient is decreased until a solution is reached for τ_1 and τ. It is possible to get more than one solution. Because underdamped characteristics are seldom experience in distillation processes the solution with the biggest damping coefficient is assumed to be the correct one. All of the solutions

predict the same ultimate gain and ultimate frequency, thus the tuning will not be significantly affected by the choice of damping coefficient.

4.4 Controller Tuning

The tuning procedure is important when comparing controller structures; therefore, a common method was used. The choice for the multiple SISO controller is the BLT procedure (Luyben, 1986).

This simple procedure uses the concepts of classical maximum closed-loop log modulus (LM) from SISO systems and the stability criterion of multivariable Nyquist plot to detune equally all loops from the single-loop Ziegler-Nichols settings.

4.5 Stability and Robustness of Closed-Loop

The stability of the closed-loop system is examined using characteristic loci plots (MacFarlane and Belletruti, 1973).

Robustness is the ability of the closed-loop to remain stable despite changes in process parameters. Doyle and Stein (1981) proposed two useful measures of robustness.

$$DSO = \underline{\sigma}\left[I - (G\,B)^{-1}\right] \tag{4.7}$$

$$DSI = \underline{\sigma}\left[I - (B\,G)^{-1}\right] \tag{4.8}$$

The final variable pairing is checked for robustness by plotting DSO and DSI as functions of frequency. Singular values below 0.2 indicate a lack of robust stability that may require further controller detuning.

Chapter 5
Control of Ethanol-Water Columns

Control systems for the conventional and vapor recompression ethanol-water columns are discussed in this chapter. The procedures outlined in Chapter 4 were used to design control structures for these processes. The goal was not to obtain the "best" control structure, but rather one which was workable and illustrated the differences between the columns' dynamic responses.

5.1 Conventional Column

The design of the conventional column has been discussed in Chapter 2 and the base case summarized in Figure 2-1.

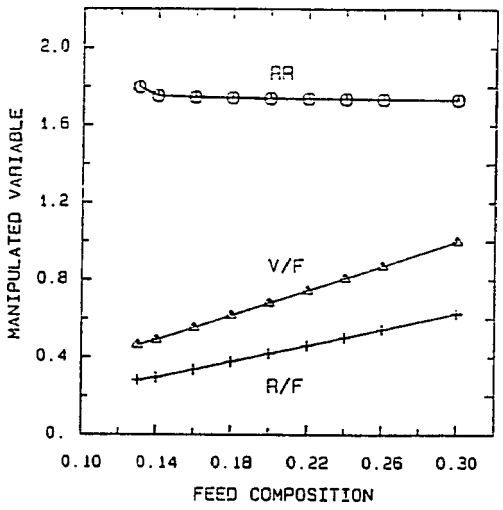

Figure 5-1: Luyben curves of the conventional column

Luyben curves of the process, plotted in Figure 5-1, were obtained to

determine the order of the control structure. The curves indicate that both vapor boilup and reflux flow must be adjusted to compensate for feed composition disturbances, while the reflux ratio remains almost constant over the range studied. This means that single-end composition control is recommended: fix the reflux ratio and control one end with heat input.

5.1.1 Single-end Control

The bottom composition is inferred from a temperature near the bottom of the column. Singular value decomposition was used to get an indication of where to place the temperature sensors to maximize sensitivity and minimize interaction (Moore, 1986). Figure 5-2 shows values of the left singular vector for each tray. The largest magnitude occurs at Tray 6, indicating that it is the most favorable location for the temperature sensor.

The temperature on Tray 6 (T_6) changes from 224.4 °F to 210.4 °F as feed composition varies from 0.14 to 0.26 with constant terminal compositions. Figure 5-3 shows the temperature effect on bottom composition when the reflux ratio (RR) is fixed at 1.8 (maximum value from the Luyben curves, Figure 5-1). It also indicates that the value of temperature selected will determine the operating feed composition range. A higher temperature allows a wider range without impairing the specified purities. Figure 5-4 shows the variations in distillate composition with changes in feed composition using a reflux ratio of 1.8 and T_6 = 221.7°F. Distillate composition varies very little over the feed composition range of interest.

The cost of working with fixed reflux ratio and controlling Tray 6 temperature is an increment in energy, which in this case is less than 2 %. The additional energy required when using the proposed control structure rather than

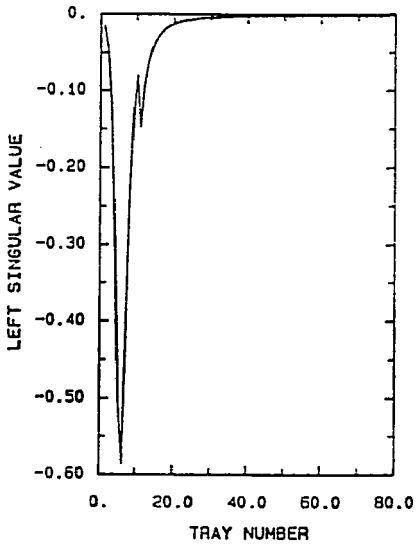

Figure 5-2: SVD analysis. Left singular values

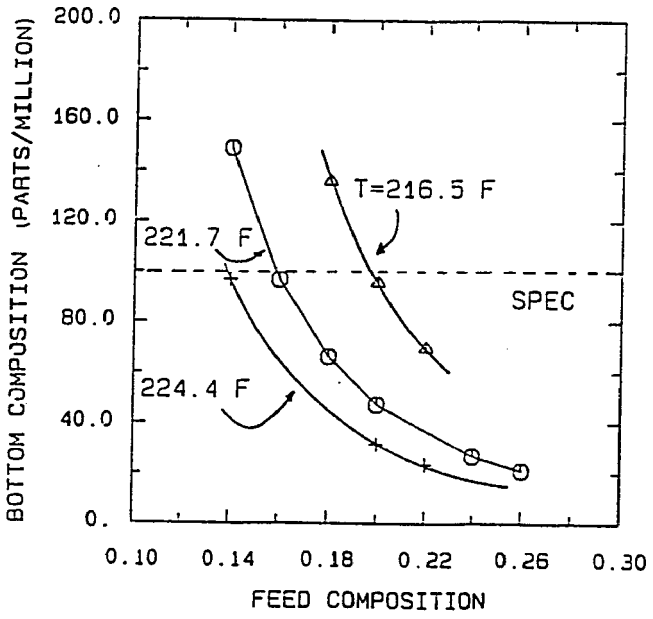

Figure 5-3: Bottom composition for reflux ratio of 1.8

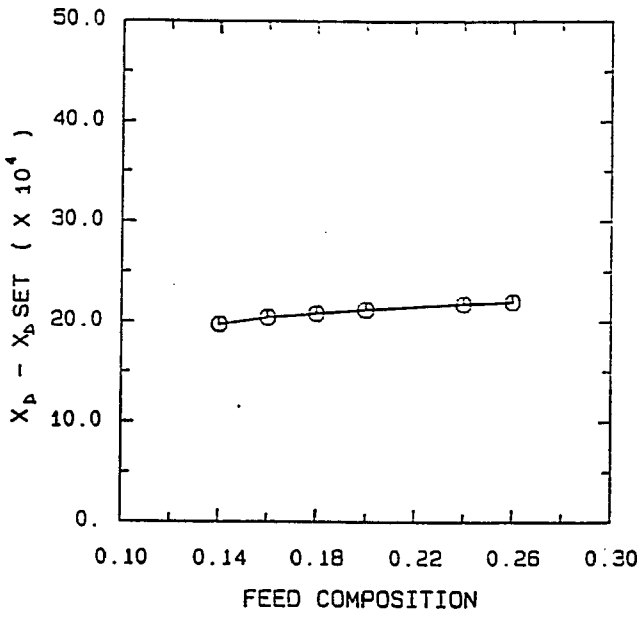

Figure 5-4: Distillate composition for RR=1.8 and T_6=221.7 °F

dual composition control is shown in Figure 5-5. The effect of Tray 6 temperature set point on distillate composition and additional energy consumption is negligible.

Figure 5-6 shows the single-end control structure selected. The following transfer function was determined using the ATV (Section 4.3) method:

$$\frac{TM(6)}{CO} = \frac{360\, e^{-0.2s}}{(1.2s+1)(590s-1)} \tag{5.1}$$

where $TM(6)$ represents the tray 6 temperature transmitter output (transmitter lag of 15 seconds) and CO is the controller output signal (valve lag of 30 seconds). Time constants and dead time are in minutes. The ATV results also

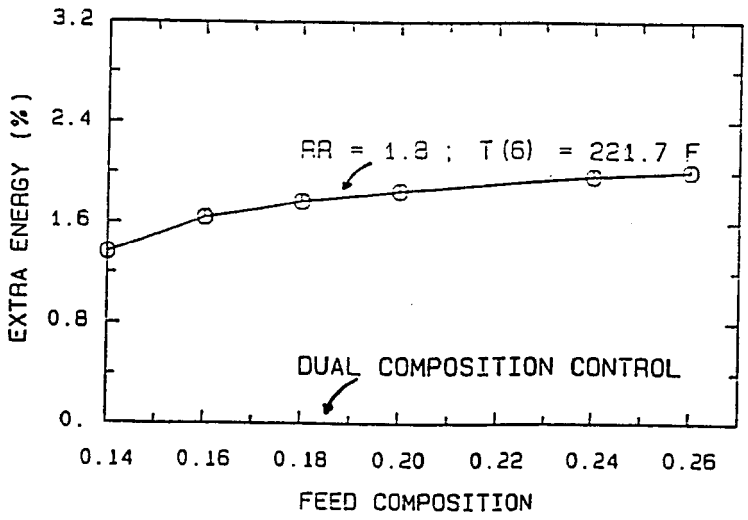

Figure 5-5: Energy consumption: single-end vs dual composition control

indicate an ultimate gain of 8.51 and ultimate period of 3.12 minutes.

For this simple SISO controller the BLT tuning criterion is used. A detuning factor of 4.8 brings the original Ziegler-Nichols tuning to a maximum closed-loop log modulus of 2.0. The final tuning uses a proportional gain of 0.8 and integral time of 12.5 minutes. Figure 5-7 shows the performance of the controller for step changes in feed composition. Distillate and bottom compositions are not directly controlled. Their response to the same disturbances is shown in Figure 5-8. These results show the ability of the control structure to keep the terminal compositions within specification.

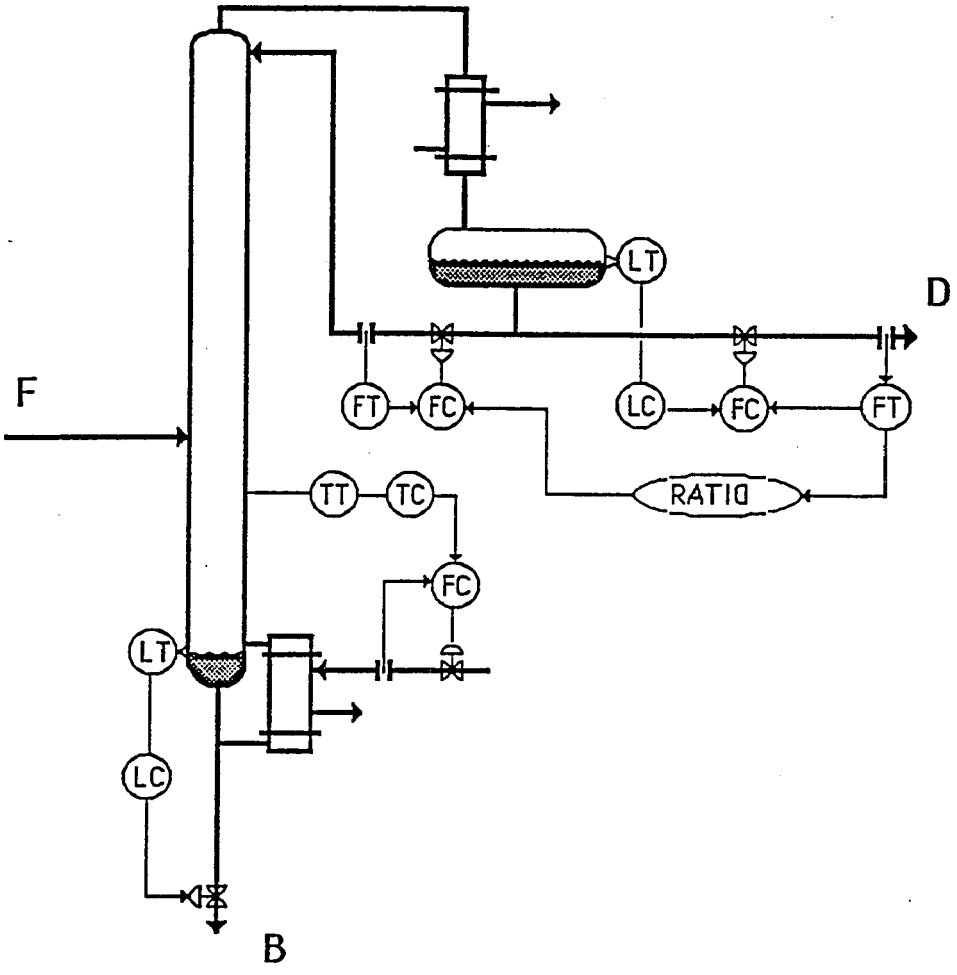

Figure 5-6: Single-end control structure

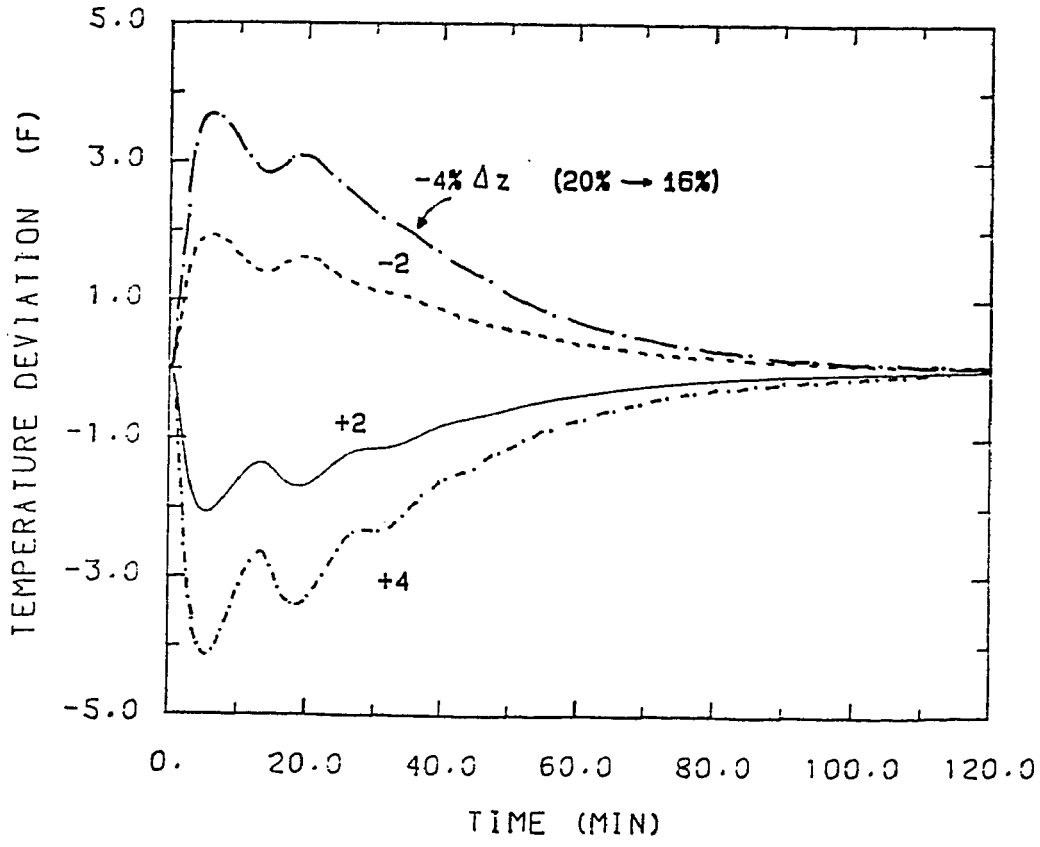

Figure 5-7: Temperature response to step changes in feed composition

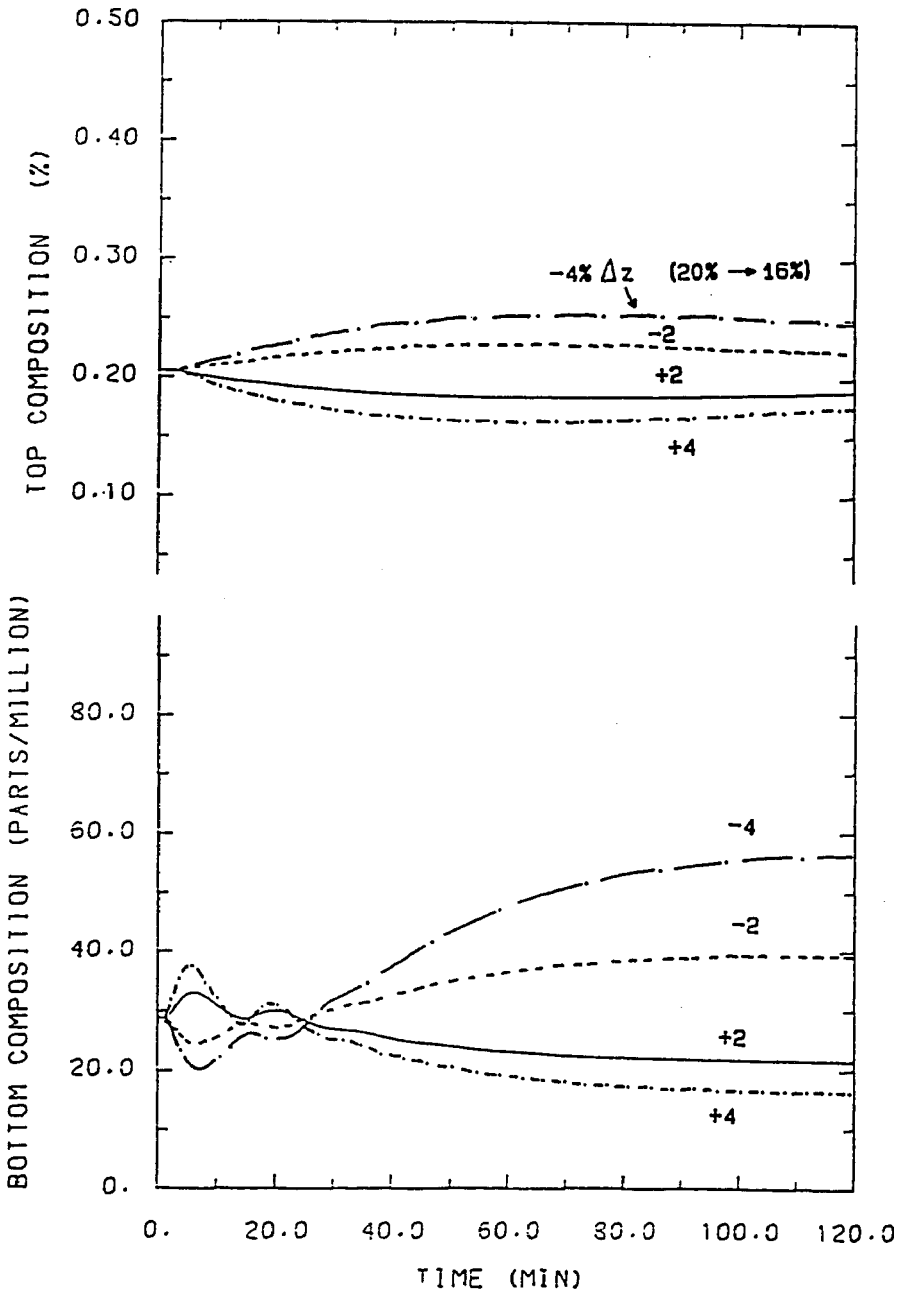

Figure 5-8: Composition response to step changes in feed composition

5.1.2 Dual Composition Control

Although dual composition is not required for the ethanol-water system, it has been examined in the interest of increasing understanding of the generic behavior of vapor recompression columns.

An analyzer is used to measure top composition instead of inferring it by temperature. This decision is based on the poor sensitivity of temperature on the top trays. Based on the singular value decomposition method, if two temperature measurements were used both of them should be located very close to the feed tray (Tray 10). Table 5-1 shows the steady-state gains of the process for different control structures. Dimensionless gains have been calculated using transmitter spans of 0.2 mole fraction for distillate composition (x_D) and 100 °F for Tray 6 temperature (T_6) and using valve gains of 2.34×10^8 Btu/hr for heat input (Q_R), 8380 lbmol/hr for reflux flow (R), 4800 lbmol/hr for distillate flow (D) and 3.5 for reflux ratio (RR).

Table 5-1: Steady-state gains $\mathbf{G_{(o)}}$ for ethanol-water system

	$G_{(o)}$	R-Q_R	D-Q_R	RR-Q_R
x_D:	g_{11}	9.5	-6.0	3.7
	g_{12}	-15.5	0.3	-5.8
T_6:	g_{21}	-438	276	-170
	g_{22}	767	42	323

Table 5-2 gives values of the RGA, Niederlinski Index (NI), Morari

Resiliency Index (MRI) and condition number for the control structures examined. The indices indicate that all possibilities are feasible. The values of the MRI are similar, therefore additional evidence is needed for rejecting any of the control structures. The condition number of the R-Q_R control structure is large but still not critical. The RR-Q_R control structure was chosen because the previous results indicate that minimum adjustment of the reflux ratio is required to keep the distillate composition within specification.

Table 5-2: Steady-state analysis of alternative control structures

control structure	variable pairing	RGA	NI	MRI	condition number
R-Q_R	x_D-R, T_6-Q_R	14.4	0.07	0.6	1550
D-Q_R	x_D-D, T_6-Q_R	0.72	1.4	1.2	230
RR-Q_R	x_D-RR, T_6-Q_R	5.6	0.2	0.6	620

The following process transfer functions were identified for the RR-Q_R control structure:

$$\begin{pmatrix} x_D \\ T_6 \end{pmatrix} = \begin{pmatrix} \dfrac{3.7\, e^{-1.2\, s}}{(6.9\, s+1)\,(162\, s+1)} & \dfrac{-5.8\, e^{-1.3\, s}}{(1.8\, s+1)\,(1190\, s+1)} \\ \dfrac{-170\, e^{-0.2\, s}}{(0.6\, s+1)\,(127\, s+1)^2} & \dfrac{323\, e^{-0.2\, s}}{(1.3\, s+1)\,(400\, s+1)} \end{pmatrix} \begin{pmatrix} RR \\ Q_R \end{pmatrix}$$

Ziegler-Nichols and BLT tuning of the diagonal controllers is summarized in Table 5-3. The characteristic loci plots of the diagonal elements shown in

Figure 5-9 indicate that the closed-loop system is stable. Figure 5-10 shows the robustness indices DSO and DSI . The curves are almost identical. The minimum value of the singular values is approximately 0.63 (-4 db) indicating that the closed-loop system is robust.

Table 5-3: Controller settings for conventional column

	Ziegler-Nichols		BLT	
Loop	K_c	τ_I(min)	K_c	τ_I(min)
x_D-RR	17.8	15.2	4.8	56.7
T_6-Q_R	3.2	2.6	0.9	9.6

The controller was evaluated using the non-linear model by introducing step disturbances in feed composition. The results are shown in Figure 5-11. A small improvement in the controller performance is obtained when dual composition control is used. The temperature loop is slightly faster than in the single-end case and the distillate composition is always on specification.

5.2 Vapor Recompression Column

The vapor recompression column operates at the same pressure as the conventional column, so to achieve a desired separation the column itself is identical. The base case design of the vapor recompression column is summarized in Figure 2-5.

The basic differences between the vapor recompression model and the conventional column are the addition of a compressor, a trim cooler and

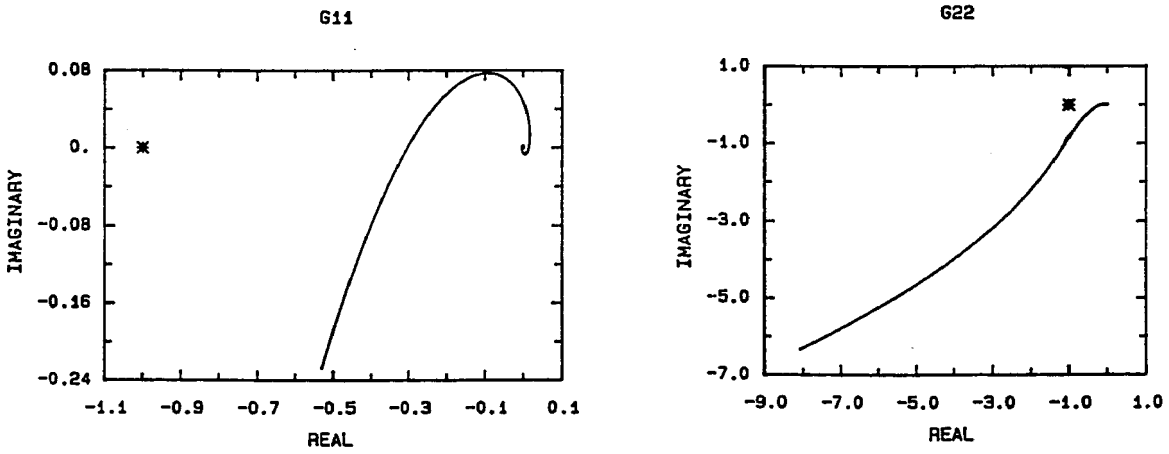

Figure 5-9: Characteristic loci of RR-Q_R control structure

consideration of pressure dynamics in the compressor suction and discharge. Open loop studies showed that the system tends to run away when disturbances occur. It appears that the compressor loop adds positive feedback into the system. For example, an increase in column pressure causes an increase in flow through the compressor and therefore an incremental increase in heat input. This produces an additional increase in column pressure. Under open loop conditions, the trim cooler is unable to compensate for this abnormality. Thus, it was necessary to control column pressure to maintain a stable system. This pressure control loop was found to be faster than the composition loops, and the interaction between the two types of loops negligible.

Because the pressure loop is essentially independent, the vapor recompression process for the ethanol-water system can be reduced from a 3x3

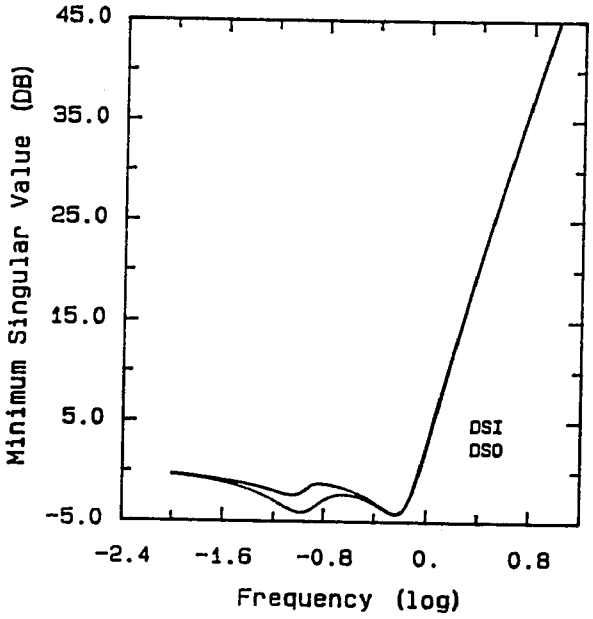

Figure 5-10: Robustness of RR-Q_R control structure

system to a single-input single-output system. The column and operating conditions are the same as in the conventional case, so a constant reflux ratio policy provides the desired control. Dual composition control was also considered to obtain results applicable to other binary mixtures requiring similar vapor recompression designs.

5.2.1 Controller Design

A control strategy similar to the conventional column can be applied to the vapor recompression column provided both columns are identical and operate at the same conditions. For the current case, the controlled variables are distillate composition (x_D) and Tray 6 temperature (T_6). The manipulated variables are reflux ratio (RR) and compressor speed (S_p).

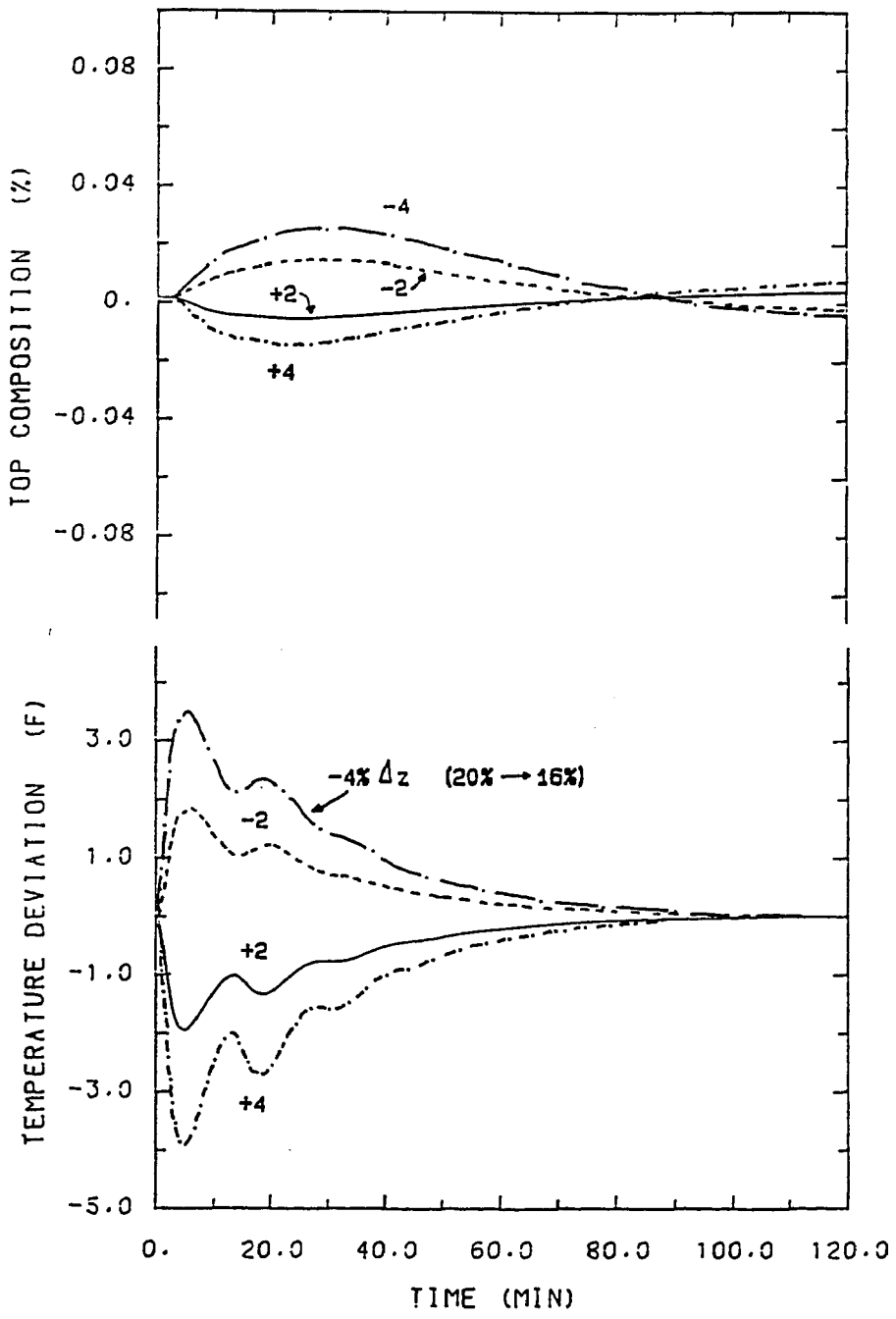

Figure 5-11: Dual composition control performance

The process steady-state gains are:

$$\begin{pmatrix} x_D \\ T_6 \end{pmatrix} = \begin{pmatrix} 1.6 & -26.6 \\ 168 & 2130 \end{pmatrix} \begin{pmatrix} RR \\ S_p \end{pmatrix}$$

For this control structure the RGA is 0.4, the MRI is 3.7 and the condition number is 580. These values indicate that the control structure is feasible. Figure 5-12 shows the control structure selected, which includes antisurge control (section 3.2).

The following are the expressions for the process transfer functions, which were identified via the ATV procedure:

$$\begin{pmatrix} x_D \\ T_6 \end{pmatrix} = \begin{pmatrix} \dfrac{1.6\, e^{-1.0\, s}}{(0.02\, s+1)(19.3\, s+1)^2} & \dfrac{-26.6\, e^{-1.0\, s}}{(0.8\, s+1)(1513\, s+1)} \\ \dfrac{168}{(0.6\, s+1)(140\, s+1)^2} & \dfrac{2130}{(1211\, s+1)(0.08\, s^2+0.6\, s+1)} \end{pmatrix} \begin{pmatrix} RR \\ S_p \end{pmatrix}$$

Table 5-4 summarizes Ziegler-Nichols and BLT tunings of the diagonal controllers. Figure 5-13 shows the characteristic loci for the system, which indicate that it is closed-loop stable. The curves for the DSO and DSI robustness indices are shown in Figure 5-14. The minimum value is 0.35 (-9 db).

To evaluate the performance of the controllers on the non-linear models, different disturbances were introduced. Figures 5-15 and 5-16 show the responses

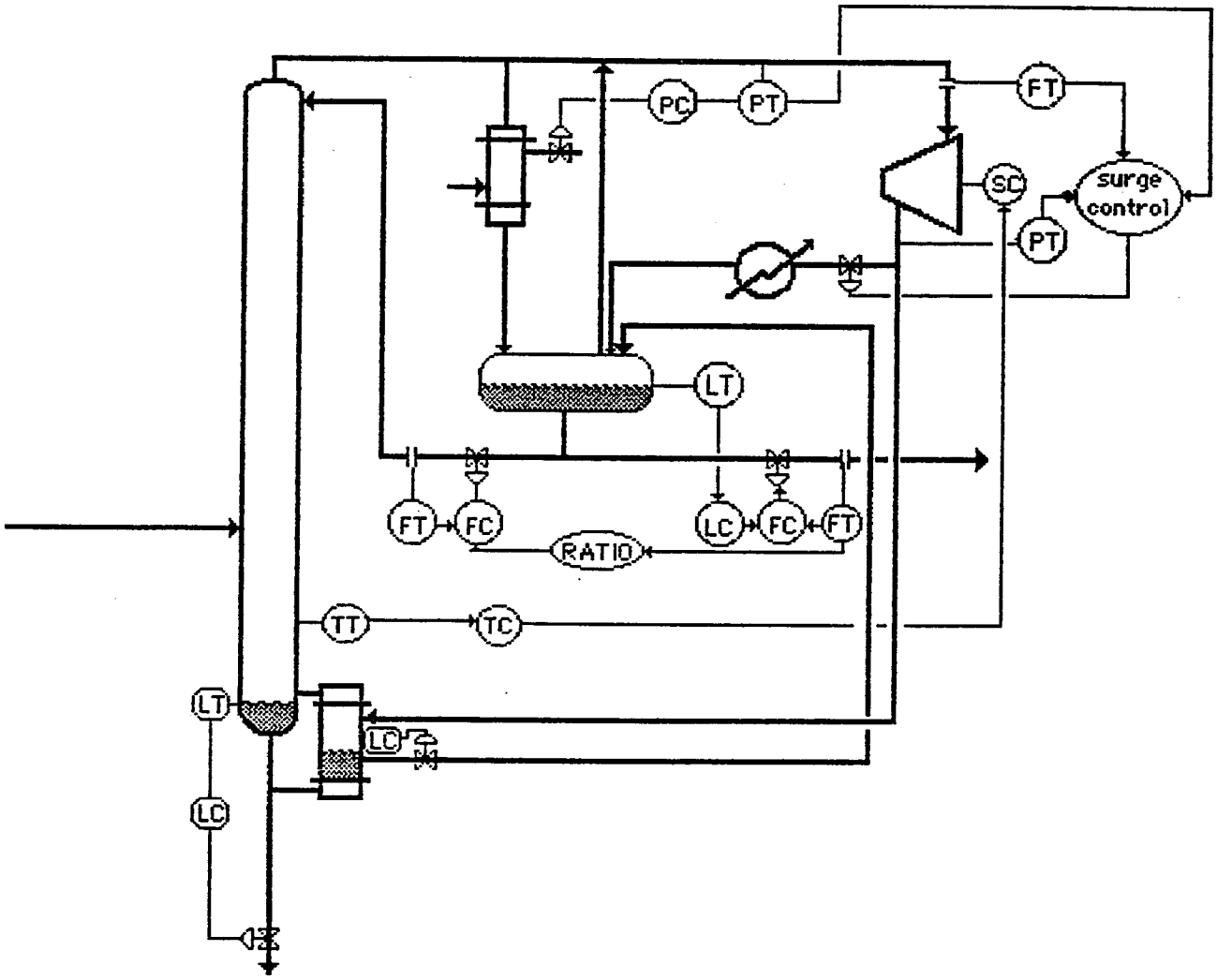

Figure 5-12: Control structure for the vapor recompression column

Table 5-4: Controller settings for vapor recompression column

	Ziegler-Nichols		BLT	
Loop	K_c	τ_I(min)	K_c	τ_I(min)
x_D-RR	11.2	16.5	5.0	36.7
T_6-S_p	1.8	1.6	0.8	3.4

of the process when feed composition and feed rate are changed. In general, the closed-loop behavior of the system is faster than in the conventional case. This behavior could be due to the effect of pressure transients (recall that pressure of the conventional column was fixed while that of the vapor recompression column varies) which have a rapid effect on the column. The smaller time delays and time constants encountered in the vapor recompression transfer functions result in smaller integral times for the controllers.

Feed rate and feed composition disturbances have a similar effect on the controlled variables. The Tray 6 temperature loop behavior is faster and more oscillatory than in the conventional column. Top composition is held almost constant.

When changes in feed temperature were made the controlled variables were only slightly affected because the feed is preheated with the top and bottom streams.

The results indicate that the control structure used in the conventional column can operate successfully in the vapor recompression column.

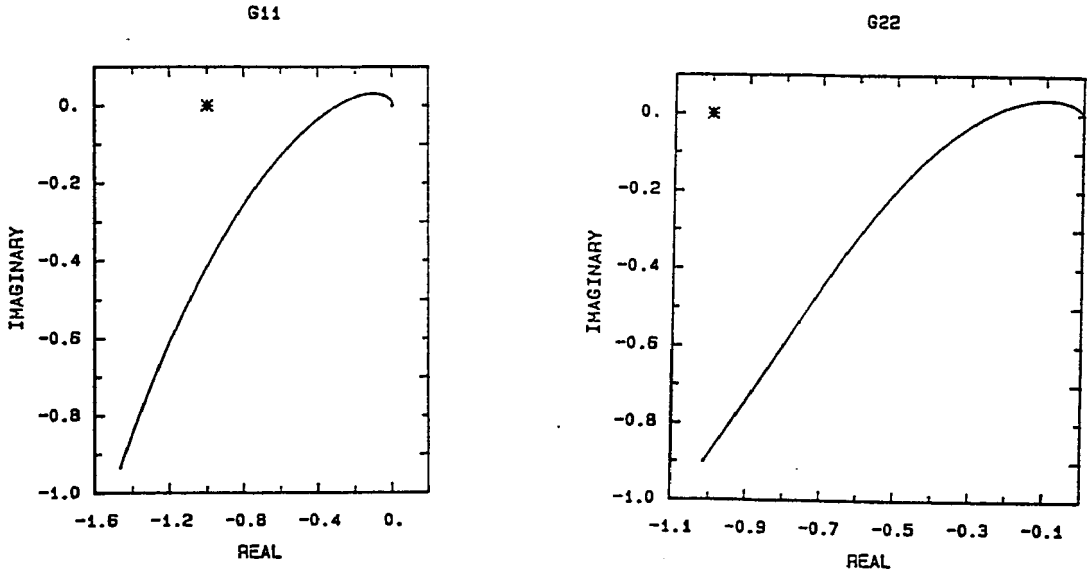

Figure 5-13: Characteristic loci of RR-S_p control structure

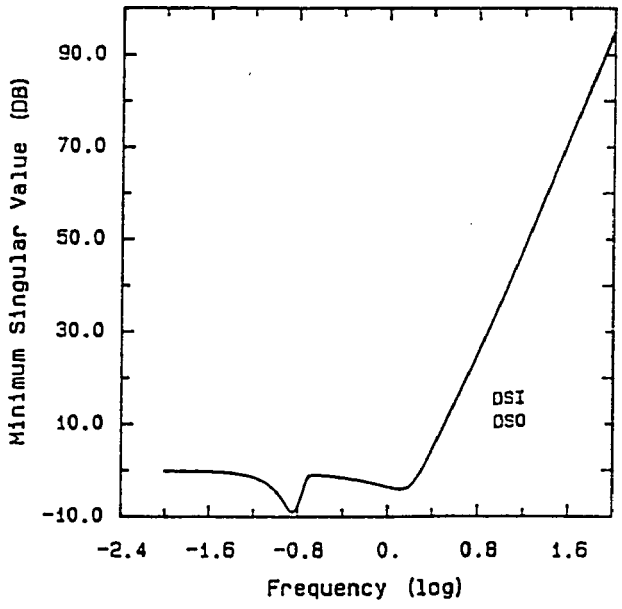

Figure 5-14: Robustness of RR-S_p control structure

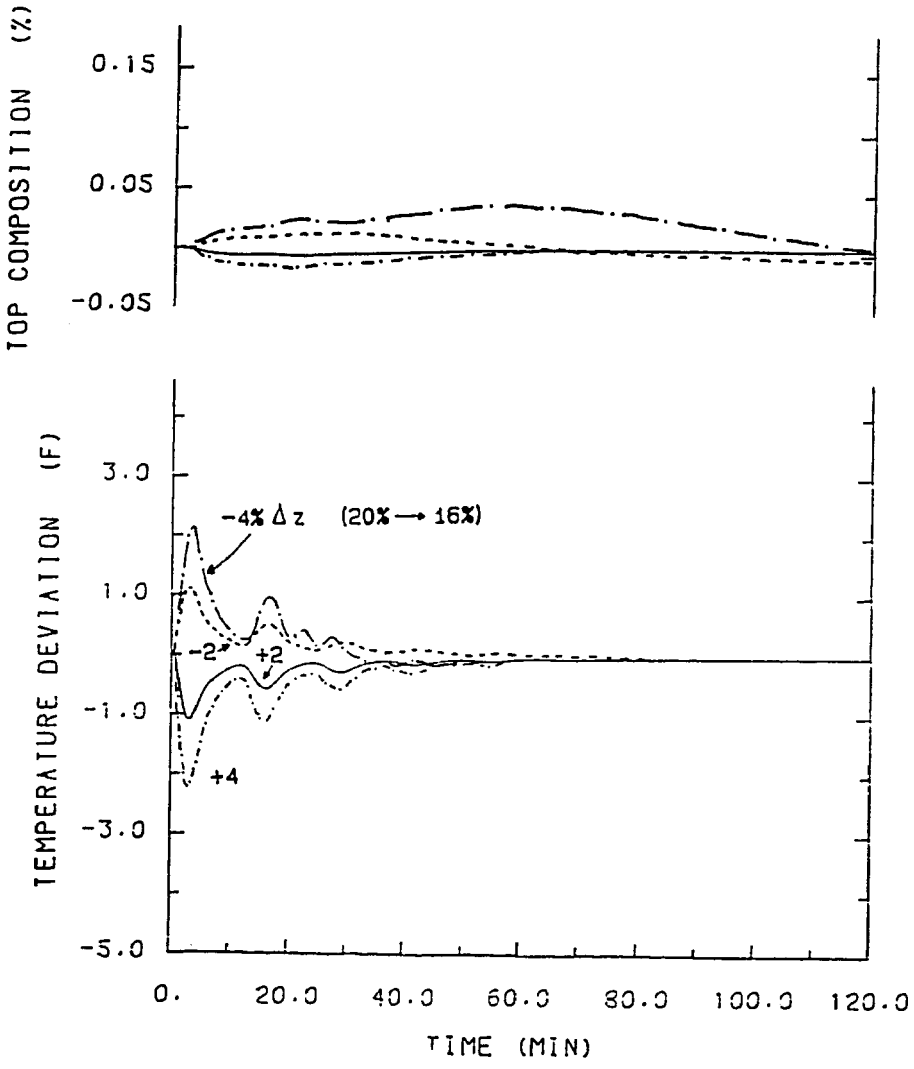

Figure 5-15: Control performance: feed composition disturbances

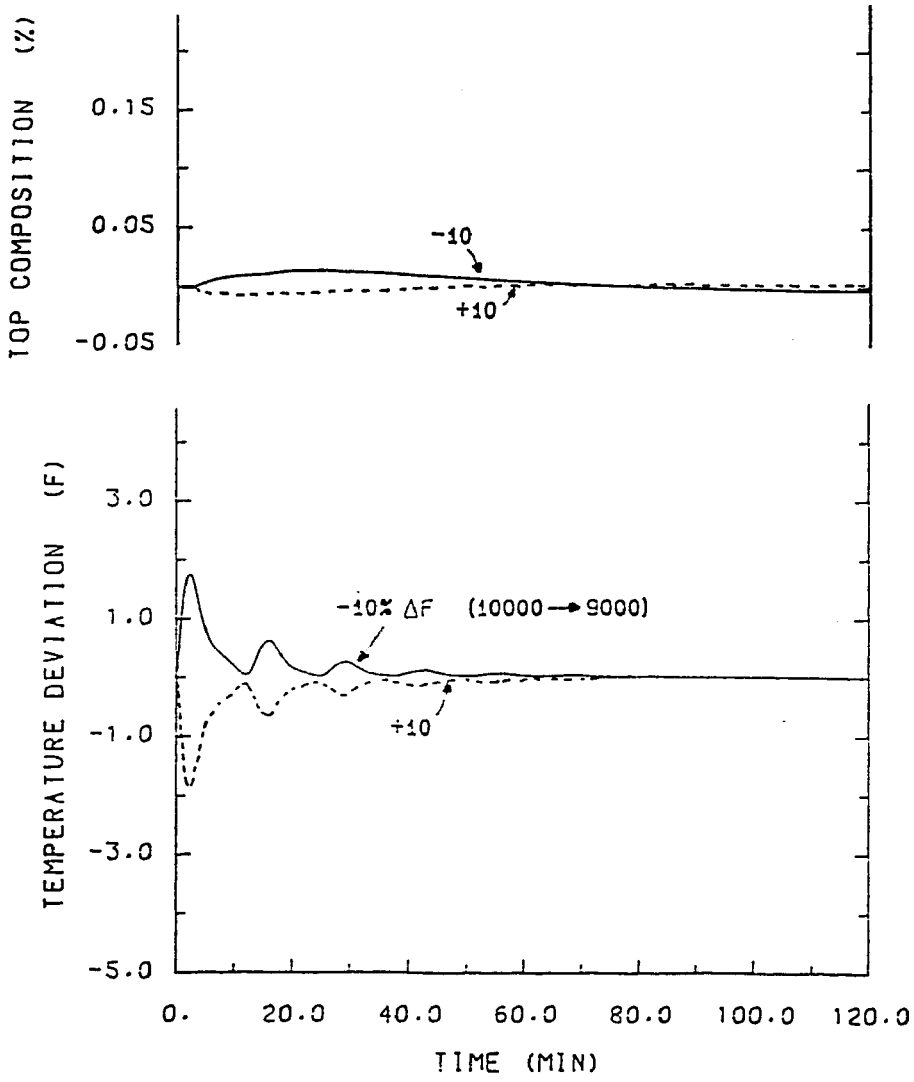

Figure 5-16: Control performance: feed rate disturbances

Chapter 6
Control of Propylene-Propane Columns

Controllers for the conventional and vapor recompression towers were designed following the procedures presented in Chapter 4.

The main characteristic of propylene-propane columns is the difficult separation resulting from the low relative volatility of the mixture. This separation requires a large number of plates. The column operates at high pressure, so that water can be used to condense the overhead vapor. The small temperature difference between top and bottom and the large number of trays make it necessary to measure compositions directly thus slowing the composition loops through the use of analyzers.

6.1 Conventional Column

The design of the conventional column has been discussed in Chapter 2 and the base case is summarized in Figure 2-6.

The incentive for dual composition control is clearly shown by the Luyben curves of the process (Figure 6-1). Vapor boilup, reflux flow and reflux ratio must be adjusted significantly to maintain the terminal composition specifications.

The controlled variables are distillate and bottoms composition. Possible manipulated variables include reflux flow, distillate flow, bottoms flow, heat input, and combinations thereof, so the number of control structures that could be considered is large. Table 6-1 shows steady-state gains for some of these alternatives. Dimensionless gains have been calculated using transmitter spans of 0.05 mole fraction for x_D and 0.2 mole fraction for x_B; valve gains of

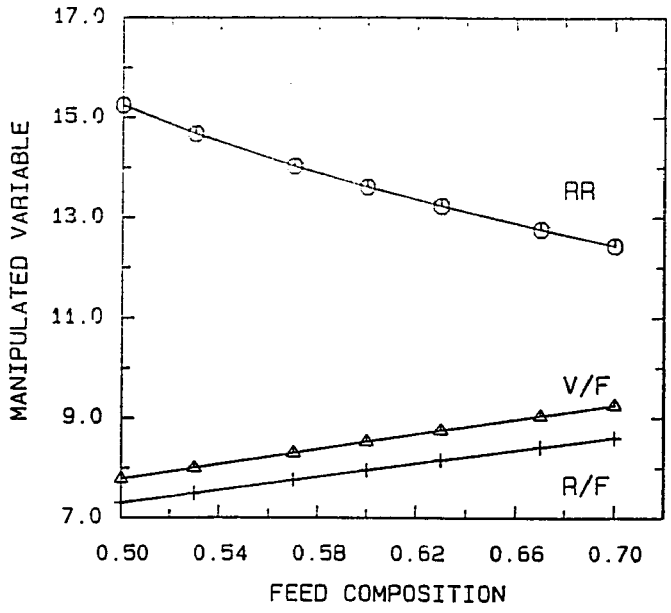

Figure 6-1: Luyben curves for propylene-propane column

5.46×10^7 Btu/hr for Q_R, 9500 lbmol/hr for reflux flow, 700 lbmol/hr for distillate flow, 500 lbmol/hr for bottoms flow, 27.0 for the reflux ratio and 2.19×10^5 Btu/lbmol for boilup ratio ($BR = Q_R / B$).

Table 6-2 lists the steady-state indices for the control alternatives considered. Since all the RGA and NI values are positive, all of the control structures are feasible. The values of MRI and condition number are similar for all structures with the exception of the R-Q_R control structure. The condition number for the R-Q_R alternative is 30 times larger than for the other structures, suggesting that controlling the process with that structure would be more difficult. This result coincides with the rule of thumb which discourages using reflux flow to control distillate composition in columns with high reflux ratio.

Table 6-1: Steady-state gains $G_{(0)}$

	$G_{(0)}$	R-Q_R	D-Q_R	RR-Q_R	RR-B	RR-BR
x_D:	g_{11}	84.76	-6.84	6.30	4.95	5.49
	g_{12}	-87.40	5.40	-1.60	1.13	-0.70
x_B:	g_{21}	135.21	-10.80	9.95	-1.76	3.10
	g_{22}	-149.40	-1.91	-12.78	9.04	-5.26

Table 6-2: Steady-state analysis of alternative control structures

control structure	variable pairing	RGA	NI	MRI	condition number
R-Q_R	x_D-R, x_B-Q_R	15.0	0.07	3.6	66
D-Q_R	x_D-D, x_B-Q_R	0.18	5.5	5.6	2.3
RR-Q_R	x_D-RR,x_B-Q_R	1.2	0.8	3.8	4.5
RR-B	x_D-RR, x_B-B	0.96	1.04	5.1	1.8
RR-BR	x_D-RR,x_B-BR	1.08	0.92	3.6	2.0

Finco (1987) studied the control of propylene-propane towers, recommending the use of the D-B control structure. Unfortunately, it is not possible to analyze this structure at steady-state. In addition to excellent performance, Finco pointed out the unconventional characteristics and the poor

integrity of this structure. The RR-BR structure is equivalent to the D-B structure assuming tight level control, but requires more complex instrumentation. The RR-Q_R, D-B and the more conventional D-Q_R structure were subjected to dynamic study for this dissertation. The different control structures are illustrated in Figures 6-2 to 6-4. To tune the level loops the following criteria were used: when the levels were controlled by external flows (distillate and bottoms), proportional only controllers were used; when the levels were controlled by internal flows (reflux and vapor rate), tight PI controllers were used.

Transfer functions of the form:

$$G(s) = \frac{K e^{-\tau_D s}}{(\tau_1 s + 1)(\tau_2 s + 1)^n}$$

have been identified for the D-Q_R and RR-BR structures using the ATV method. Dead time is mostly composition measurement time (5 minutes). Values of the transfer function parameters are shown in Table 6-3 for the different loops and structures.

To analyze the unusual D-B structure, ATV tests were tried and an ultimate gain and period were identified for D-x_D and B-x_B loops. The D-x_D loop behaves similar to the RR-x_D loop, while the ultimate gain of the B-x_B resembles the BR-x_B, but its period is half that of the BR-x_B. For the D-B structure, the tuning is the same as the RR-BR structure but with half as much reset time in the bottom loop. This tuning can be improved, but since the procedures differ, comparison with the other structures is not a fair one. Table 6-4 summarizes the settings and detuning factors for each composition

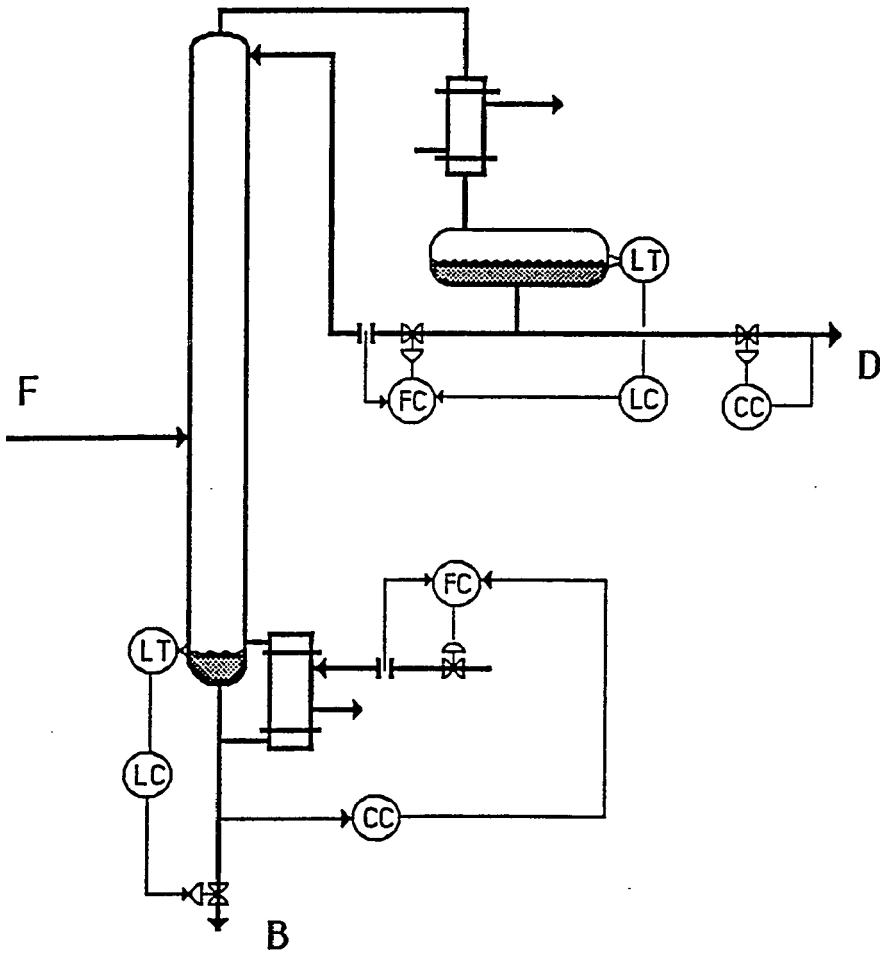

Figure 6-2: D-Q_R Control structure

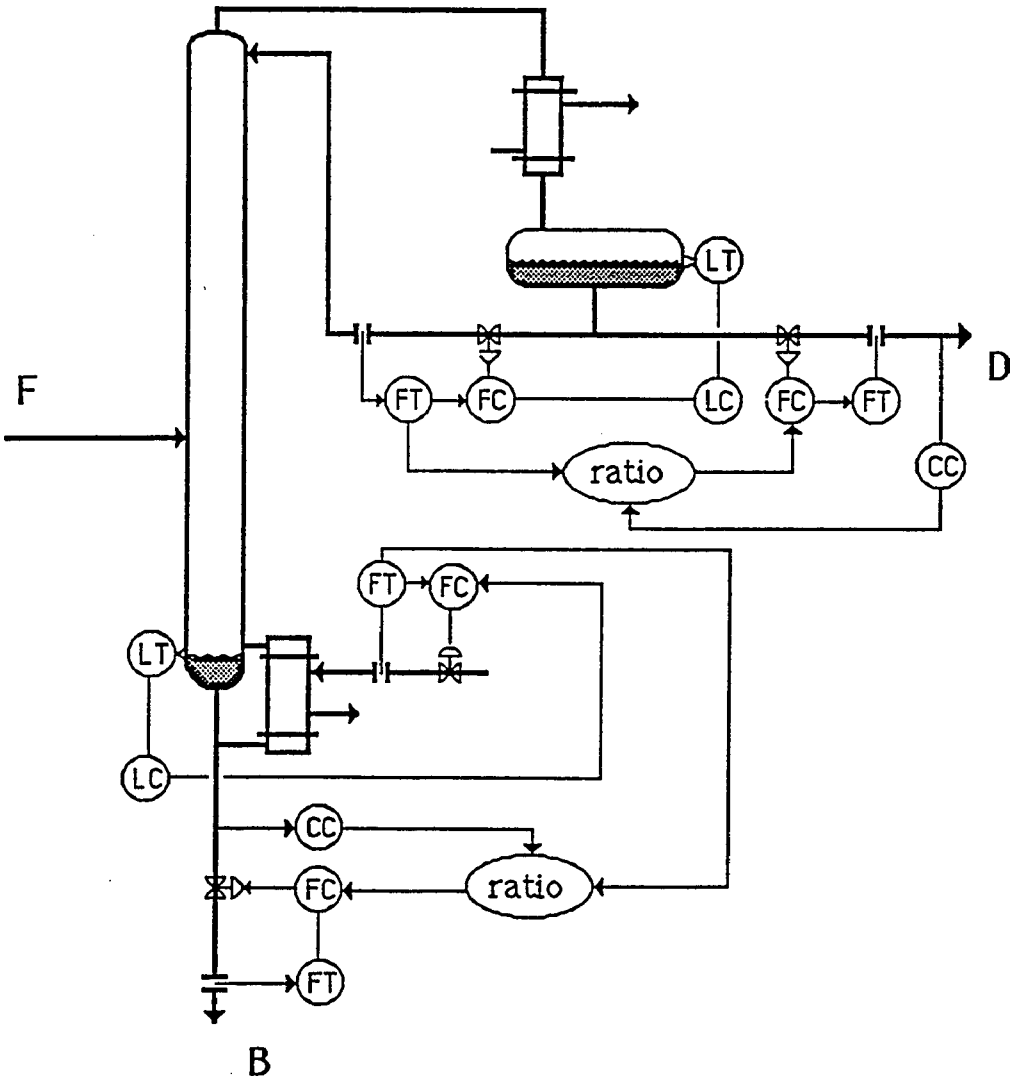

Figure 6-3: RR-BR Control structure

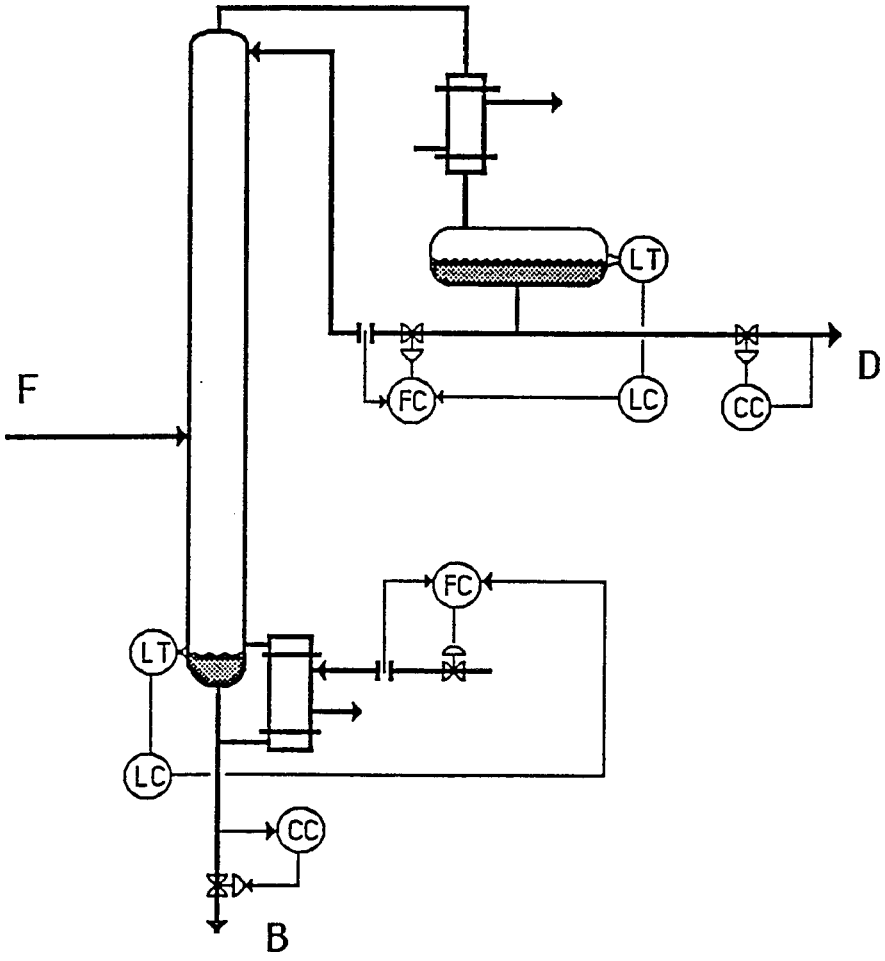

Figure 6-4: D-B Control structure

Table 6-3: Transfer function parameters

Structure	Loop	K	τ_D	τ_1	τ_2	n
D-Q_R	D-x_D	-6.8	5.0	1.6	4300	1
	D-x_B	-10.8	10.0	46	470	1
	Q_R-x_D	5.4	5.0	0.8	175	2
	Q_R-x_B	-1.9	5.0	3.2	7.2	2
RR-BR	RR-x_D	5.5	5.0	1.7	3375	1
	RR-x_B	3.1	19.0	5.3	5390	1
	BR-x_D	-0.7	5.0	1.2	3470	1
	BR-x_B	-5.3	19.0	5.2	4610	1

control structure.

The control structures are compared based on how well the composition controllers performed on the rigorous, nonlinear models. The process response to a step change in feed composition from 0.6 to 0.55 mole fraction of propylene is presented in Figures 6-5 and 6-6. Figure 6-5 illustrates the changes in terminal compositions when the D-Q_R and RR-Q_R control structures were used. Figure 6-6 shows the manipulated variable movement for both structures. The performance of the D-B structure is presented in Figure 6-7.

The results indicate that any of these control structures is able to effectively regulate the process. The performance of these structures differ less than reported by Finco, perhaps because lower purity columns were studied in

Table 6-4: Controller settings for conventional column

Structure	Loop	Gain	Reset time	Detune factor
D-Q_R	Overhead	-36	44	2.0
	Bottom	-0.4	60	2.0
RR-BR	Overhead	21	76	3.4
	Bottom	-8	270	3.4
D-B	Overhead	21	76	--
	Bottom	-8	135	--

this dissertation (Finco used 99.5% in the top and 2.5% in the bottoms).

6.2 Vapor Recompression Column

The propylene-propane mixture requires a high pressure reflux drum design for the vapor recompression column. Open loop responses to different disturbances showed that the process was stable, in contrast to the openloop instability observed in the ethanol-water system.

The base case is illustrated in Figure 2-7. Initially, the process was treated as a 3x3 system where compositions and pressure in the column were the controlled variables. The Luyben curves for reflux flow, reflux ratio and vapor boilup are similar to these presented in Figure 6-1. The use of vapor recompression introduces additional candidate manipulated variables: compressor speed and cooling water flow. Figure 6-8 shows that both these variables must be adjusted to maintain the desired set points. No reduction in the order of the system appeared to be possible.

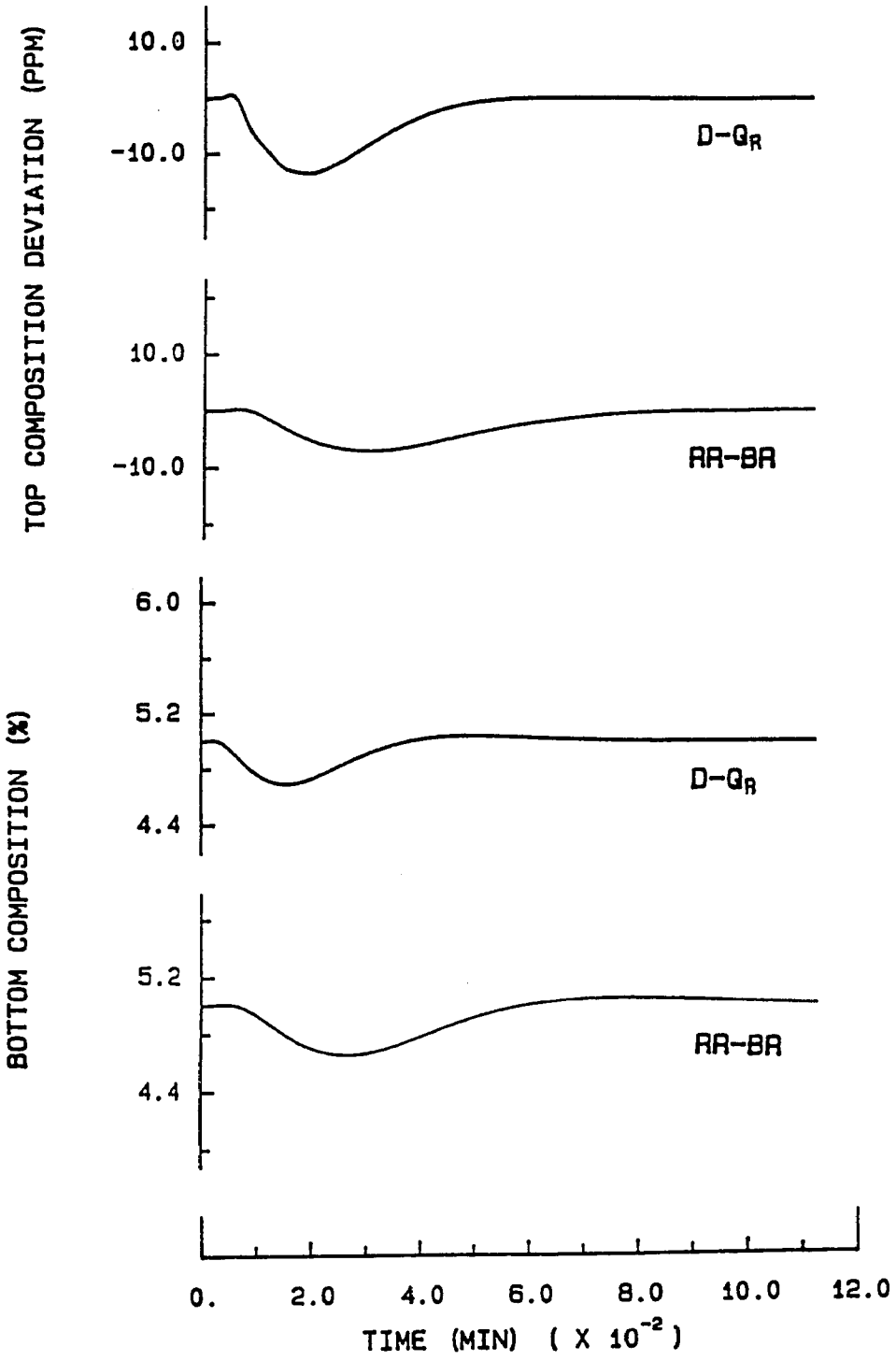

Figure 6-5: Closed-loop response of controlled variables z from 0.6 to 0.55. $x_D(\text{set}) = 0.99$. $x_B(\text{set}) = 0.05$

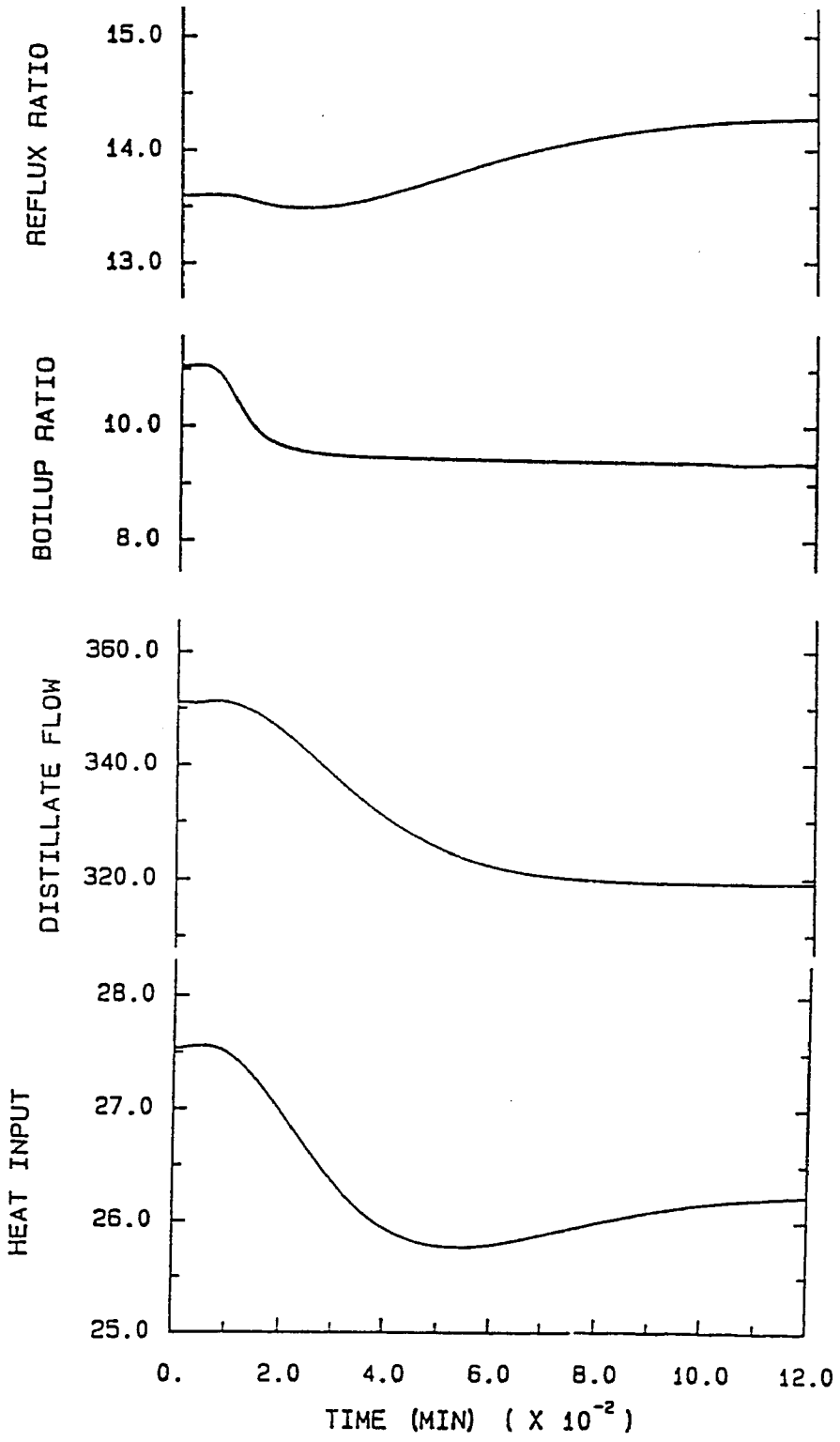

Figure 6-6: Closed-loop response of manipulated variables z from 0.6 to 0.55. $x_D(\text{set}) = 0.99$, $x_B(\text{set}) = 0.05$

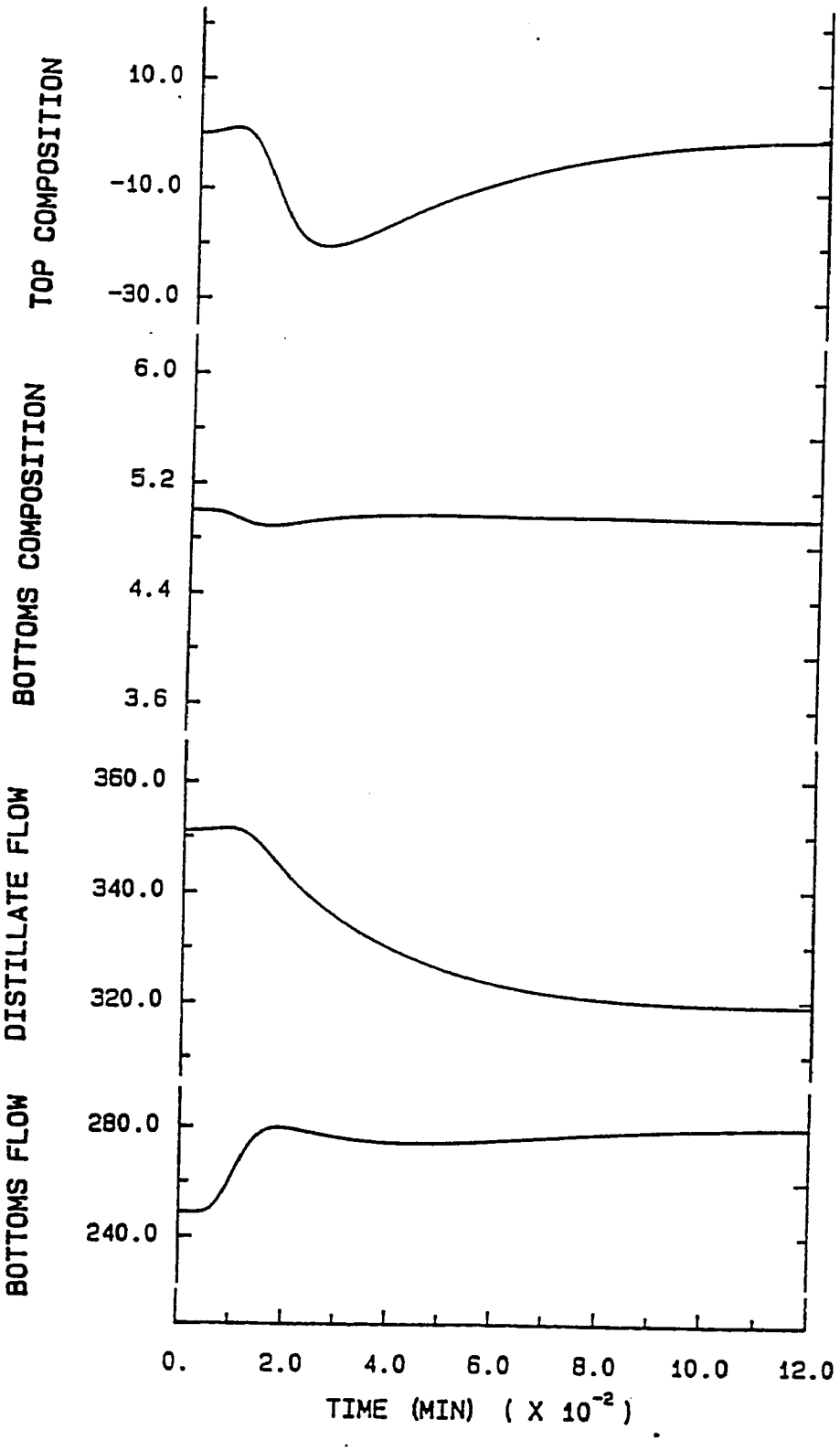

Figure 6-7: Closed-loop response of D-B control structure z from 0.6 to 0.55. $x_D(set) = 0.99$, $x_B(set) = 0.05$

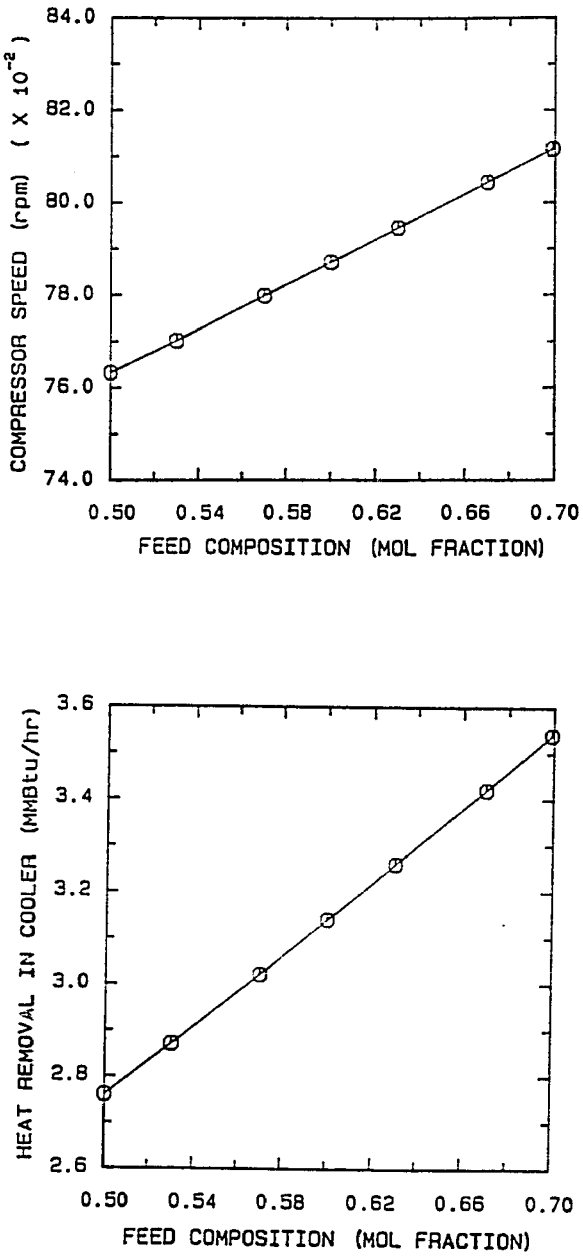

Figure 6-8: Luyben curves for the vapor recompression column

Knowledge of the conventional column was used to select a control strategy for the vapor recompression column. For the conventional column, it was found that any of the control structures considered gave satisfactory results. Since the D-Q_R structure is widely used, the vapor recompression controller design was based on a control structure that used distillate flow and compressor speed. Cooling water flow rate to the trim cooler was the third manipulated variable. For this 3x3 case the steady-state gains are:

$$\begin{pmatrix} x_D \\ x_B \\ P \end{pmatrix} = \begin{pmatrix} -9.2 & 7.9 & -0.3 \\ -10.0 & -2.8 & 0.1 \\ -0.9 & 1.0 & -0.3 \end{pmatrix} \begin{pmatrix} D \\ \text{Speed} \\ F_w \end{pmatrix}$$

The relative gain array is:

$$\Lambda = \begin{pmatrix} 0.24 & 0.89 & -0.13 \\ 0.75 & 0.26 & -0.01 \\ 0.01 & -0.15 & 1.14 \end{pmatrix}$$

The RGA indicates that the pairing is feasible. The negative values for the pairing x_D-F_w and x_B-F_w show that cooling water should not be used to control either composition. The RGA for the remaining 2x2 system (x_D, x_B; D, Speed) suggests an inversion in the pairing as in the conventional column; however the dynamics of that pairing are poor leaving only the pairing shown as the only viable alternative for this particular structure. Figure 6-9 shows the suggested control structure, including compressor antisurge control.

Dynamic studies of the process revealed that the pressure loop was much faster than the composition loops (natural period of 1.2 minutes), so the loop

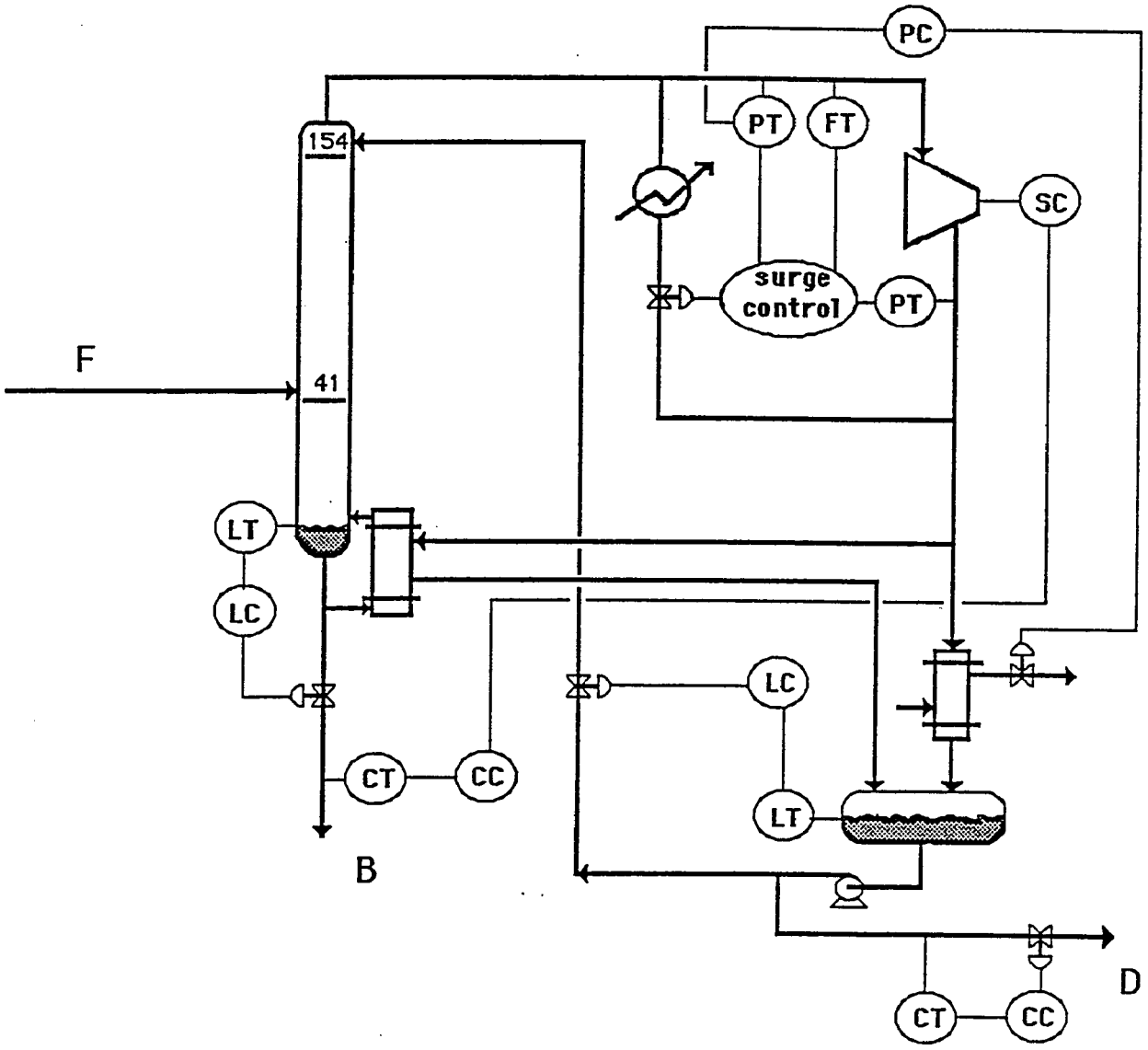

Figure 6-9: Vapor recompression control structure

was tuned independently and the order of the system reduced to 2x2.

The transfer functions of the process are:

$$\begin{pmatrix} x_D \\ x_B \end{pmatrix} = \begin{pmatrix} \dfrac{-9.2\,e^{-5.0\,s}}{(1.5\,s+1)\,(4800\,s+1)} & \dfrac{7.9\,e^{-5.0\,s}}{(7\,s+1)\,(141\,s+1)} \\ \dfrac{-10\,e^{-5.0\,s}}{(3\,s+1)\,(115\,s+1)^2} & \dfrac{-2.8\,e^{-5.0\,s}}{(4.5\,s+1)\,(14\,s^2+6\,s+1)} \end{pmatrix} \begin{pmatrix} D \\ S_p \end{pmatrix}$$

In contrast to the conventional column, the vapor recompression process has smaller dead times and underdamped characteristics in the transfer function between bottoms composition and compressor speed. The vapor recompression process responds faster because of the lower operating pressure (higher relative volatility) and because of the process itself, which has linked the heat addition and removal.

Table 6-5 gaves the Ziegler-Nichols and BLT tuning for the diagonal controllers. Figure 6-10 shows that the system would be closed-loop stable using the BLT setting. Figure 6-11 illustrates the DSO and DSI indices for robustness. The minimum value is 0.22 (-13 db), indicating that further detuning of the controller parameters is not necessary.

The performance of the control system for step changes in feed composition is illustrated in Figure 6-12. The response is slightly faster than that obtained by the conventional column. Figure 6-13 shows the manipulated variable movements, indicating that the range of controllability could be wider without running into valve saturation. These responses do not consider process constraints, which are covered in the next chapter.

Feed rate, feed temperature and setpoint changes were applied to test the

Table 6-5: Controller settings for vapor recompression column

	Ziegler-Nichols		BLT	
Loop	K_c	τ_I(min)	K_c	τ_I(min)
x_D-D	-62	21.4	-31	42.8
x_B-S_p	-0.6	27.3	-0.3	54.6

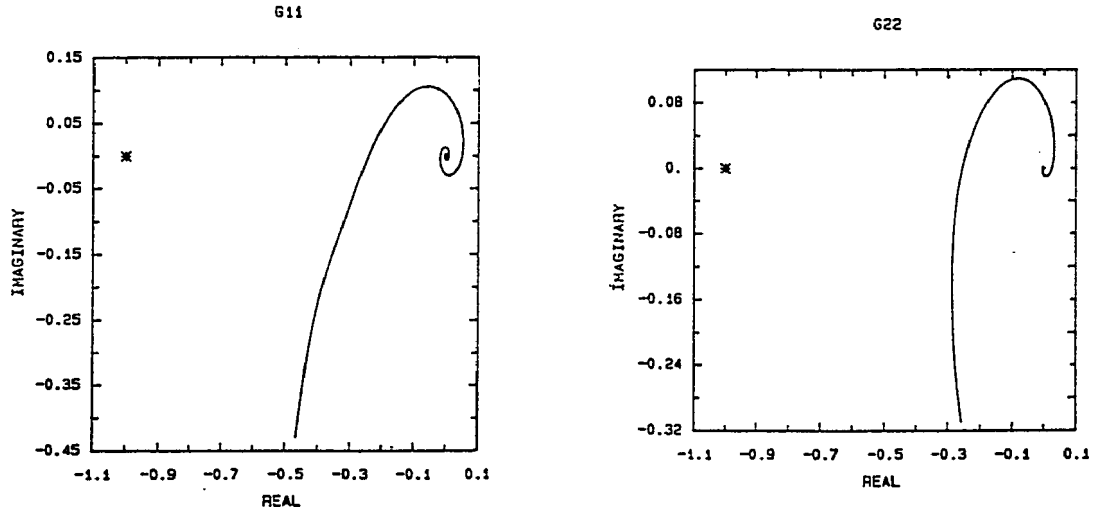

Figure 6-10: Characteristic loci for vapor recompression column

ability of the control structure to keep the compositions within specification. Figure 6-14 shows the effect of feed rate disturbances. which resembles that resulting from feed composition disturbances. The feed temperature effect is

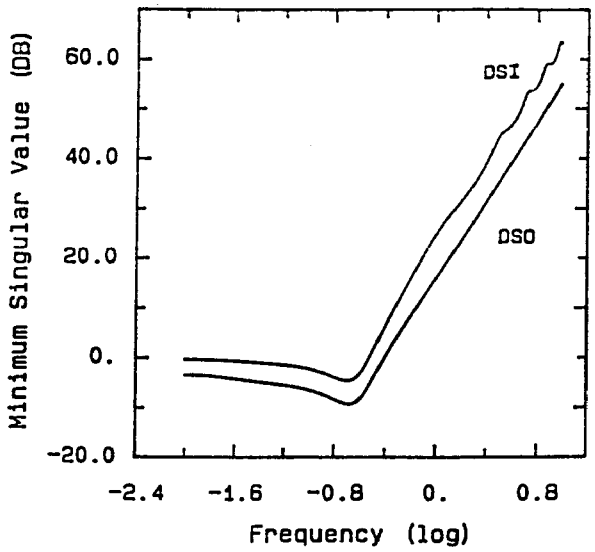

Figure 6-11: Controller robustness

negligible. It becomes more important when the temperature is lower than 90 °F, because the feed is subcooled at feed tray conditions. The response of the system to a setpoint change in bottoms composition from 5 to 3% is given in Figure 6-15. The response is particularly oscillatory for the top composition loop due to steady-state interaction between the loops. Detuning the loops can reduce the oscillation, as is shown by the additional curves in Figure 6-15. These represent new controller tunings: BLT with a log modulus of −2 db. Since the response of the bottom loop was satisfactory, detuning of the top loop only was considered. However, no improvement with respect to BLT−2 was found. To see if detuning degraded load rejection a feed composition disturbance was made and little deterioration was found (see Figure 6-16).

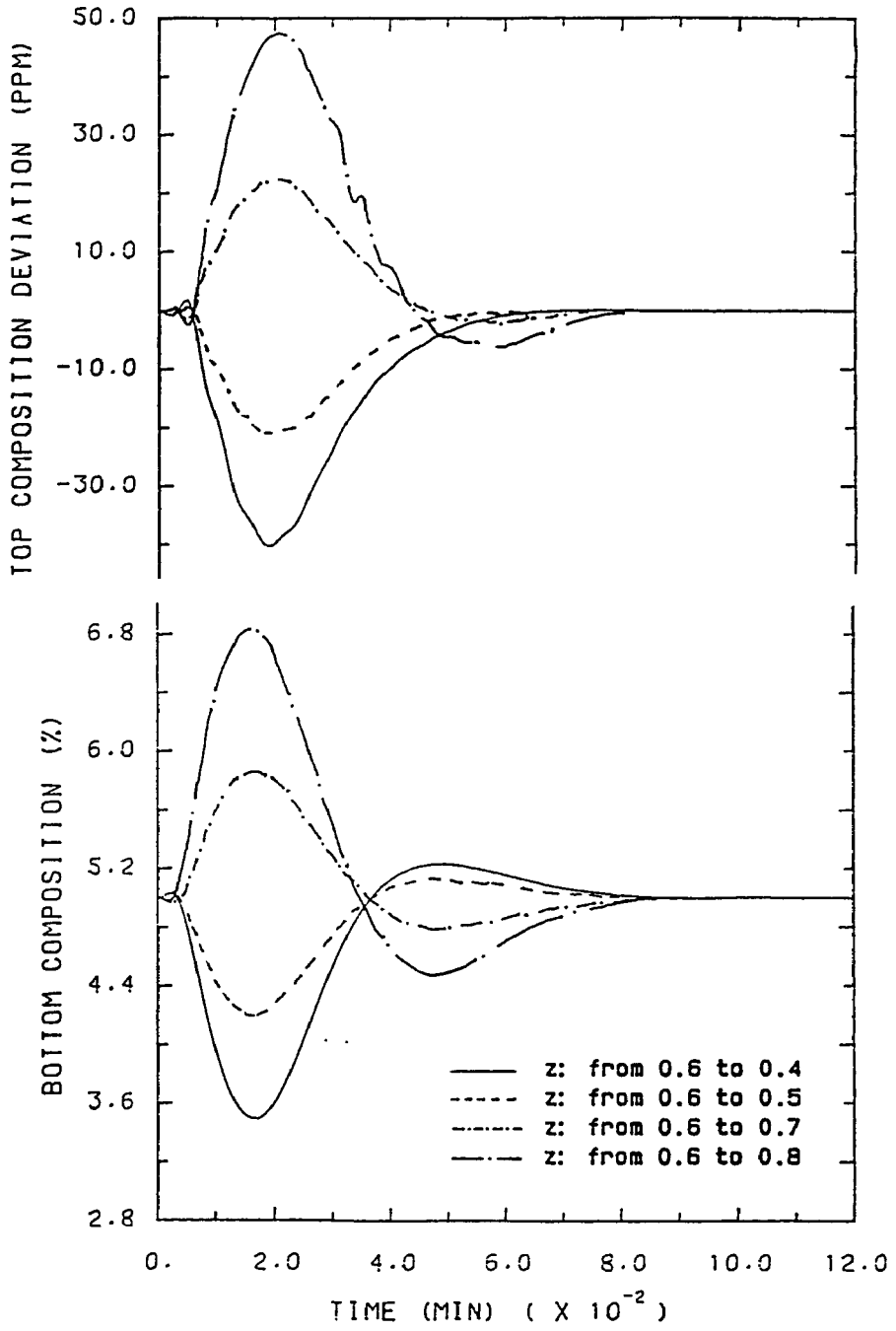

Figure 6-12: Controller performance: controlled variables

$x_D(\text{set}) = 0.99$; $x_B(\text{set}) = 0.05$

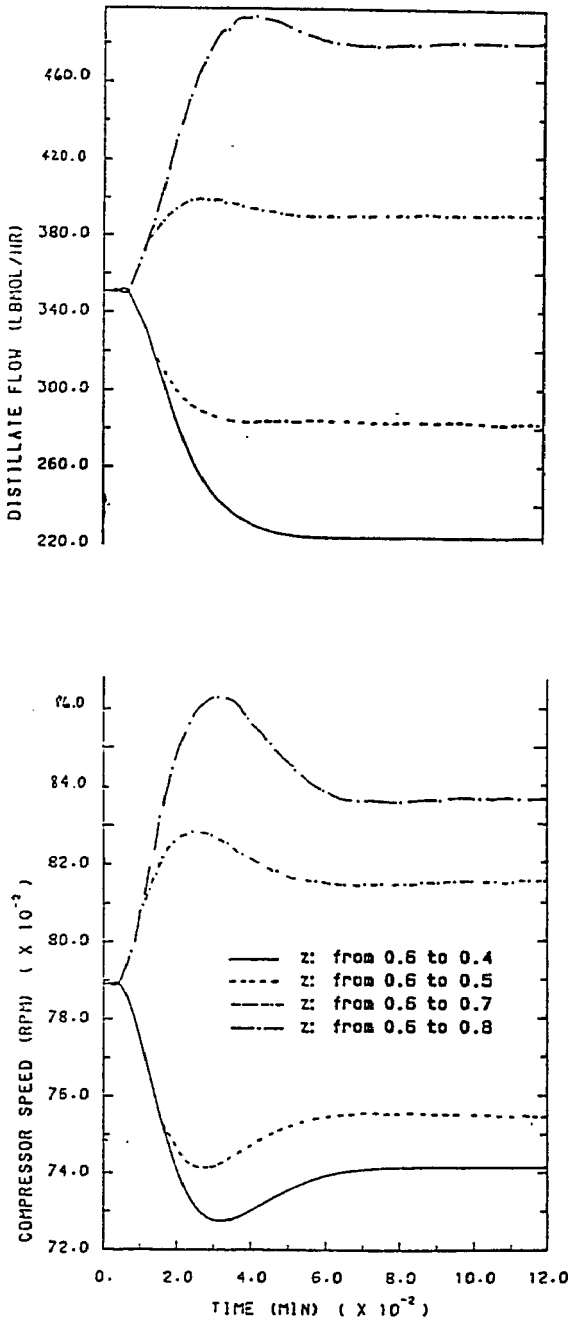

Figure 6-13: Controller performance: manipulated variables $x_D(\text{set}) = 0.99$; $x_B(\text{set}) = 0.05$

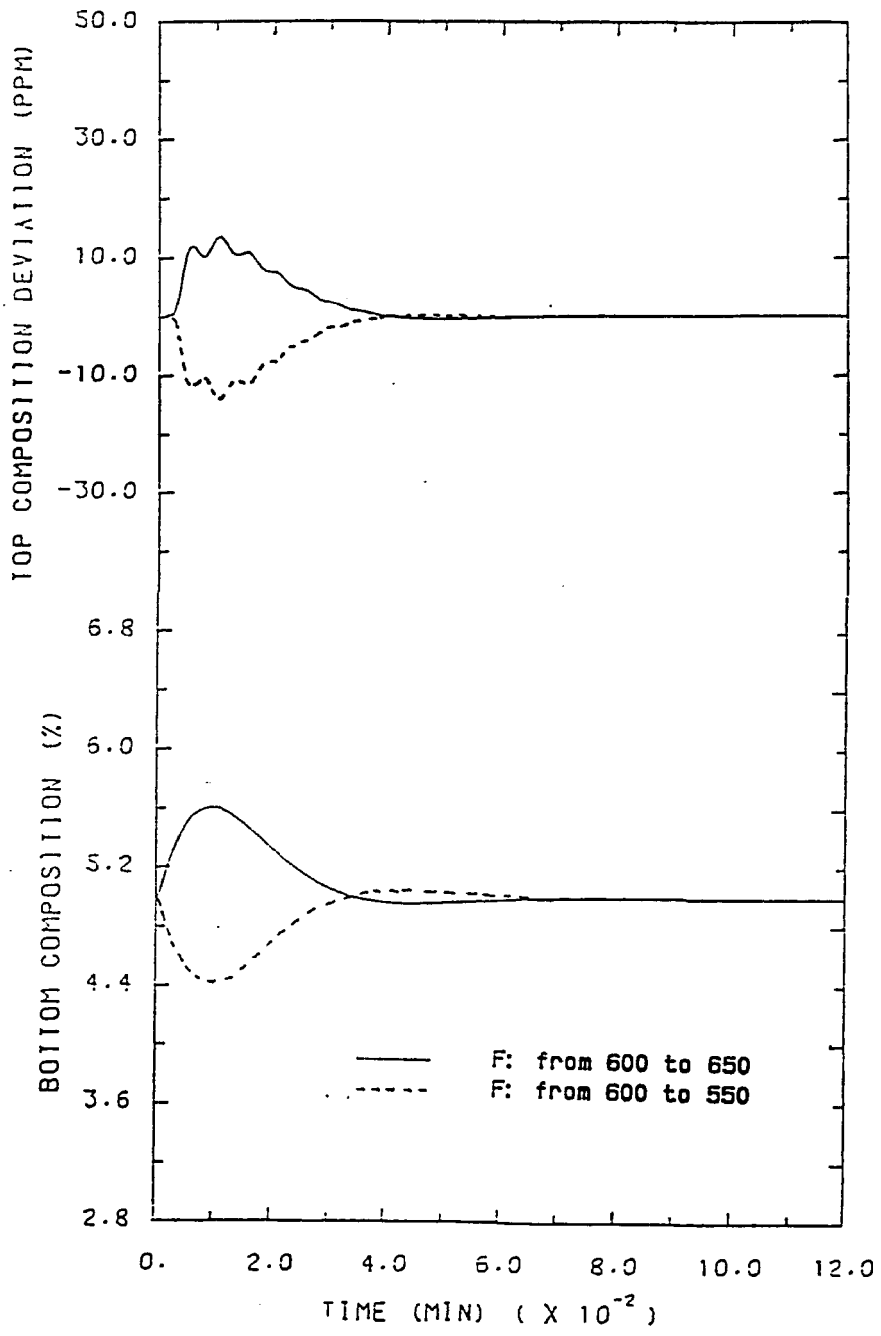

Figure 6-14: Controller performance: feed rate changes
$x_D(\text{set}) = 0.99$: $x_B(\text{set}) = 0.05$

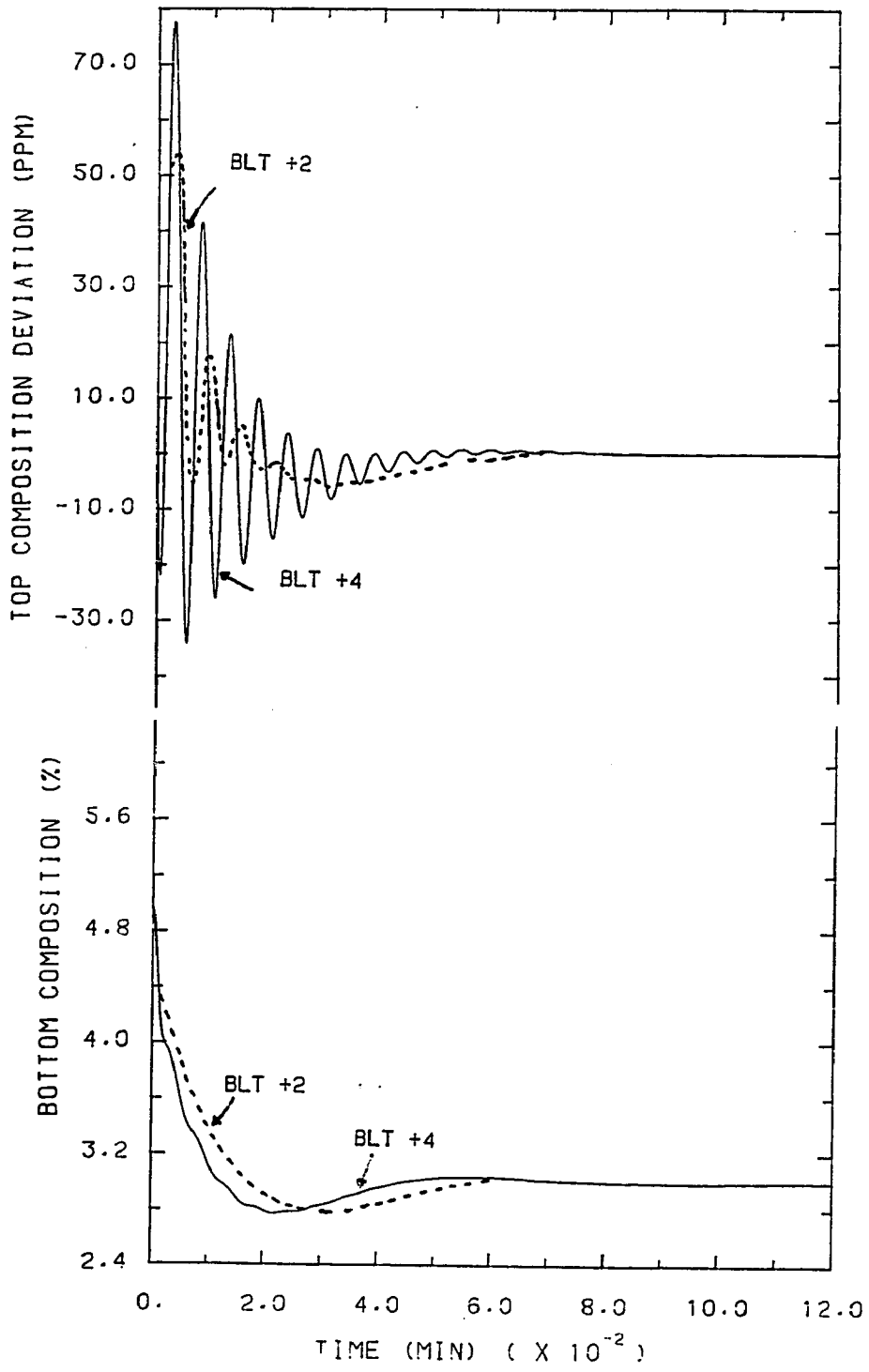

Figure 6-15: Controller performance: setpoint change $x_D(\text{set}) = 0.99$; $x_B(\text{set}) = 0.03$

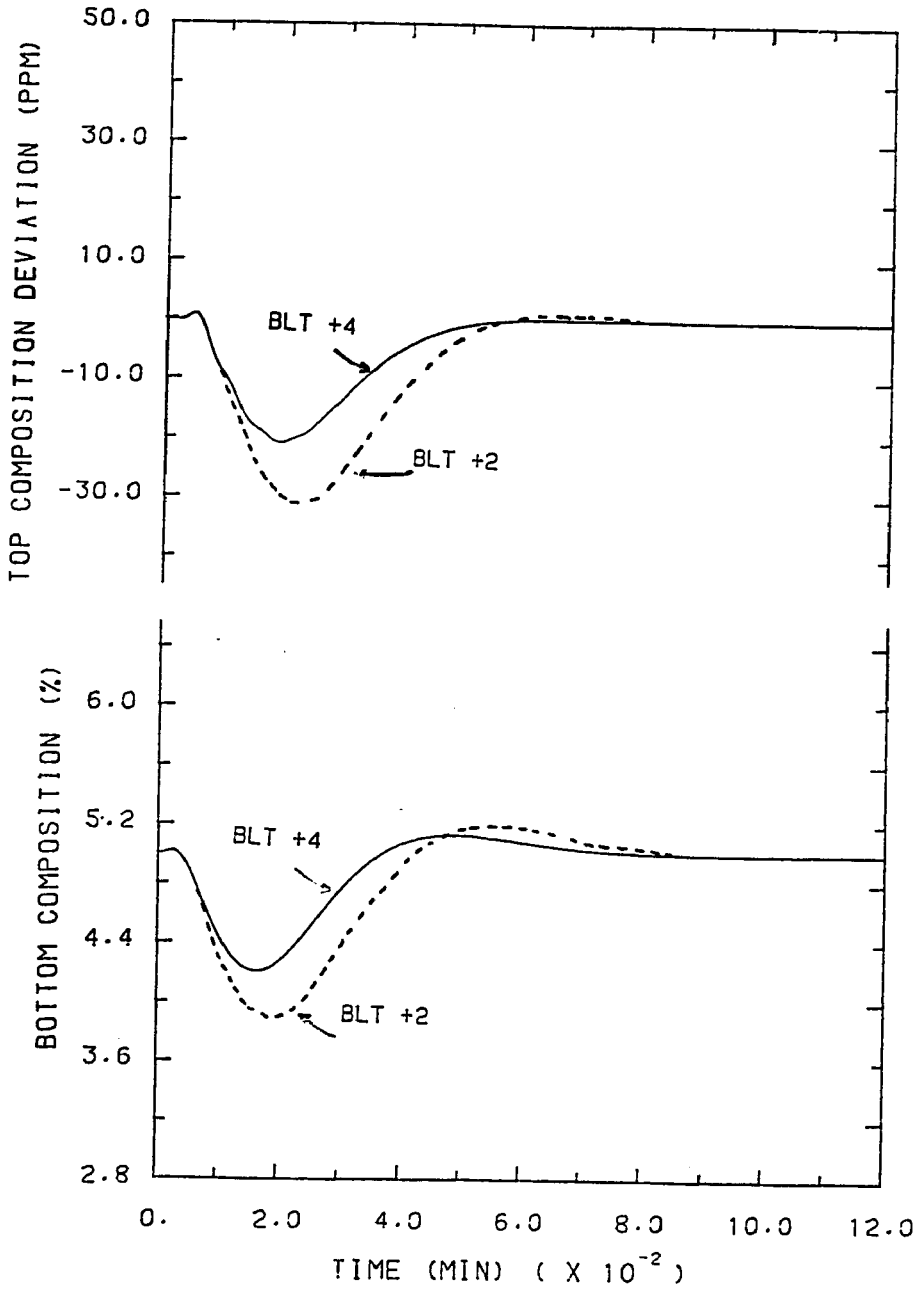

Figure 6-16: Tuning effect for feed composition disturbances z from 0.6 to 0.5. $x_D(set) = 0.99$; $x_B(set) = 0.05$

Chapter 7
Compressor Control Alternatives and Process Constraints

The effects of process constraints and alternative methods of controlling the compressor (instead of variable speed) are explored in this chapter. Analysis is based on the propylene-propane system, but should be applicable to any vapor recompression system.

7.1 Effect of Process Constraints

The economic situation determines the operating point of a plant. The plant would operate above or below the design operating point depending on the demand for the products. For the distillation column, this might cause the process to run against a physical limitation such as valve saturation, column flooding, compressor surge, etc. For example, when maximum production is the objective, column flooding, speed saturation and cooling water valve saturation constraints must be considered.

To maximize profit it is desirable to produce the product demanded using the minimum energy. In a binary column, it is typical for the purity of one product to be determined by the quality requirements of the market and that of the second by the energy cost - product value trade-off. For the propylene-propane tower it is necessary to produce propylene at 99%. The bottoms composition is set at 5% propylene because it is assumed to be the optimum. A composition higher than 5% of propylene in the bottoms means that the cost of wasted propylene exceeds the energy savings. Based on this economic criterion, when the process encounters a constraint, the first loop that should be sacrificed

is the one associated with energy.

For the propylene-propane system a constraint that hits primarily the energy loop is the one associated with changes in cooling water temperature. In summertime the cooling water valve may be completely open, so that column pressure is no longer controllable. When the cooling water temperature goes from 85 to 95 °F the pressure setpoint of 10.9 atm is no longer attainable and the column steady-state pressure increases to 11.7 atm. This higher operating pressure makes the separation more difficult because it lowers relative volatility. Figure 7-1 shows the controller performance during this type of summer operation. For small disturbances the controller performance is almost unaffected, but as the perturbation increases the distillate composition loop performance degrades some what. The loop becomes slower and the tuning tighter. It would be advisable to detune the loop to avoid the oscillatory behavior shown during summer operation. The bottoms composition loop is less affected.

Column flooding might be caused by an increase in feed rate or feed composition. An override control can be designed to prevent this situation by holding the compressor speed at a safe value. Figure 7-2 shows the control performance when the flooding override control is active. For a step change in feed composition from 0.6 to 0.8 mole fraction in propylene. the bottoms composition is no longer controllable at the desired setpoint.

It has been established that when faced with process constraints it is preferable to maintain product composition rather than pressure. Flooding velocity is a function of vapor rate and vapor density. An increase in operating pressure increases the vapor density and decreases the vapor rate. Usually this

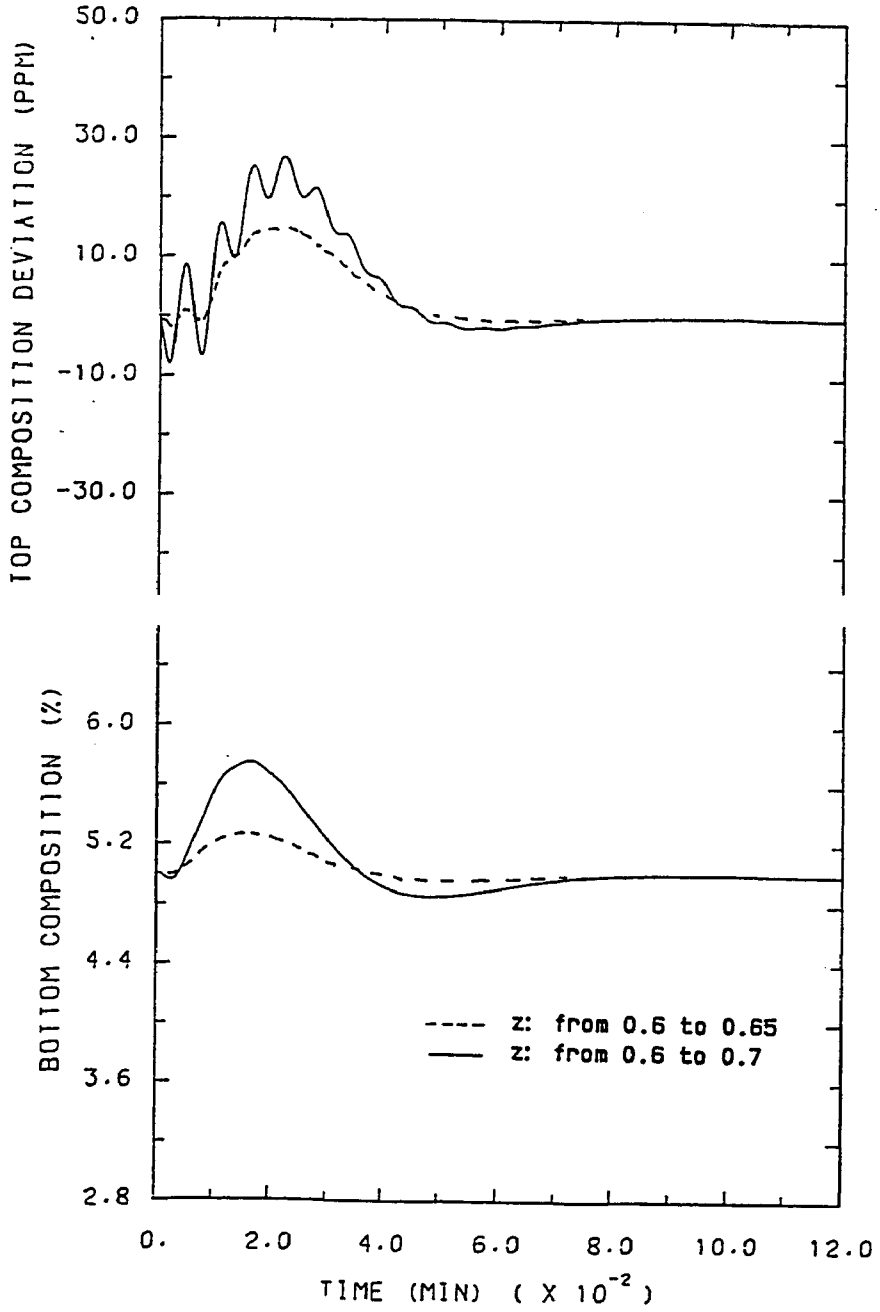

Figure 7-1: Step changes in feed composition: summer operation
$x_D(set)=0.99$ $x_B(set)=0.05$

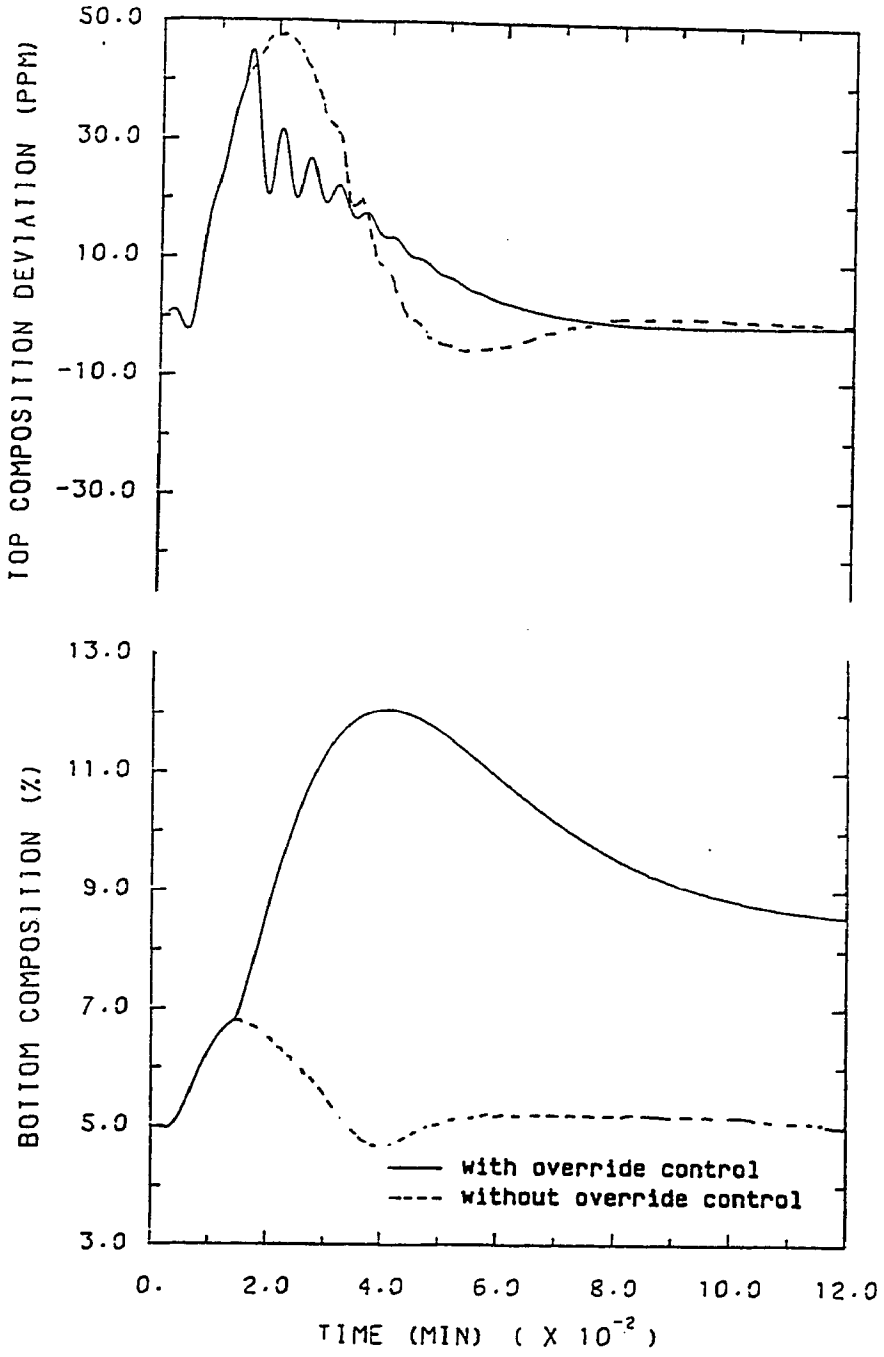

Figure 7-2: Override controller performance

$x_D(set)=0.99$ $x_B(set)=0.05$/ z: 0.6 to 0.8

change affects the actual velocity more than the flooding velocity and may remove the flooding limitations.

The effect of operating pressure was studied from a steady-state point of view. Let

A_{net} = net area (ft^2)
F_L = liquid flow (lbmol/hr)
V_V = vapor flow (lbmol/hr)
MW = average molecular weight
v = vapor velocity (ft/s)
v_f = flooding velocity (ft/s)
ρ_L = liquid density (lb/ft^3)
ρ_V = vapor density (lb/ft^3)
σ = surface tension (dynes/cm)

Then, flooding velocity is given by (Wankat, 1988):

$$v_f = K\sqrt{\frac{\rho_L - \rho_V}{\rho_V}} \qquad (ft/s) \tag{7.1}$$

where $K = C_{SB}(\sigma/20)^{0.2}$

For a tray spacing of 24 in., Wankat suggests the following correlation for C_{SB}:

$$log(C_{SB}) = -0.94506 - 0.70234\, log(F_{LV}) - 0.22618\, [log(F_{LV})]^2 \tag{7.2}$$

$$F_{LV} = \frac{F_L}{F_V}\sqrt{\frac{\rho_V}{\rho_L}}$$

Surface tension can be calculated using a correlation for hydrocarbons reported by Henley and Seader (1981):

$$\sigma = \left(\frac{\rho_L - \rho_V}{18.5}\right)^4 \tag{7.3}$$

The operating vapor velocity can be calculated by

$$v = \frac{F_V MW}{\rho_V A_{net} 3600} \qquad (ft/s) \tag{7.4}$$

Table 7-1 shows the effect of operating pressure (P) on the reflux ratio (RR), relative volatility (α), vapor density (ρ_V), surface tension (σ), vapor velocity (v), flooding velocity (v_f) and the ratio of vapor to flooding velocity when the feed composition is 0.8 mole fraction of propylene and the required bottoms composition is 0.05.

The results indicate that, for the propylene-propane system, raising the pressure does not remove the flooding constraint. This appears to be due to the high sensitivity of relative volatility (on a relative basis) to pressure in this system. As pressure is increased, relative volatility decreases which increases the reflux ratio. This increases the required molar vapor flow rate. The increase in vapor density with increasing pressure does not have a large enough effect to compensate for this higher molar vapor rate, and the result is only a small decrease in the actual vapor velocity as pressure is increased. Higher pressure decreases flooding velocity because of the higher density.

Table 7-1: Pressure effect on flooding limitations

P	RR	α	ρ_V	σ	v	v_f	v/v_f
12.0	9.95	1.200	1.69	4.97	0.83	0.77	1.08
11.5	9.76	1.202	1.62	5.15	0.84	0.80	1.05
10.9	9.55	1.206	1.55	5.39	0.87	0.84	1.03
10.5	9.41	1.208	1.50	5.56	0.88	0.87	1.01
10.0	9.25	1.210	1.43	5.77	0.90	0.91	0.99

7.2 Compressor Control Alternatives

The control strategies for vapor recompression towers presented so far have been designed using a variable speed compressor. Compressor control can be accomplished in several other ways: suction throttling, bypassing outlet flow back into the compressor suction, or varying the heat-transfer area in the reboiler-condenser using a flooded reboiler design (condensate-throttling). For the propylene-propane application the compressor is controlled to regulate heat input to the column. thus controlling bottoms composition. Figure 7-3 shows the control scheme for the bottoms composition using different compressor control structures.

In this section. compressor control alternatives are explored and the impact of the compressor characteristic curves is discussed.

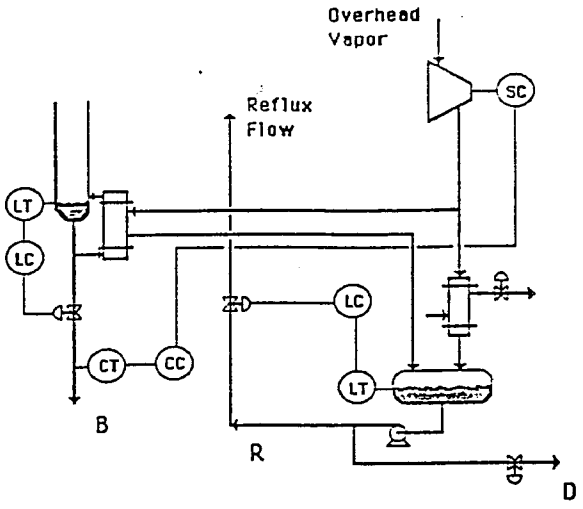

Variable Speed Control

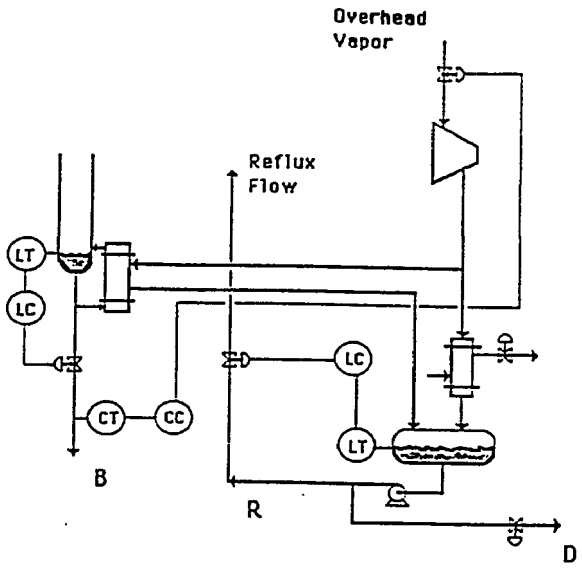

Suction Throttling Control

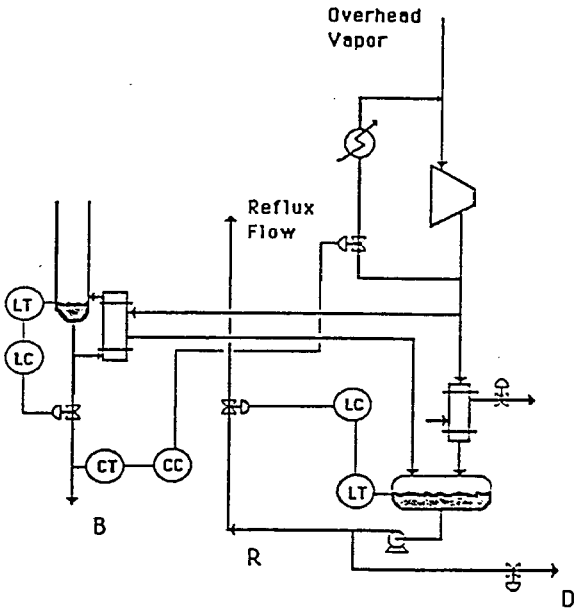

Bypass Control

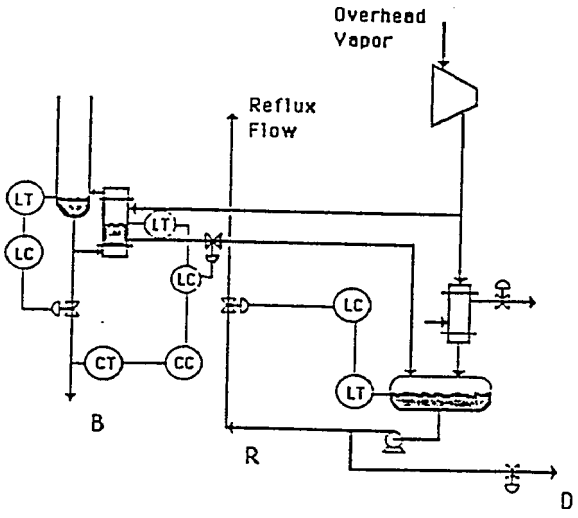

Variable Heat Transfer Area Control

Figure 7-3: Compressor control structures

7.2.1 Plant Characteristic Curve

In order to analyze the effect of the compressor control alternatives and the compressor characteristic curves on the process, the plant characteristic curve is needed. It was obtained using a steady-state rating program. The column feed rate was varied while the compositions were held constant to see the result of changing the compressor throughput.

Figure 7-4 illustrates the base compressor characteristic curves given by Equations 3.7 to 3.9 as well as the plant characteristic curve. Figure 7-5 shows the use of steeper compressor characteristic curves.

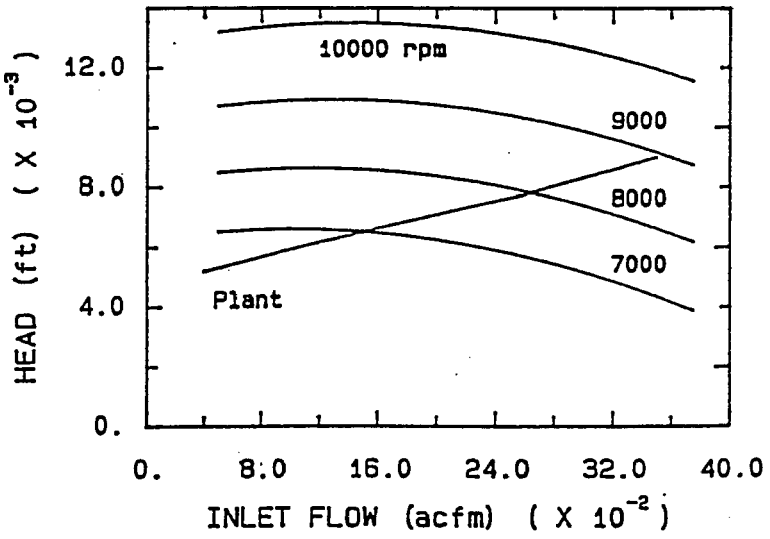

Figure 7-4: Basic compressor characteristic curves

It is interesting to note that the plant curve displays a unique quasi-linear relationship between head and compressor flow, instead of the typical upward sloped quadratic shape. Also unusual is the fact that when the throughput of

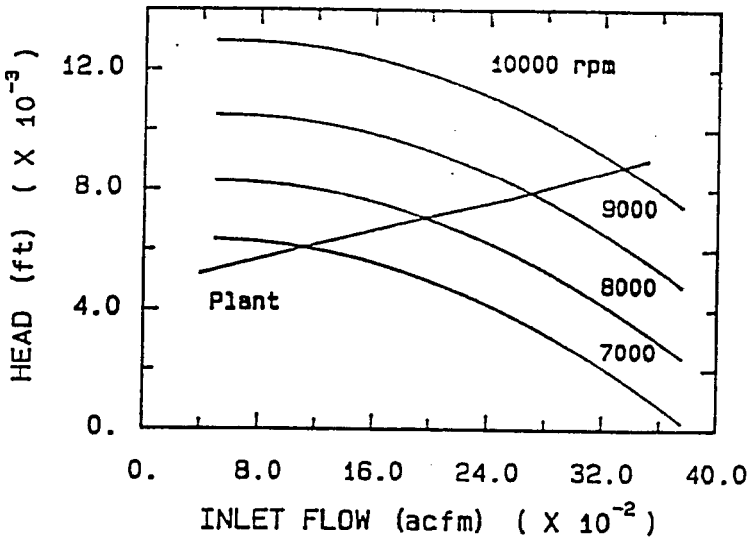

Figure 7-5: Steeper compressor characteristic curves

the compressor tends to zero the head tends to a nonzero value.

The same type of relationship is found between pressure difference across the compressor and compressor flow (see Figure 7-6). This behavior can be explained by the fact that the plant curve is determined by heat addittion and removal in the reboiler-condenser, which is given by:

$$Q = U\,A\,(T_{RC} - T_B) \tag{7.5}$$

where:

A : area of the reboiler-condenser (ft^2)
Q : heat addition/removal (Btu/hr)
U : heat transfer coefficient (Btu/ft^2 °F hr)
T_{RC} : saturated temperature at discharge pressure (°F)

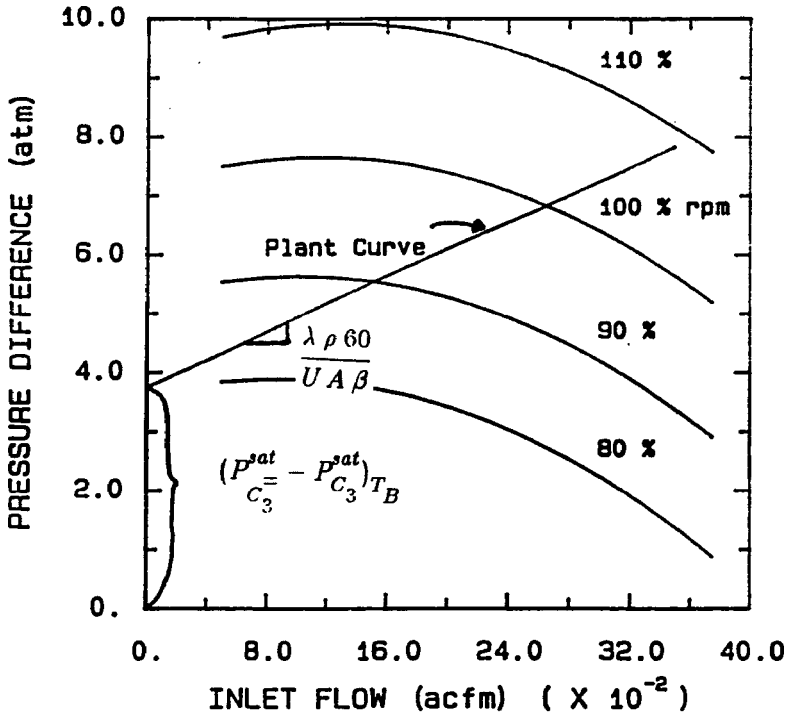

Figure 7-6: Generic vapor recompression plant curve

T_B : bottoms temperature (°F)

From the compressor discharge side the heat is given by:

$$Q = \lambda \rho 60 V \tag{7.6}$$

where:

λ : latent heat (Btu/lb)
ρ : suction density (lb/ft^3)
V : suction flow (ft^3/min)

For the small range over which discharge pressure changes, a linear relationship between saturated pressure and temperature can be assumed:

$$T_{RC} = \alpha - \beta P_d \tag{7.7}$$

Then, the discharge pressure can be calculated from:

$$P_d = \frac{\lambda \rho 60}{U A \beta} V + \frac{T_B - \alpha}{\beta} \tag{7.8}$$

or the pressure difference by:

$$P_d - P_s = \frac{\lambda \rho 60}{U A \beta} V + \frac{T_B - \alpha}{\beta} - P_s \tag{7.9}$$

It can be seen that the intercept of this linear relationship is nothing else that $(P^{sat}_{C_3} - P^{sat}_{C_3})_{T_B}$ for this system, because the heat would be zero when T_{RC} is equal to T_B. This expression is a generic relationship that provides the plant characteristic curve of any vapor recompression system.

The physical properties predict values of 0.0014 and 3.72 for the slope and intercept of this relationship. Fitting the data obtained from the rating program which uses a rigorous model the values are 0.0012 and 3.75.

7.2.2 Variable Speed

Compressor speed is adjusted to compensate for process disturbances. Figure 7-7 shows how the compressor speed must change to maintain compositions when additional heat is required by the column. The operating point moves to a higher speed curve. increasing the flow and head of the compressor. To analyze the effectiveness of the variable speed control structure different sizes of feed composition disturbances were introduced into the dynamic nonlinear model. Figure 7-8 shows the maximum peak of the dynamic compressor speed responses and the final values (steady-state) required to keep bottoms composition within specification when feed composition disturbances

occur.

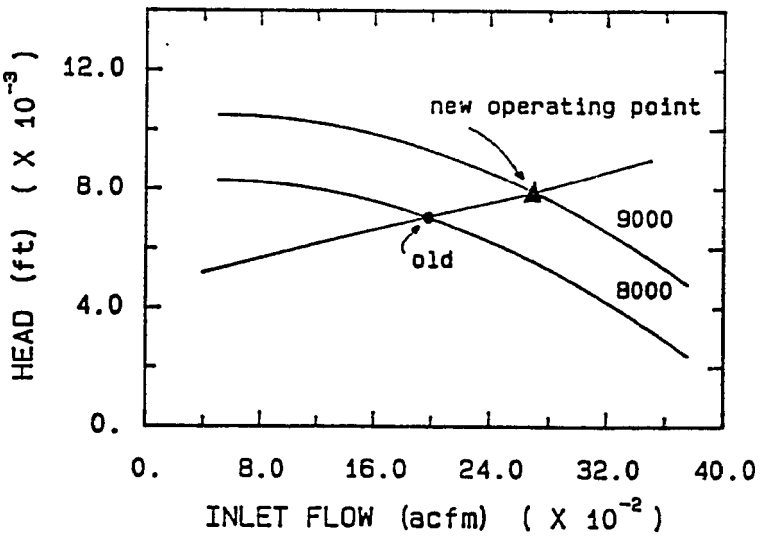

Figure 7-7: Variable speed effect

The shapes of the plant and compressor characteristic curves determine the changes in speed required to meet the new operating point. Table 7-2 gives the adjustments in speed (S_p) for two different compressor characteristic curves. For a given process, the steeper the compressor curves the larger the changes in speed. For a specific feed composition (z), energy consumption (hp) is the same for both sets of curves because the operating point dictated by the process is the same, and speed is determined by the head and flow provided by the compressor.

There should be a column operating pressure that minimizes compressor horsepower. A reduction in pressure decreases the vapor rate in the column and through the compressor but increases the ratio of suction to discharge pressure.

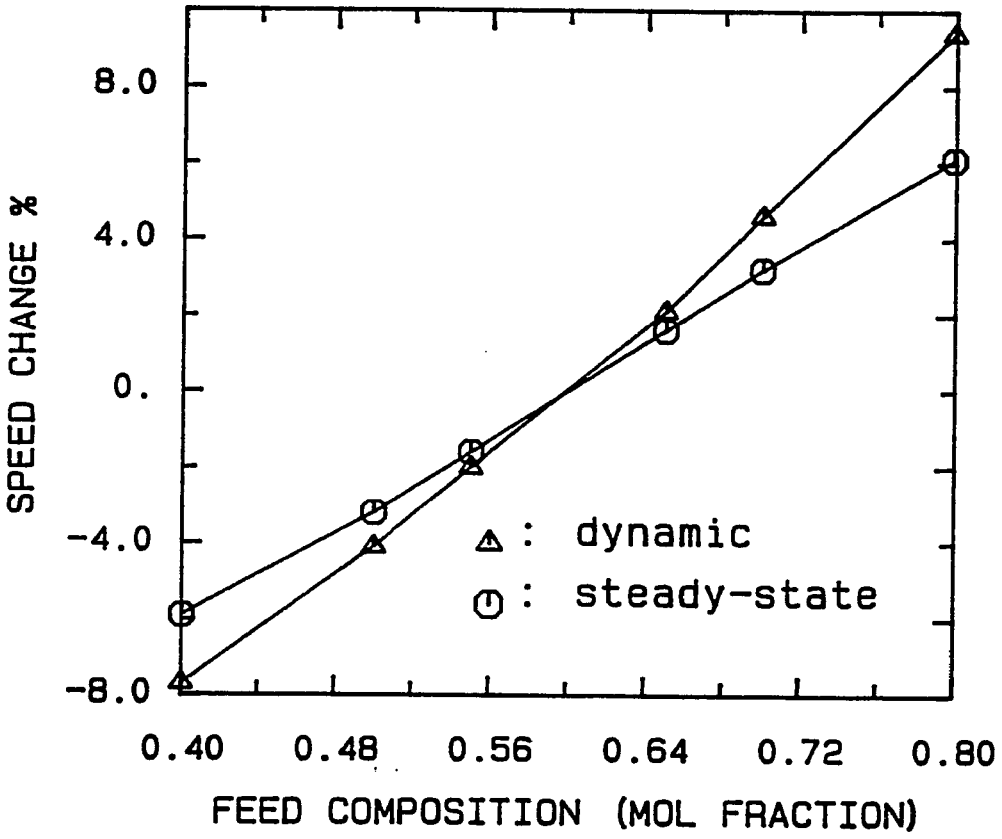

Figure 7-8: Speed changes vs. feed composition

$x_D(set)=0.99$ $x_B(set)=0.05$

Table 7-2: Compressor curve effect on speed

	basic curves		steeper curves		
z	S_p	%change	S_p	%change	hp
0.8	8370	6.1	9748	11.1	1520
0.7	8145	3.2	9150	4.3	1360
0.6	7890	--	8769	--	1190
0.5	7640	-3.2	8394	-4.3	1016
0.4	7420	-5.9	8065	-8.0	870

Table 7-3 shows the effect of pressure (P) on energy. Cooling water temperature (T_{cw}) and saturation of the water valve (F_w = 20000 lbmol/hr) would limit the available pressure range. A change in pressure from 10.9 atm to 10 atm reduces energy consumption by 1% and increases compressor speed by 2%. Thus it seems clear that for the variable speed configuration, energy consumption is only slightly effected by the operating pressure. On the other hand, running at the minimum pressure means that the system cannot handle load disturbances without requiring a pressure change. The small reduction in power (1%) may not be worth the increased operability and control problems.

Table 7-3: Pressure effect on speed

T_{cw}	P	S_p	hp	F_w
85	12	7742	1208	4324
	10.9	7890	1186	8245
	10.4	7968	1180	14300
	10.0	8036	1174	35300*
75	10.9	7890	1186	3827
	10.0	8036	1174	6064
	9.0	8236	1169	17981
	8.8	8281	1169	29730*

* Exceeds valve design capability

7.2.3 Suction Throttling

The suction throttling strategy adjusts suction pressure to compensate for process disturbances. Figure 7-9 shows the case when additional heat is required by the column. The operating point is moved along a constant speed curve to a higher flow by reducing the pressure difference across the compressor. The higher temperature differential driving force in the reboiler-condenser increases the discharge pressure. The increased opening of the suction valve decreases pressure drop over it, increasing suction pressure. The increase in suction pressure though is higher than the increase in discharge pressure. thus the pressure difference across the compressor is reduced. The changes in suction pressure resulting from feed composition disturbances are illustrated in Figure 7-10.

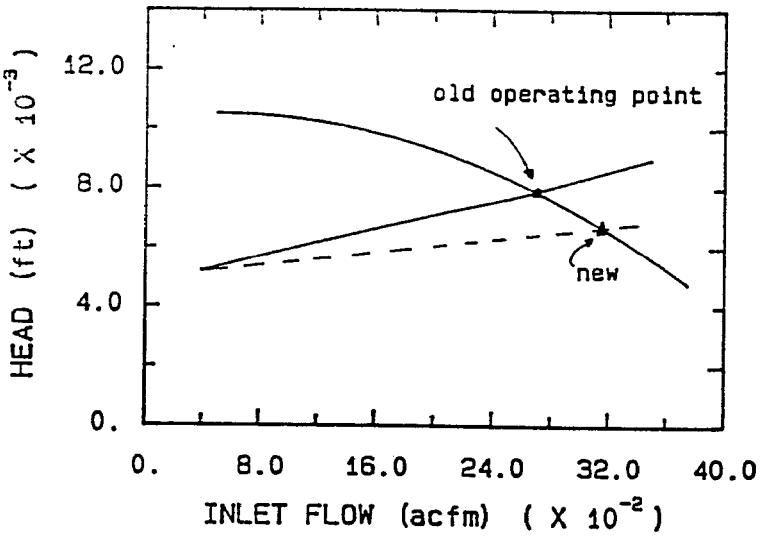

Figure 7-9: Suction throttling effect

The suction valve was designed to be completely open when the feed composition rises to values close to 0.8 mole fraction propylene. Because of the valve on the suction line, the head of the process characteristic curve for a specific throughput is higher than in the variable speed case, so a higher compressor speed is needed to meet process requirements, resulting in increased energy consumption at the design point. Table 7-4 indicates the differences in suction pressure (P_s) when a compressor with steeper characteristic curves is used.

Table 7-5 shows the effect of the operating pressure on energy consumption. A change in pressure from 10.9 atm to 10 atm reduces the energy requirements by 5% and decreases suction pressure by 6.8%. However, reducing the pressure also reduces the range in which suction pressure can be varied.

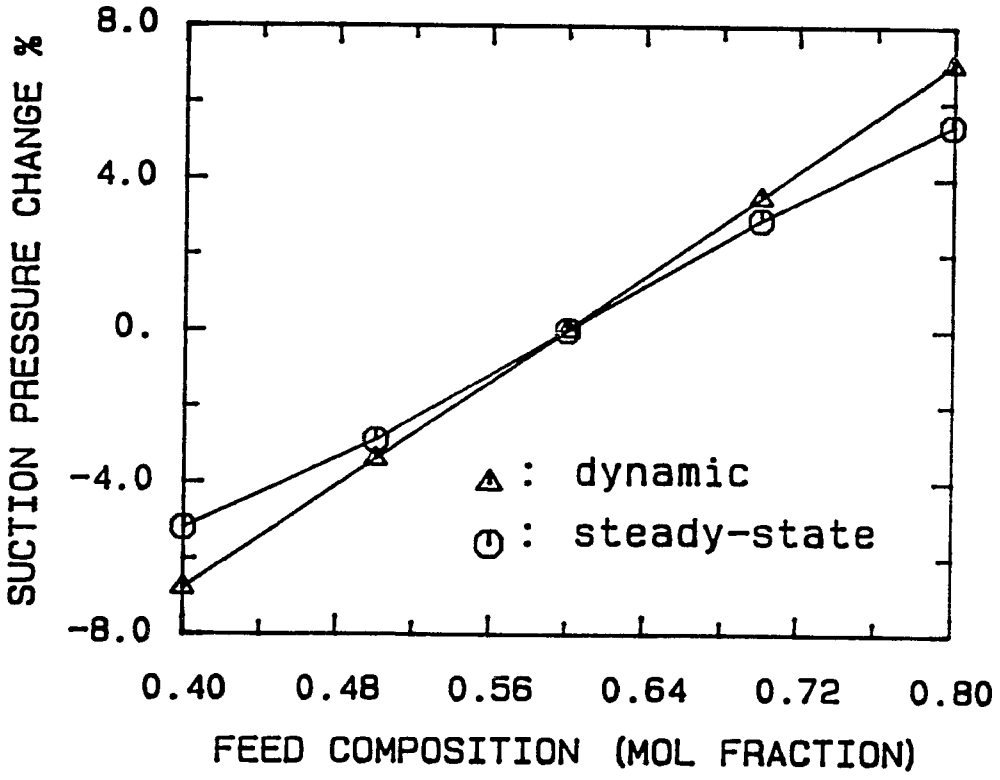

Figure 7-10: Suction pressure changes vs. feed composition

$x_D(set)=0.99$ $x_B(set)=0.05$

Table 7-4: Compressor curve effect on suction throttling

	basic curves			steeper curves			
z	P_s	%change	hp	P_s	%change	hp	F_c
0.8	10.86	5.4	1529	10.86	7.5	1529	6081
0.7	10.6	2.9	1447	10.5	4.0	1470	5625
0.6	10.3	--	1342	10.1	--	1391	5085
0.5	10.02	-2.9	1227	9.7	-4.0	1299	4536
0.4	9.76	-5.2	1115	9.4	-6.9	1205	4040

thus reducing the capability of handling load disturbances. The lowest attainable pressure is limited by cooling water flow and temperature.

7.2.4 Variable Heat Transfer Area

The heat transfer area of the reboiler-condenser is adjusted to compensate for process disturbances. The heat input to the column is regulated by changing the setpoint of the level controller in the reboiler-condenser. thus varying the heat transfer area available. The changes in heat transfer area modify the plant characteristic curve. Figure 7-11 shows how the operating point of the compressor is moved by increasing the heat transfer area when the column requires more heat. The new operating point is farther down the constant speed curve allowing more flow to go through the compressor. The compressor head is lower because increasing the available heat transfer area decreases the temperature differential driving force in the reboiler-condenser. This

Table 7-5: Pressure effect on suction throttling

T_{cw}	P	P_s	hp	F_w
85	10.9	10.3	1342	13298
	10.4	9.9	1308	26971*
75	10.9	10.3	1342	5089
	10.4	9.9	1308	6256
	10.0	9.6	1281	7762
	9.5	9.2	1248	11440
	9.0	8.84	1214	22738*

* Exceeds valve design capability

means that the compressor discharge pressure decreases.

At the design operating point the process conditions are the same as in the variable speed compressor case, but a bigger reboiler-condenser must be used to make it possible handle disturbances. Figure 7-12 indicates the dynamic and steady-state changes in heat transfer area when feed composition disturbances upset the column. Table 7-6 illustrates that the changes in heat transfer area become larger and changes in energy consumption become smaller when a compressor with a steeper characteristic curves is used. The same heat transfer area is used for both sets of compressor characteristic curves at the design point. so a higher compressor speed is needed for the steeper curves.

The effects of pressure are illustrated in Table 7-7. These are similar to the behavior in the other alternatives. in that a reduction in pressure reduces

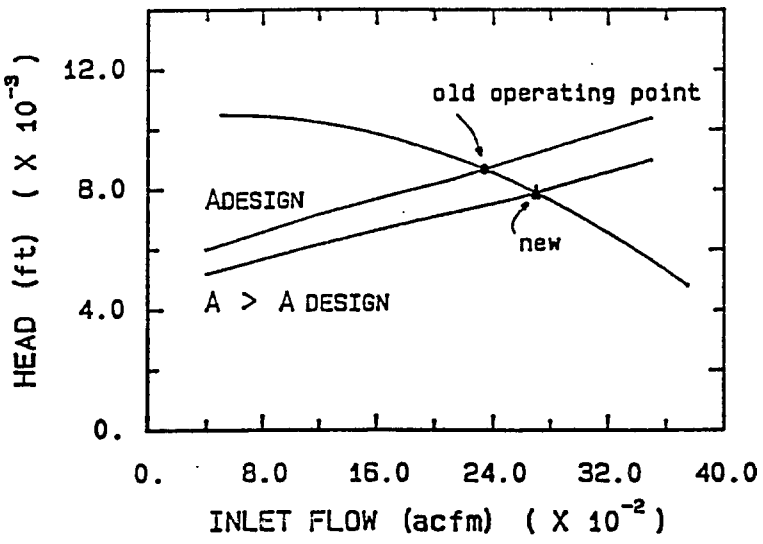

Figure 7-11: Variable heat transfer area effect

energy requirements but also reduces the ability of handling load disturbances. A change from 10.9 atm to 10 atm in pressure causes a reduction in energy of 6% and increases the area by 12%.

7.2.5 Bypassing

The bypass control alternative operates with more flow through the compressor than is necessary to meet the column heat input requirements. The excess flow is recycled to the compressor suction. Figure 7-13 shows that to increase the heat input to the column the bypass flow must decrease causing a corresponding increase in the compressor head: the heat input increases due to the higher temperature differential driving force in the reboiler-condenser. The net effect is increased flow through the reboiler, less flow through the

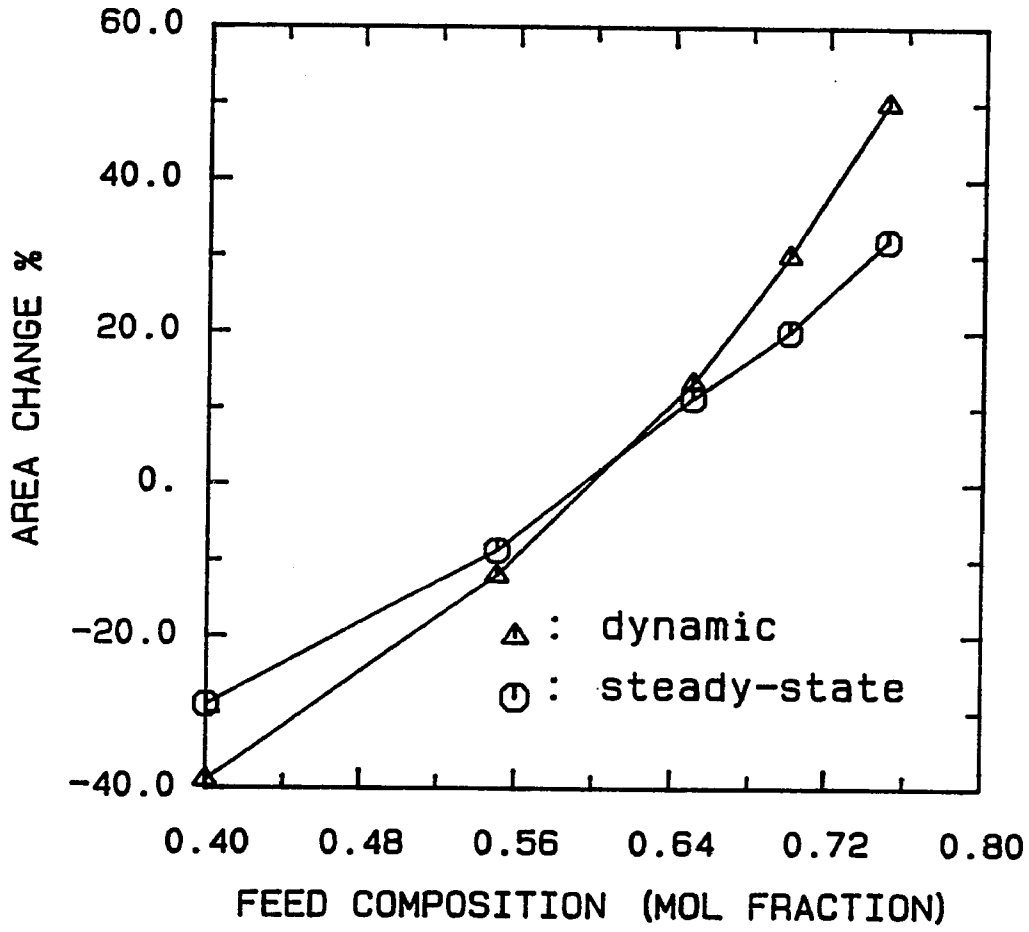

Figure 7-12: Heat transfer area changes vs. feed composition
$x_D(set)=0.99$ / $x_B(set)=0.05$

Table 7-6: Compressor curve effect on heat transfer area

	basic curves			steeper curves		
z	area	%change	hp	area	%change	hp
0.8	7106	66	1306	7338	71	1200
0.7	5137	20	1240	5635	31	1198
0.6	4280	--	1190	4280	--	1190
0.5	3640	-15	1110	3320	-22	1148
0.4	3053	-29	1020	2657	-38	1094

Table 7-7: Pressure effect on heat transfer area

T_{cw}	P	area	hp	F_w
85	10.9	4280	1190	8200
	10.4	4530	1150	13800
	10.0	4780	1120	41000*
75	10.9	4280	1190	3690
	10.0	4780	1120	5850
	9.5	5162	1080	9247
	9.0	5670	1040	23500*

* Exceeds valve design capability

compressor, and much less flow through the bypass.

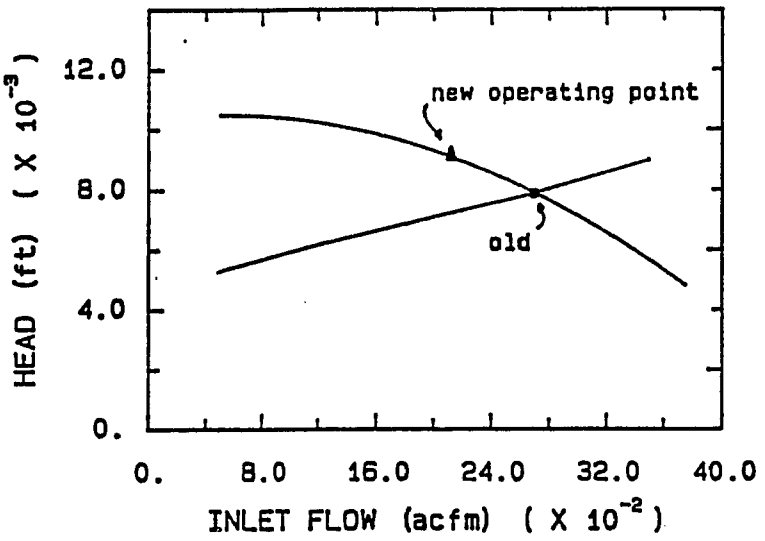

Figure 7-13: Bypass flow effect

A design bypass flow of 3000 lbmol/hr was selected to provide a reasonable capability to handle process disturbances. This high flow causes a dramatic increase in energy consumption in comparison to the other alternatives. Steady-state and dynamic changes in bypass flow to compensate for feed composition disturbances are illustrated in Figure 7-14.

The effect of the compressor characteristic curves is the opposite of that in the other cases. Steeper compressor characteristic curves reduce the changes in bypass flow. This is because the temperature differential driving force in the reboiler determines heat input and the flow through the exchanger. The steeper compressor characteristic curves. give smaller changes in pressure for given changes in flow. Table 7-8 shows the bypass flow and energy consumption for

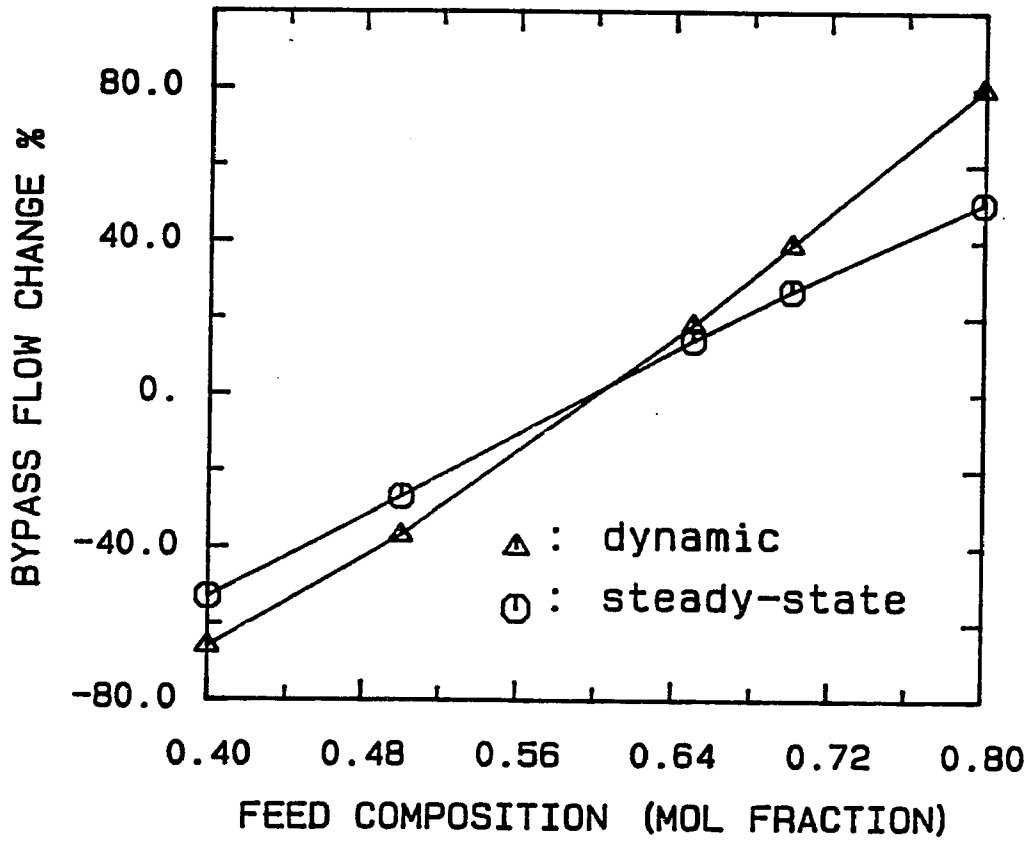

Figure 7-14: Bypass flow changes vs. feed composition
$x_D(set)=0.99$/ $x_B(set)=0.05$

Table 7-8: Compressor curve effect on bypass flow

	basic curves			steeper curves		
z	F_d	%change	hp	F_d	%change	hp
0.8	1450	-52	1880	1710	-43	1945
0.7	2160	-28	1887	2300	-23	1920
0.6	3000	--	1886	3000	--	1886
0.5	3840	28	1876	3700	23	1850
0.4	4590	53	1860	4350	45	1800

Table 7-9: Pressure effect on bypass flow

T_{cw}	P	F_d	hp	F_w
85	10.9	3000	1886	8245
	10.4	2635	1803	14300
	10.0	2340	1735	35290*
75	10.9	3000	1886	3420
	10.0	2340	1735	6064
	9.5	1967	1649	9055
	9.0	1562	1588	17980

* Exceeds valve design capability

the two sets of compressor curves.

Table 7-9 illustrates the effect of pressure on the amount of flow bypassed and the energy consumed. A reduction in pressure reduces the internal vapor in the column and the bypass flow, and thus reduces the energy consumption. In this case, a lower operating pressure reduces operating costs more significantly than in the other alternatives.

7.2.6 Dynamic Performance

For the propylene-propane system Figure 7-15 shows that all of the compressor control alternatives perform well. They differ in control action effort and energy consumption. Variable speed and suction throttling require smaller adjustments in the manipulated variable than bypassing or variable heat transfer area. Variable heat transfer area is inherently slower than the other alternatives because of the liquid dynamics in the heat exchanger. For the propylene-propane system, this difference is not appreciable due to the slow composition responses.

Figure 7-16 shows an energy consumption comparison of the compressor control alternatives for different feed compositions. Bypass control is the simplest alternative, but requires much more energy than the others. In general, selection of an approach depends on the specific application. Variable heat exchanger area could be advantageous when feed composition disturbances are usually over the design value because energy consumption is less sensitive than in the variable speed or suction throttling cases. For a plant that operates over a wide range of feed rates and compositions, it would be advisable to have a variable speed compressor.

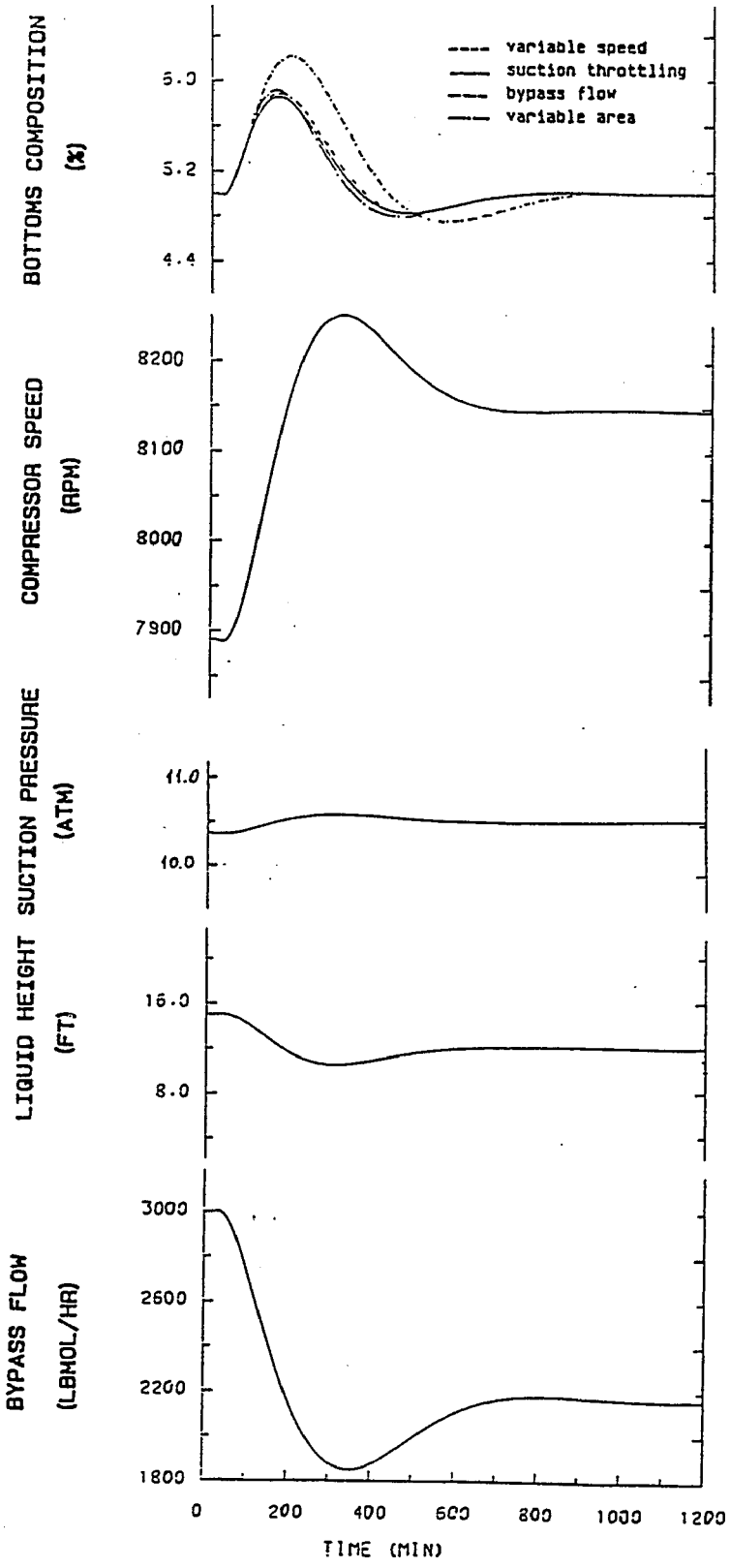

Figure 7-15: Compressor controller performance
x_D(set)=0.99/ x_B(set)=0.05/ z: 0.6 to 0.7

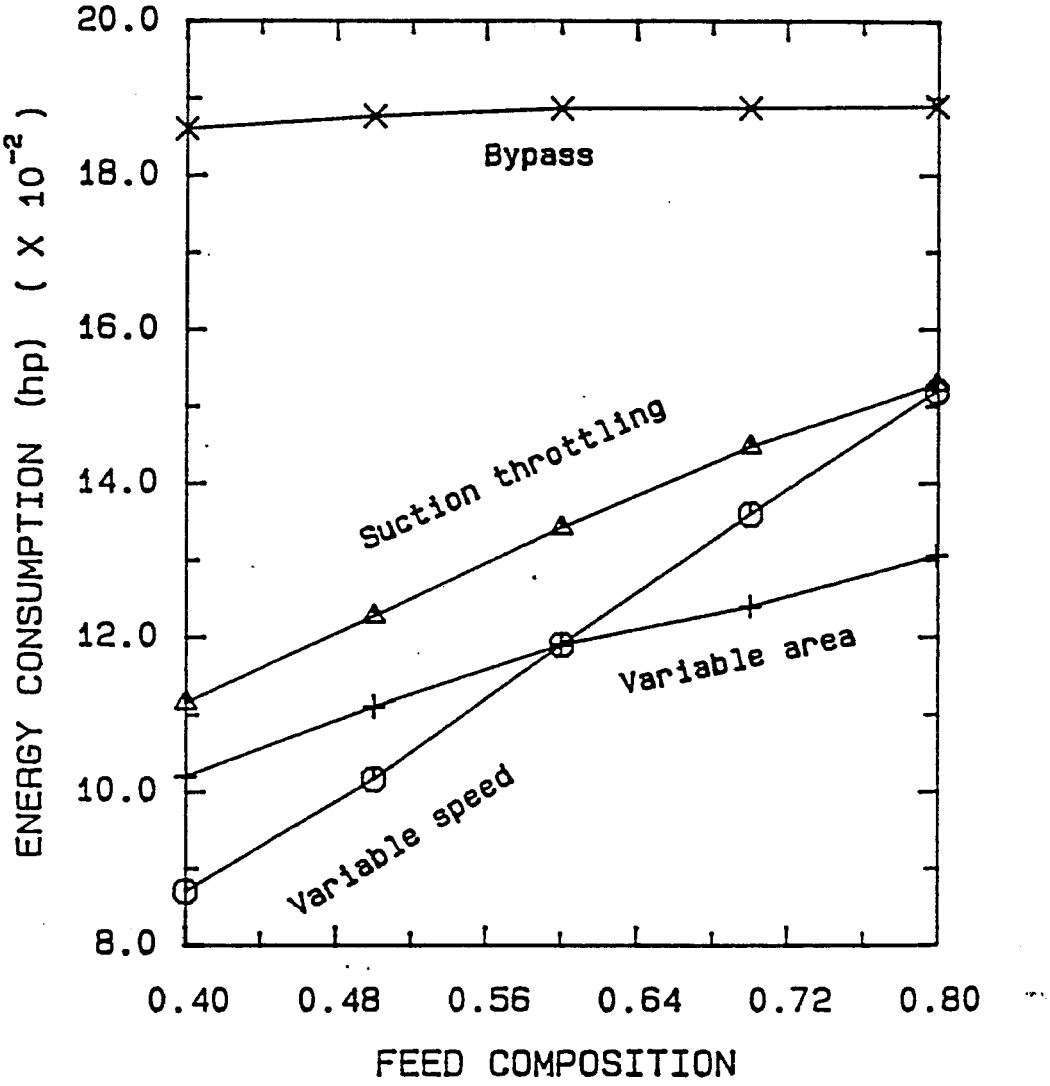

Figure 7-16: Energy consumption comparison

Chapter 8
Generic Conclusions

This study has shown that the control system used on a vapor recompression column can be the same as the control system of the corresponding conventional column by replacing heat input control with compressor control. The pressure loop will be faster than the compositions loops, so it can be tuned independently. For this conclusion to be valid, two conditions are necessary: (1) the composition time constants of the column should be at least 5 times larger than the pressure time constant; (2) the time constants of the reboilers of the two systems should be approximately the same. In terms of a distillation design parameter, the first condition coresponds to having a temperature difference between top and bottom of the column that is no greater than approximately 60 °F, which represents the upper limit for vapor recompression under today's economic conditions.

To reach this generic conclusion, we have explored two specific systems, ethanol-water and propylene-propane, which differ in many ways:

- Operating pressure: The ethanol-water system operates at low pressure (1 atm), whereas the propylene-propane system operates at a much higher pressure (10-20 atm).
- VLE characteristics: The ethanol-water mixture has very non-ideal liquid behavior and rather ideal vapor phase behavior because of the low operating pressure. The propylene-propane mixture behaves as an ideal liquid and non-ideal vapor.
- Mixture properties: Composition changes have an important impact on mixture properties in the case of ethanol-water because the individual component properties differ significantly. Propylene and propane have similar properties throughout the range of interest, so mixture properties are less dependent on composition.
- Vapor holdup: Because of the low operating pressure and consequent

low vapor densities, the vapor holdup of the ethanol-water system is negligible. Vapor holdup must be considered for the propylene-propane system.

- Vapor recompression design: The two systems require different vapor recompression designs so that water can be used as the cooling medium.

- Temperature difference (ΔT): The ΔTs between column top and bottom are 62 °F and 22 °F for the ethanol-water and propylene-propane systems respectively. The ΔT has a major impact on the economic attractiveness of vapor recompression systems, because a large ΔT implies a high compression ratio and increased compressor power.

Vapor recompression is generally considered to be economically viable (late 1980's energy costs) for separations with a column ΔT of about 65 °F or less. In light of this, the propylene-propane and ethanol-water systems can be seen as approximating boundary conditions of the region where economic incentives exist. Because of their representative nature, these systems provide a basis for a general study of vapor recompression.

The steady-state and dynamic aspects of conventional columns were analyzed to provide a comparative basis for the vapor recompression systems. Clearly, the main difference between vapor recompression and conventional distillation is the way in which energy is added and removed from the columns. For the conventional column, the dynamic changes in energy addition (reboiler duty) or removal (condenser duty) occur very rapidly compared to the dynamics of the column. Additionally, these two parameters can be varied independently. In the vapor recompression columns, energy addition and removal are linked because of the reboiler-condenser. The trim cooler does allow for some independent energy removal, but the quantity of energy removed is small compared to the total amount of energy flowing through the column.

Originally, it was thought that the pressure behavior of the columns might differ in the two structures. In the conventional columns, pressure dynamics are fast and so can be regulated by manipulating the condenser duty without interaction with composition loops. In the vapor recompression columns, the relationship between compressor speed and pressure initially appears complex. For example, one would expect an increase in compressor speed to increase suction flow and decrease suction pressure; however, the same increase in speed should increase the heat added to the column, and thus increase vapor rates and suction pressure. The speed and net effect of these changes were unknown, so the vapor recompression columns were considered truly multivariable systems of order 3x3 and a significant control challenge.

For the specific cases we have studied, the pressure loop dynamics were found to be significantly faster than the dynamics of the composition loops, thus it was possible to degrade the control systems to order 2x2.

Looking at the vapor recompression columns as a 2x2 system, important similarities between the conventional and vapor recompression systems become apparent. The vapor recompression columns were controlled by extending a control structure successfully employed on the specific conventional column to the corresponding vapor recompression column. To achieve this, compressor control in the vapor recompression column (speed, area, suction or bypass) replaced heat input control in the conventional column.

The ethanol-water and propylene-propane systems display a common pattern: the similarities between the conventional and vapor recompression processes outweigh the differences. There are two key similarities: the pressure loop can be treated independently of composition loops, and compressor control

emulates heat input control.

When these two conditions are present we believe that we have provided a generic solution to the problem of control of columns with direct vapor recompression. In the following sections these conditions are explained and the limitations of the generic solution addressed.

8.1 Pressure Control

The fact that the pressure loop can be treated (tuned) independently of composition loops implies that the interactions between these types of loops are negligible. Consequently, the system can be seen as 2x2 like the conventional column. Independence can be assumed because pressure dynamics are fast relative to composition dynamics.

A. Composition Dynamics

The inherent composition dynamics are primarily determined by the holdup of material in the column. Since almost all systems considered for vapor recompression represent difficult separations (low relative volatility), the column will always have a large number of trays, which results in slow composition dynamics. Composition control loop dynamics will be slowed by delays and lags associated with the sensors and other column hardware.

For the propylene-propane system, the column ΔT is small so two analyzers must be used to measure compositions. Use of analyzers will slow composition responses. In this particular application a delay of 5 minutes was assumed. The distillate composition control loop responds with a natural period of 26 minutes and the bottoms composition control loop responds with a period of 33 minutes.

For the ethanol-water system, with its substantial ΔT, only one analyzer is required; bottoms composition can be inferred from Tray 6 temperature. The natural periods are 20 and 2 minutes for the top composition and temperature in Tray 6 control loops respectively.

In both cases, a turbine speed lag of 0.5 minutes was assumed. A larger lag will further slow composition dynamics because the speed of changes in heat input will decrease. The same effect is produced when condensate throttling is used to control the compressor and regulate column heat input.

B. Pressure Dynamics

The pressure dynamics are fast because the vapor residence time (time constant) of the column is small. Changes in the rate of vapor boilup or condensation rapidly effect pressure.

For the propylene-propane system, the pressure loop control responds with a natural period of 1.2 minutes. The vapor residence time is 7.8 minutes.

For the ethanol-water system. the pressure loop control responds with a period of 0.4 minutes. The vapor residence time is 0.58 minutes.

The results indicate that pressure dynamics are in a range of 5 to 50 times faster than composition dynamics. This difference in the speed of response of pressure and composition loops is typical of systems where the separation is difficult (small ΔT). Since small ΔTs are currently a prerequisite for vapor recompression columns. it seems likely that the independence of the pressure loop can be assumed for most vapor recompression systems.

8.2 Compressor Control

A. Dynamic

To maintain in the vapor recompression column the same control system as in the conventional column it is necessary that the compressor control loop (variable speed, variable area, suction throttling or bypass) has an equivalent dynamic response to the heat input control in the conventional column. This means that if the dynamics of the reboiler is slow in the conventional column, then the same should apply to the vapor recompression reboiler dynamics. Typically, the compressor loop in the vapor recompression column behaves similar to the steam heat input control loop in the conventional column. This is because the vapor holdup in the compressor is relatively small compared to the vapor holdup in the column (ratio 1/20), thus changes in compressor speed (or other compressor control variables) rapidly effect the vapor rates in the column, emulating the steam effect on the conventional columns.

For the propylene-propane system, the vapor holdup in the compressor section (pipes, compressor, heat exchangers) was 750 ft^3 and the vapor holdup in the column was 16000 ft^3. The time constants (V/F) were 0.3 and 7.8 minutes for the compressor section and column respectively.

For the ethanol-water column the vapor holdups were 1200 and 20000 ft^3 and the time constants 0.022 and 0.58 minutes for the compressor part and column respectively.

B. Steady-State

The steady-state interactions of vapor recompression control systems are

similar to those of conventional column systems with the same control structures. The pathways by which a disturbance effects the system are similar whether the column uses vapor recompression or not. For example, for a (D,Q_R) control structure, an increase in heat input increases vapor rate and reflux flow. The increase in reflux pushes the column back toward steady-state. The presence of a compressor does not alter this sequence; the same effect occurs when the compressor speed is increased in a (D,S_p) control structure.

8.3 Limitations

A small ΔT is the key to slow composition dynamics (fast pressure dynamics) and small time constants in the compressor section relative to the column. Therefore, the vapor recompression control design procedure outlined in this dissertation can be considered generic as long as the column temperature difference is less than about 60 °F. This is the "rule of thumb" limitation for vapor recompression systems under today's economic conditions.

This study has been conducted for commercial scale columns. The conclusions obtained here may not be valid in pilot plants or laboratory scale columns where the volume of the columns will be closer to the compressor section volumes.

References

Astrom, K. J. and T. Hagglund. Automatic Tuning of Simple Regulators with Specifications on Phase and Amplitude Margins. *Automatica*, 1984, *20*, 645-651.

Black, C. Vapor Phase Imperfections in Vapor-Liquid Equilibria. *Ind. Eng. Chem.*, 1963, *50*, 391-402.

Bristol, E. On a New Measure of Interaction for Multivariable Process Control. *IEEE Trans. Autom. Control*, 1966, *AC-11*, 133-140.

Brousse, E., B. Claudel and C. Jallut. Modeling and Optimization of the Steady State Operation of a Vapor Recompression Distillation Column. *Chem. Eng. Sci.*, 1985, *40*, 2073-2078.

Buckley, P. S, Luyben W. L. and J. P. Shunta. *Design of Distillation Column Control Systems.* Research Triangle Park: Instrument Society of America, 1985.

Choe, Y. S. *Rigorous Dynamic Models of Distillation Columns.* Master's thesis. Lehigh University, 1985.

Choe, Y. S. and W. L. Luyben. Rigorous Dynamic Models of Distillation Columns. *Ind. Eng. Chem. Res.*, 1987, *26*, 2158-2161.

Collura. M. A. *Energy Saving Distillation in Fuel Ethanol Production: Steady-State and Dynamic Analysis.* Doctoral dissertation, Lehigh University, 1985.

Danzinger, R. Distillation Columns with Vapor Recompression. *Chem. Eng. Prog.*, 1979, *75*, 324-328.

Davies, W. D. *System Identification of Self-Adaptive Control.* New York: John Wiley & Sons. Inc.. 1972.

Davis. F. T. and A. B. Corripio. Dynamic Simulation of Variable Speed Centrifugal Compressors. In *Advances in Instrumentation.* Instrument Society of America. 1974.

Doyle. J. C. and G. Stein. Multivariable Feedback Design: Concepts for a Classical/Modern Synthesis. *IEEE Trans. Autom. Control.* 1981. *AC-26.* 4-16.

Ferre. J. A.. F. Castells and J. Flores. Optimization of a Distillation Column with a Direct Vapor Recompression Heat Pump. *Ind. Eng. Chem. Process Des. Dev.*. 1985. *24*. 128-132.

Finco. M. V. *The Modeling and Control of Low Relative Volatility Splitters.* Master's thesis. Lehigh University. 1987.

Fuentes, C. and W. L. Luyben. Comparison of Energy Models for Distillation Columns. *Ind. Eng. Chem. Fundam.*, 1982, *21*, 323-325.

Hall, R. S., J. Matley and K. J. McNaughton. Current Costs of Process Equipment. *Chem. Eng.*, 1982, *89*, 80-116.

Henley E. J. and J. D. Seader. *Equilibrium-Stage Separation Operations in Chemical Engineering.* New York, N.Y.: John Wiley & Sons., 1981.

Hernandez, E. *Feasibility Analysis, Dynamics, and Control of Distillation with Vapor Recompression.* Doctoral dissertation, The Louisiana State University, 1981.

Hindmarsh, A. C. and A. H. Sherman. *LSODES* (Tech. Rep.). Lawrence Livermore National Laboratory, 1983.

Lapina. R. P. How to Use the Performance Curves to Evaluate Behavior of Centrifugal Compressors. *Chem. Eng.*, 1982, *89*, 86-93.

Ljung, L. *System Identification: Theory for the User.* Englewood Cliffs, New Jersey: Prentice Hall, Inc., 1987.

Luyben, W. L. *Process Modeling, Simulation, and Control for Chemical Engineers.* New York: McGraw Hill Book Co., 1973.

Luyben, W. L. Steady-State Energy Conservation Aspects of Distillation Column Control System Design. *Ind. Eng. Chem. Fundam.*, 1975, *14*, 321-325.

Luyben. W. L. Simple Method for Tuning SISO Controllers in Multivariable Systems. *Ind. Eng. Chem. Process Des. Dev.*, 1986, *25*, 654-660.

Luyben. W. L. Derivation of Transfer Function for Highly Nonlinear Distillation Columns. *Ind. Eng. Chem. Res.*, 1987, *26*, 2490-2495.

MacFarlane, A. G. and J. J. Belletrutti. The Characteristic Locus Design Method. *Automatica.* 1973. *9*, 575-588.

Meili, A. Experience with Heat Pump System for Energy Saving in Distillation Column. In *Distillation and Absorption 1987.* European Federation of Chemical Engineering. 1987.

Meili, A. and A. Stuecheli. Distillation Column with Direct Vapor Recompression. *Chem. Eng.*, 1987, *94*, 133-143.

Miller, J. S. and W. A. Kapella. Installed Costs of a Distillation Column. *Chem. Eng.*, 1977, *84*, 129-133.

Mix, T. J., *et al.* Energy Conservation in Distillation. *Chem. Eng. Prog.*, 1978, *74*, 49-56.

Moore, C. Application of Singular Value Decomposition to the Design Analysis, and Control of Industrial Processes. Paper presented at a meeting of the

American Control Conference. 1986.

Morari, M. Design of Resilient Processing Plants III. *Chem. Eng. Sci.*, 1983, *38*, 1881-1888.

Mostafa, H. A. Thermodynamic Availability Analysis of Fractional Distillation with Vapor Recompression. *Can. J. Chem. Eng.*, 1981, *59*, 487-491.

Muhrer C. A., M. A. Collura and W. L. Luyben. Concentration Profile Inversion in Distillation Rating Programs with Tray Efficiencies. *Ind. Eng. Chem. Res.*, 1988, *27*, 716-718.

Mulet, A., A. B. Corripio and L. B. Evans. Estimate Costs of Distillation and Absorption Towers Via Correlations. *Chem. Eng.*, 1981, *88*, 77-82.

Neerken, R. F. Keys to Compressor Selection. *Chem. Eng.*, 1975, *82*, 78-94.

Niederlinski, A. A Heuristic Approach to the Design of Linear Multivariable Interacting Control Systems. *Automatica*, 1971, *7*, 691-701.

Null, H. R. Heat Pumps in Distillation. *Chem. Eng. Prog.*, 1976, *73*, 58-64.

Prausnitz J. M., R. N. Lichtenthaler and E. Gomes. *Molecular Thermodynamics of Fluid-Phase Equilibria.* Englewood Cliffs, N.J.: Prentice-Hall Inc., 1986.

Quadri, G. P. Use Heat Pump for P-P Splitter. Part 1: Process Design. *Hydrocarbon Processing*, 1981, *60*, 119-126.

Quadri, G. P. Use Heat Pump for P-P Splitter. Part 2: Process Optimization. *Hydrocarbon Processing*, 1981, *60*, 147-151.

Rijnsdorp, J. P. Interaction in Two-Variable Control Systems for Distillation Columns. *Automatica*, 1965, *1*, 15-24.

Robinson, C. S. and E. R. Gilliland. *Elements of Fractional Distillation.* New York: McGraw Hill Company, 1950.

Shinskey, F. G. *Process Control Systems.* New York: McGraw-Hill Company, 1979.

White, M. H. Basics of Surge Control for Centrifugal Compressors. *Chem. Eng.*, 1972, *79*, 54-62.

Yu, C. C. and W. L. Luyben. Design of Multiloop SISO Controllers in Multivariable Processes. *Ind. Eng. Chem. Process Des. Dev.*, 1986, *25*, 498-503.

Appendix A
Thermodynamic and Physical Properties

A.1 Ethanol-Water System

A.1.1 Vapor-liquid equilibrium

The form of the equilibrium model is that suggested by Black (1963). The model is as follows:

$$K_i = \frac{y_i}{x_i} = \frac{\gamma_i p_i^o}{\phi_i' P} \qquad (A.1)$$

where:

y_i : vapor mole fraction of component i
x_i : liquid mole fraction of component i
γ_i : liquid phase activity coefficient of component i
p_i^o : vapor pressure of pure component i
ϕ_i' : imperfection pressure coefficient of component i (similar to fugacity coefficient)
P : total pressure

The parameters and accuracy of the model are described by Collura (1986).

A.1.2 Enthalpy functions

A model developed by Collura (1986) was used. The following assumptions and simplifications are included:

- enthalpy defined as zero for pure liquids at 0°C and saturation pressure
- vapor phase heat of mixing is not included (ideal vapor solution)
- ideal gas heat capacities are used

A.1.3 Density functions

Liquid density is estimated using Amagat's rule for mixtures. This method simply assumes that liquid volumes are additive, and hence neglects the volume change on mixing.

Vapor density is estimated based on the ideal gas volume.

A.2 Propylene-Propane System

A.2.1 Vapor-liquid equilibrium

A correlation developed by Finco (1987) is used.

$$\alpha = A_0 - A_1 x - A_2 x^2 \qquad (A.2)$$

$$A_0 = 1.2855 - 0.000446 P$$

$$A_1 = 0.088008 - 0.0001035 P$$

$$A_2 = 0.052215 - 0.00014607 P$$

where

α : relative volatility
x : liquid composition (mole % propylene)
P : pressure (70 psia $\leq$ P $\geq$ 250 psia)

A.2.2 Enthalpy functions

Liquid and vapor enthalpies were calculated using the Redlich-Kwong equation of state. The correlation and parameters were obtained from Henley and Seader (1981).

A.2.3 Density functions

Amagat's rule was used to obtain the liquid mixture density. For the pure components the following correlations were developed:

(A.3)

$$\rho_{1,L} = 0.6 - 0.0011\,T$$

$$\rho_{2,L} = 0.57 - 0.001\,T \tag{A.4}$$

for temperatures on the range of 70 to 140 °F.

Vapor density was calculated from:

$$\rho_v = \frac{MW\,P}{z\,R\,T} \tag{A.5}$$

$$z = 1 + \frac{B_{mix}\,P}{RT} \tag{A.6}$$

$$\frac{B}{v_c} = 0.43 - 0.886\,\frac{T_c}{T} - 0.694\,\frac{T_c^2}{T^2} - 0.075\,\frac{T_c^{4.5}}{T^{4.5}} \tag{A.7}$$

The virial coefficient was obtained from the corresponding-states correlations described by Prausnitz *et al.* (1986).

Appendix B
Columns Design Specifications

B.1 Ethanol-Water Columns

	Conventional	VRC
column diameter, ft	13.5	13.5
number of trays	78	78
feed tray location	10	10
weir height, in	2.0	2.0
weir length, ft	10.4	10.4
tray spacing, in	24	24
reboiler area, ft^2	6760	39400
condenser area, ft^2	7560	
top preheater area, ft^2	1860	1860
bottom preheater area, ft^2	1320	1320
trim cooler area, ft^2		1400

B.2 Propylene-Propane Columns

	Conventional	VRC
column diameter, ft	9.5	8.5
number of trays	208	154
feed tray location	58	41
weir height, in	2.0	2.0
weir length, ft	7.3	6.6
tray spacing, in	24	24
reboiler area, ft^2	1420	4280
condenser area, ft^2	12500	
trim cooler area, ft^2		800

Vita

Cristian A. Muhrer

Personal Background

Date of Birth : June 12, 1956

Place of Birth : Vina del Mar, Chile

Parents : Frank and Elena Muhrer

Education

Montreal University, Montreal, Canada
Master of Science in Chemical Engineering. July 1982
Thesis Title: "Temperature Profile Control in Extruders by Microprocessor"

Santa Maria University, Valparaiso, Chile
Bachelor of Science in Chemical Engineering. December 1979
Graduated 1st in class

Work Experience

Research Assistant, Lehigh University, Pennsylvania, USA (January 1986 to November 1988).

Teaching Assistant, Lehigh University, Pennsylvania, USA (August 1985 to December 1985).

Instructor, University of Concepcion, Concepcion, Chile
Taught Fluid Mechanics, Process Dynamics, Digital Control and Distillation. Performed Process Control research (March 1983 to August 1985).

Research Associate, Santa Maria University, Valparaiso, Chile
Developed an on-line feedback control and data acquisition system (July 1982 to January 1983).

Research Assistant, Ecole Polytechnique de Montreal, Canada (May 1980 to June 1982).

Papers and Publications

"Concentration Profile Inversion in Distillation Rating Programs with Tray Efficiencies"
I&EC Research, **1988**, *27*, 716.
with W. Luyben and M. Collura.

"Tuning of Digital PID Controllers"
Proceedings of the X Interamerican Congress in Chem. Eng., Santiago (1983).
with J. Yianatos and E. Pizarro.

" Extruder Temperature Behavior"
Annual Congress of the Society of Plastic Engineers, Chicago, SPE, ANTEC, Preprints, Vol. 8 (1983).
with I. Patterson and C. Guerrero.

"Optimal Tuning of Digital PID Controllers Using Ratio Variances Contours"
Proceedings of the 33rd Canadian Society for Chemical Engineering Conference, Toronto (1983).
with J. Yianatos.

"Temperature Response of Extruders"
Proceedings of the 25th Conference of the Canadian Chemist Institute, Toronto (1982).
with I. Patterson.

"Technological Forecast of the Pulp and Paper Industry at Quebec"
Proceedings of the 20th Conference of the Canadian Paper Asociation, Montreal (1982).
with L. Binette, M. Duran, S. Ponce and I. Rossini.

"On the Use of Box and Jenkins Technique to Identify and Control a Tank Level"
Proceedings of the IV Chilean Conference of the Automatic Control Association. Santiago (1980).
with J. Yianatos.

"Simulation of Digital Controllers and Searching for Optimal Tuning for P, PI. PID Controllers"
Proceedings of the V Chilean Congress of Chem. Eng., Valparaiso (1979).
with J. Yianatos.